Universidad de Valladolid

Final Thesis

Optimization of Hybrid Fiber Amplifiers in uncompensated links designed for NyWDM transmission

---

Author:
Carlos Gomez Tome

Supervisors:
Vittorio Curri
Andrea Carena

Politecnico di Torino

February, 2015

A mis padres por dejarme aprovechar todas las oportunidades que he tenido hasta ahora, a mi abuela por todo su cariño y a Sara y los dos canijos por alegrarme todos los días.

Abstract

Uncompensated links are the state of art in nowadays optical communications. Its deployment is being carried-out instead of the typical compensated links (such as Chirped fibers). This project focus on the optimization of the link through the use of hybrid Raman-EDFA amplifiers, HFA. Therefore, we propose optimization rules for HFA in NyWDM transmission over these uniform uncompensated links and for it, we introduce a fiber Raman merit parameter showing that noise reduction is always dominant on NLI enhancement. Before that, a basical explanation of optical communications performance is explained where we will treat the optical fiber, optical amplifiers and the GN-Model.

Contents

1 Introduction **1**

2 The optical fiber **3**
2.1 Basic Concepts 3
2.1.1 Geometrical description 3
2.1.2 Wave Propagation Theory 6
2.2 Single-Mode Fibers, SMF 8
2.2.1 Dispersion in Single-Mode Fibers 8
2.3 Main problems of the fiber in our system scenario 10
2.3.1 Fiber Losses 10
2.3.2 Nonlinear Optical Effects 13
2.4 Nonlinear Optical effects. Stimulated Raman Scattering, SRS 15

3 Optical Amplifiers **19**
3.1 Basic concepts 19
3.1.1 Amplifier Gain 20
3.1.2 Amplifier Noise 20
3.2 Erbium-doped fiber amplifier, EDFA 21
3.2.1 Stimulated Emission 21
3.2.2 ASE Noise 23
3.2.3 EDFA Gain 23
3.2.4 EDFA Noise Figure 24
3.3 Raman Amplifiers 25
3.3.1 Raman Gain 25
3.3.2 Raman Noise Figure 28
3.3.3 Raman amplifier efficiency 29
3.4 Hybrid Raman/Erbium-Doped Fiber Amplifiers (HFA) 29

4 The GN Model **32**
4.1 The GN Model reference formula 32
4.2 The IGN Model 34

4.3 GN model in our system scenario 34

5 Simulation Results **39**
5.1 Code Performance 39
5.2 Analyzed scenario 40
5.2.1 Simulation considerations 42
5.3 First Scenario. Counter propagating Pump, No extra losses when RA is on 43
5.3.1 NZDSF results 45
5.3.2 SMF results 50
5.3.3 PSCF results 55
5.3.4 Comparison between fibers 60
5.4 Second Scenario. Co and Counter propagating Pump, No extra losses with RA on 64
5.4.1 NZDSF results 66
5.4.2 SMF results 69
5.4.3 PSCF results 72
5.4.4 Comparison between fibers 75
5.5 Third Scenario. Co and Counter propagating Pump, Extra losses with RA on 76
5.5.1 NZDSF results 77
5.5.2 SMF results 80
5.5.3 PSCF results 83
5.5.4 Comparison between fibers 86
5.6 Comparison between Second Scenario and Third Scenario . . . 87
5.6.1 NZDSF comparison 88
5.6.2 SMF comparison 89
5.6.3 PSCF comparison 90

6 Conclusions **91**

Chapter 1

Introduction

The overall global Ip traffic rate has suffered a big growth last years [1]. To be able to handle these rates, and to avoid congestion, carriers are exploring multiple ways to increase the capacity in their installed infrastructure (without replacing field fiber) [2]. One of these ways consist in using hybrid fiber amplifiers, HFA, in other words, the use Raman amplification together with EDFA's. This manner is a seamless solution for C-band transmission in order to improve OSNR and consequently allowing higher capacity [2], or increasing reach maintaining the capacity [3]. Another application of the HFA is related with the purpose to enlarge the link bandwidth to C+L [4].

This project focus on the analysis of HFA used to enhance C-band transmission supposing to add counterpropagating and copropagating pumps to supplement EDFA. It is supposed to operate with Nyquist WDM (NyWDM) transmission on uniform uncompensated links based on a comb of channels modulated with multilevel modulation formats with coherent R_x. In this system scenario, propagation introduces a noise-like disturbance called nonlinear interference (NLI) whose strength can be analytically evaluated using the GN-model [5], also in presence of Raman amplification [6]. Using the GN-model, it is derived a general optimization procedure for HFA, and for moderate pumping regime ($P_{pump} \leq 500$ mW) [7, 8, 9] it is proposed a Raman merit parameter for different fiber types.

Before explaining the analysis and the results, a general explanation of the basis of optical communications is reviewed. The concepts of optical fiber performance will be explained and also, its main problem such as attenuation, dispersion and non-linearities. Then, the amplificators of this project will be explained separetely, describing its main characteristics and the advantages of the use of both of them will be discussed. Finally, the main theoretical

ideas of the GN-model will be showed and explained.

The design rules aimed at OSNR or reach maximization in NyWDM uniform links are also reviewed, showing what the optimal power level is and the scaling of design targets with HFA noise reduction and NLI enhancement.

Finally, the project focus on moderate pumping and define the Raman merit parameter related to the fiber type. It shows the dominant Raman positive effect of noise reduction versus the NLI enhancement due to power regrowth at fiber end. In order to apply the developed results we consider three typical fiber types showing that only for the lowloss PSCF it is not convenient to pump Raman up to 500 mW, while for standard-loss NZDSF and SMF the merit of noise reduction is marginally impaired by NLI enhancement.

Chapter 2

The optical fiber

In this chapter we will introduce the basic concepts of optical fibers, what kind of fibers do exist and what are their main characteristics and problems. We will focus on the single mode fiber and on the stimulated Raman scattering non linnearity.

2.1 Basic Concepts

There are two main points of view to describe the performance of the optical fiber. The first one is the geometrical description, a very simple description, and the second one is based on the Maxwell laws of electrical and magnetic fields.

2.1.1 Geometrical description

An optical fiber consists of a cylindrical core of silica glass surrounded by a cladding whose refractive index is lower than that of the core [10].

We can difference two kinds of optical fiber, one called *step-index fiber* in which there is an abrupt index change at the core-cladding interface and another one known as *graded-index fiber* in which the refractive index decreases gradually inside the core. In figure 2.1 the index profile and the cross section for the two kinds of fibers are represented.

The *step-index fiber* performance is showed in figure 2.2. A light beam incides at the core center making an angle θ_i with the fiber axis. Because of refraction at the fiber-air interface, the beam bends toward the normal.

The angle of the refracted beam is θ_r:

$$n_0 sin\theta_i = n_1 sin\theta_r, \tag{2.1}$$

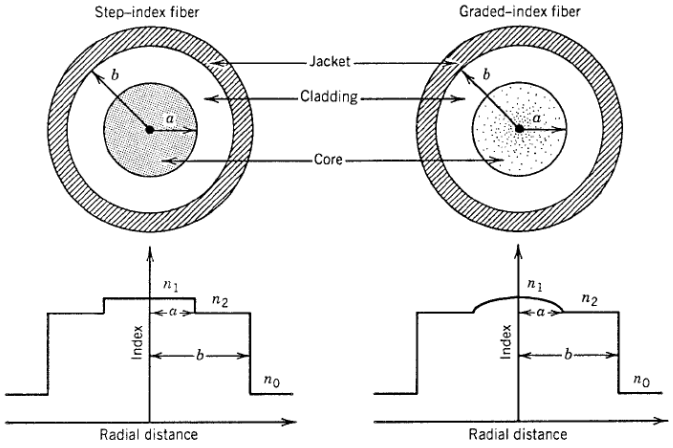

Figure 2.1: Cross section and refractive-index profile for step-index and graded-index fibers [10].

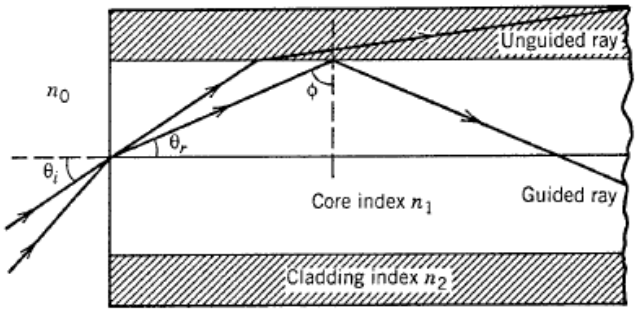

Figure 2.2: Step-index fiber performance [10].

where n_1 and n_0 are the refractive indices of the fiber core and air, respectively. The refracted beam hits the core-cladding interface and is refracted again. However, refraction is possible only for an angle of incidence ϕ such that $sin\phi < n_2/n_1$ (where n_2 is the cladding index). We define then the *critical angle* ϕ_c, the angle that produces the total internal reflection at the core-cladding interface of the beam, in equation: 2.2.

$$sin\phi_c = \frac{n_2}{n_1} \tag{2.2}$$

A remarkable effect on the *step-index fiber* is the multipath dispersion or modal dispersion. It can be understood by looking at figure 2.2, where different beams travel along paths of different lengths. As a result, these beams get dispersed in time at the output of the fiber even if they were coincident at the input and traveled at the same speed inside the fiber. By taking the velocity of propagation $v = c/n_1$, the time delay is given by:

$$\triangle T = \frac{n_1}{c}\left(\frac{L}{sin\phi_c} - L\right) = \frac{L}{C}\frac{n_1^2}{n_2}\frac{(n_1 - n_2}{n_1}. \tag{2.3}$$

The time delay between the two rays taking the shortest and longest paths is a measure of broadening experienced by an impulse launched at the fiber input.

In a different way, the performance of the *graded-index fiber* is showed in figure 2.3. The refractive index of the core in graded-index fibers is not constant but decreases gradually from its maximum value n_1 at the core center to its minimum value n_2 at the core-cladding interface.

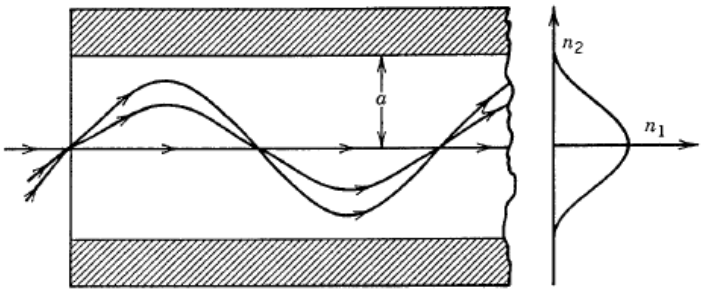

Figure 2.3: Graded-index fiber performance.

In these fibers intermodal or multipath dispersion is reduced. Figure 2.3 shows schematically paths for different beams. Similar to the case of

step-index fibers, the path is longer for more oblique rays. However, the beam velocity changes along the path because of variations in the refractive index. More specifically, the beam propagating along the fiber axis takes the shortest path but travels more slowly as the index is largest along this path. Oblique beams have a large part of their path in a medium of lower refractive index, where they travel faster. It is therefore possible for all beams to arrive together at the fiber output.

In any case, graded-index fibers are rarely used for long-haul links and graded-index plastic optical fibers provide an ideal solution for transferring data among computers. They are becoming increasingly important for Ethernet applications requiring bit rates in excess of 1 Gb/s.

The geometrical description aproximates to the real results but it is truly valid when the core radius a is much larger than the light wavelength λ . When the two become comparable, it is preferable and even necessary, to use the wave-propagation theory.

2.1.2 Wave Propagation Theory

The study of the fiber in terms of wave propagation theory is based on the Maxwell formulas explained in [10]. This analysis gives us the wave equation (shown in equation 2.4)

$$\nabla^2\tilde{\mathbf{E}} + n^2(\omega)k_0^2\tilde{\mathbf{E}} = 0, \tag{2.4}$$

where the free-space wave number k_0 is defined as:

$$k_0 = \omega/c = 2\pi/\lambda, \tag{2.5}$$

and λ is the vacuum wavelength of the optical field oscillating at the frequency ω.

Equation 2.4 is solved to obtain the optical modes of step-index fibers. It is referred to a specific solution that satisfies the appropriate boundary conditions and has the property that its spatial distribution does not change with propagation. Fiber modes can be classified as guided modes, leaky modes and radiation modes. It seems obvious that signal transmission in fiber-optic communication systems takes place through the guided modes only. A mode is uniquely determined by its propagation constant β. This constant can be determined solving the equations for the electric and the magnetic field derived from the equation 2.4 [10]. For a given set of parameters we get different values of β and this variable gives us different optical modes. Depending on whether the axial component along z coordinate of the electric field, E_z, or the axial component along z of the magnetic field, H_z, they can

be differentiated: *hybrid modes* (EH or HE), TE modes (where $E_z = 0$) and TM modes (where $H_z = 0$). A different notation LP is sometimes used for weakly guiding fibers for which both E_z and H_z are nearly zero (LP stands for linearly polarized modes). It is important to underline that it is been avoided the correct use of β_{mn} because this is a simple explanation to understand the foundations of the wave propagation theory.

It is useful to introduce a quantity $\tilde{n} = \beta/k_0$, called the mode index or effective index and having the physical significance that each fiber mode propagates with an effective refractive index $\tilde{n}$ whose value lies in the range $n_1 > \tilde{n} > n_2$. It is important to remark that every mode has a *cutoff* situation in which they can not propagate the signal along the waveguide (in our case the fiber). A parameter that plays an important role in determining the cutoff condition is defined as:

$$V = k_0 a (n_1^2 - n_2^2)^{1/2}. \tag{2.6}$$

It is called the *normalized frequency*, or simply the V parameter. The other factors are the same that appear in figure 2.1.

It is also useful to introduce a normalized propagation constant b as:

$$b = \frac{\beta/k_0 - n_2}{n_1 - n_2} = \frac{\tilde{n} - n_2}{n_1 - n_2}. \tag{2.7}$$

Figure 2.4 shows a plot of b as a function of V for a few low-order fiber modes. A fiber with a large value of V supports many modes and below a certain value of V all modes except one (HE_{11}) reach cutoff.

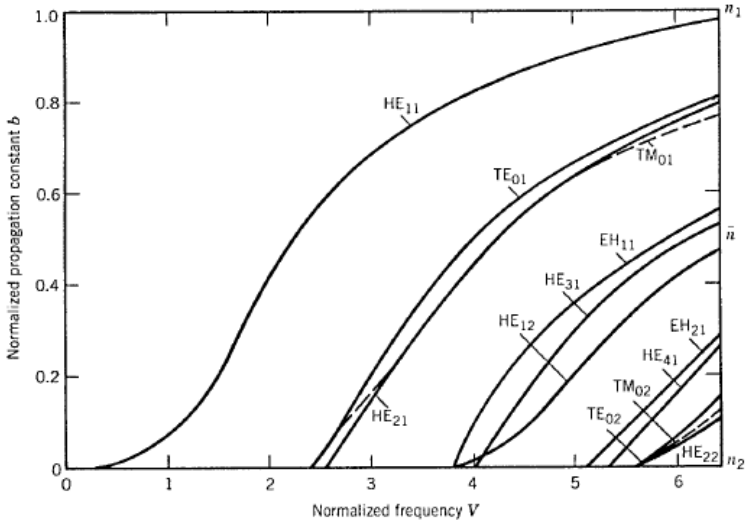

Figure 2.4: Normalized propagation constant b as a function of normalized frequency V for a few low-order fiber modes. The right scale shows the mode index $\tilde{n}$ [10].

Finally, the intermodal dispersion is related to the different mode indices (or group velocities) associated with different modes under the wave propagation theory.

2.2 Single-Mode Fibers, SMF

Single-mode fibers support only the HE_{11} mode, also known as the fundamental mode of the fiber. This mode has no cutoff situation and it is always supported by a fiber. The fiber is designed such that all higher-order modes are cut off at the operating wavelength. The design condition to obtain a single mode fiber is that $V < 2.405$. In such a way the fiber will support only the fundamental HE_{11} mode.

2.2.1 Dispersion in Single-Mode Fibers

The main advantage of single-mode fibers is that intermodal dispersion is absent simply because the energy of the injected pulse is transported by a single mode. However, pulse broadening does not disappear. The group velocity associated with the fundamental mode is frequency dependent because of *chromatic dispersion*. As a result, different spectral components of

the pulse travel at slightly different group velocities, a phenomenon referred to as *group-velocity dispersion* (GVD).

Different dispersion effects that take place in SMF fibers will be explained but as it was explained in the introduction of this project, uncompensated links are suposed to work with and therefore, the dispersion problem will be solved by a DSP at the receiver.

Chromatic Dispersion. Chromatic dispersion arises for two reasons. The first is that the refractive index of silica, is frequency dependent. Thus different frequency components travel at different speeds in silica. This component of chromatic dispersion is termed ***material dispersion***. Although this is the principal component of chromatic dispersion for most fibers, there is a second component, called ***waveguide dispersion*** [11].

To understand the physical origin of waveguide dispersion it must be said that the light energy of a mode propagates partly in the core and partly in the cladding of the fiber (where the effective index of a mode lies between the refractive indices of these parts). If most of the power is contained in the core, the effective index is closer to the core refractive index; if most of it propagates in the cladding, the effective index is closer to the cladding refractive index. The power distribution of a mode between the core and cladding of the fiber is itself a function of the wavelength. More accurately, the longer the wavelength, the more power in the cladding. Thus, even in the absence of material dispersion (so that the refractive indices of the core and cladding are independent of wavelength) if the wavelength changes, the power distribution changes, causing the effective index or propagation constant of the mode to change.

The shape of pulses propagating in optical fiber is not preserved, in general, due to the presence of chromatic dispersion. The parameter governing the evolution of pulse shape is $\beta_2 = d^2\beta/d\omega^2$. β_2 is called the group velocity dispersion parameter (GVD parameter). For most optical fibers, there is a so-called zero-dispersion wavelength, which is the wavelength at which the GVD parameter $\beta_2 = 0$. If $\beta_2 > 0$, the chromatic dispersion is said to be normal. When $\beta_2 < 0$, the chromatic dispersion is said to be anomalous.

Group velocity dispersion is commonly expressed in terms of the chromatic dispersion parameter D that is related to β_2 as:

$$D = -\left(\frac{2\pi c}{\lambda^2}\right)\beta_2 \quad \left[\frac{ps}{nm \cdot km}\right]. \tag{2.8}$$

The chromatic dispersion parameter expresses the temporal spread (ps)

per unit propagation distance (km), per unit pulse spectral width (nm). D also can be written as $D = D_M + D_W$, where D_M is the material dispersion and D_W is the waveguide dispersion, both of which we have explained earlier [11].

Polarization-Mode Dispersion. One important effect that takes place in the SMF fibers is that light launched into the fiber with linear polarization quickly reaches a state of arbitrary polarization due to the *fiber birefringence*. This effect happens because fibers exhibit considerable variation in the shape of their core along the fiber length causing a periodic power exchange between the two polarization components. Moreover, different frequency components of a pulse acquire different polarization states, resulting in pulse broadening. This phenomenon is called *polarization-mode dispersion* (PMD).

Once the main dispersion in SMF have been explained we recall that in our anaylisis we will supose uncompensated links. That is to say, there are not solutions on the fiber to the dispersion (for example the use of Chirped Gaussian Pulses [10]). The DSP is suposed to solve this problem at the end of the fiber.

2.3 Main problems of the fiber in our system scenario

Optical fibers face up to three instrinsecal problems. One of them has already been explained, it is the dispersion. The other two problems are fiber losses and nonlinear optical effects.

2.3.1 Fiber Losses

Fiber losses represent another limiting factor because they reduce the signal power reaching the receiver. As optical receivers need a certain minimum amount of power for recovering the signal accurately, the transmission distance is inherently limited by fiber losses [10].

Attenuation Coefficient. Considering P_{in} as the power launched at the input end of a fiber of a length L, the output power, P_{out} is:

$$P_{out} = P_{in} exp(-\alpha L), \tag{2.9}$$

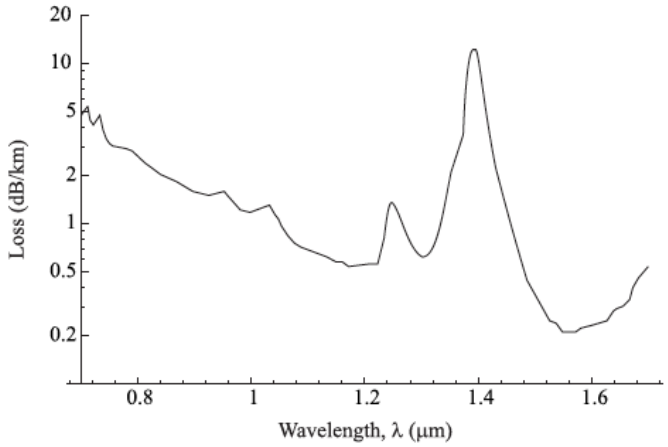

Figure 2.5: Attenuation loss in silica as a function of wavelength.

where α is the fiber-loss parameter expressed in [dB/km]. This parameter is also known as attenuation coefficient. The two main loss mechanisms in optical fibers are *material absorption* and *Rayleigh scattering*.

Material Absorption Material absorption includes absorption by silica as well as the impurities in the fiber. The material absorption of pure silica is negligible in the entire 800-1600 nm band that is used for optical communication systems. The reduction of the loss due to material absorption by the impurities in silica has been very important in making optical fiber the remarkable communication medium that it is today. The loss has now been reduced to negligible levels at the wavelengths of interest for optical communication (so much so that the loss due to Rayleigh scattering is the dominant component in today's fibers in all three wavelength bands used for optical communication). These bands are:

- 'First' band at 800 nm.
- 'Second' band at 1300 nm.
- 'Third' band at 1550 nm.

The attenuation for the range of those bands is represented in figure: 2.5. We see that the loss has local minima at these three wavelength bands with typical losses of 2.5, 0.4, and 0.25 dB/km.

The usable bandwidth of fiber in most of today's long-distance networks is limited by the bandwidth of the erbium-doped fiber amplifiers (they will

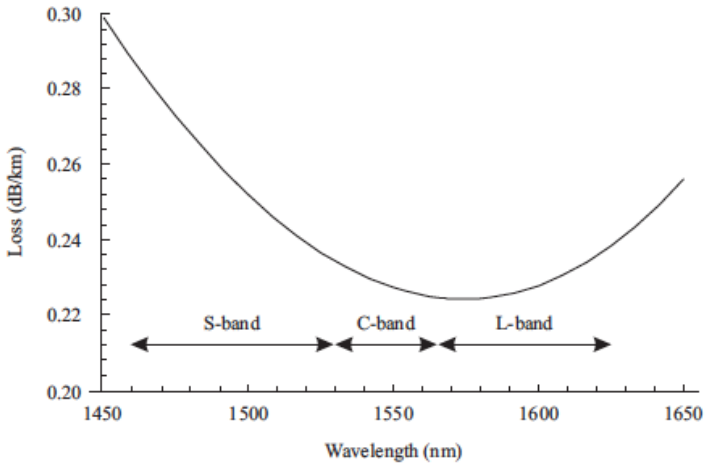

Figure 2.6: The three bands, S-band, C-band, and L-band, within the low-loss region around 1550 nm in silica fiber.

be explained on the next chapter), rather than by the bandwidth of the silica fiber. Based on the availability of amplifiers, the low-loss band at 1550 nm is divided into three regions, as shown in Figure: 2.6. The middle band from 1530 to 1565 nm is the conventional or C-band where WDM systems have usually operated. WDM systems are those which are based on wavelength-division multiplexing, that is to say, a technology which multiplexes a number of optical carrier signals onto a single optical fiber by using different wavelengths of laser light. The band from 1565 to 1625 nm, which consists of wavelengths longer than those in the C-band, is called the L-band and is today being used in high-capacity WDM systems. The band below 1530 nm, consisting of wavelengths shorter than those in the C-band, is called the S-band.

Rayleigh Scattering. Rayleigh scattering is a fundamental loss mechanism arising from local microscopic fluctuations in density. Silica molecules move randomly in the molten state and freeze in place during fiber fabrication. Density fluctuations lead to random fluctuations of the refractive index on a scale smaller than the optical wavelength λ . Light scattering in such a medium is known as Rayleigh scattering. The intrinsic loss of silica fibers from Rayleigh scattering can be written as:

$$\alpha_R = C/\lambda^4, \tag{2.10}$$

where the constant C (Rayleigh scattering coefficient) is in the range 0.7-0.9 (dB/km) μm^4, depending on the constituents of the fiber core.

On the last chapter we will explain the Ryaleigh Scattering limitations in distributed Raman Pre-amplifiers.

Waveguide Imperfections. Imperfections at the core-cladding interface (e.g., random core-radius variations) can lead to additional losses which contribute to the net fiber loss. Such variations can be kept below 1%, and the resulting scattering loss is typically below 0.03 dB/km.

Bends in the fiber constitute another source of scattering loss. Bending leads to "leakage" of power out of the fiber core into the cladding, resulting in additional loss. A bend is characterized by the bend radius (the radius of curvature of the bend). The "tighter" the bend, the smaller the bend radius and the larger the loss.

A major source of fiber loss, particularly in cable form, is related to the random axial distortions that invariably occur during cabling when the fiber is pressed against a surface that is not perfectly smooth. Such losses are referred to as *microbending losses*. Microbends cause an increase in the fiber loss for both multimode and single-mode fibers and can result in an excessively large loss.

Finally, other sources of optical loss must be taken into account. For example, those related to splices and connectors used in forming the fiber link.

2.3.2 Nonlinear Optical Effects

At higher bit rates such as 10 Gb/s and above and/or at higher transmitted powers, it is important to consider the effect of nonlinearities [11].

In the case of WDM systems, nonlinear effects can become important even at moderate powers and bit rates. There are two categories of nonlinear effects. The first arises due to the interaction of light waves with phonons (molecular vibrations) in the silica medium (one of several types of scattering effects has been already showed, Rayleigh scattering). The two main effects in this category are *stimulated Brillouin scattering* (SBS) and *stimulated Raman scattering* (SRS). In scattering effects, energy gets transferred from one light wave to another wave at a longer wavelength (or lower energy). The lost energy is absorbed by the molecular vibrations, or phonons, in the medium. This second wave is called the *Stokes* wave. The first wave can be thought of as being a "pump" wave that causes amplification of the Stokes wave. As the pump propagates in the fiber, it loses power and the Stokes wave gains power.

The other nonlinear effects arises due to the dependence of the refractive index on the intensity of the applied electric field, which in turn is proportional to the square of the field amplitude. The most important nonlinear effects in this category are *self-phase modulation* (SPM) and *four-wave mixing* (FWM).

Before explaining this effects other parameters will be introducided, we are talking about the *effective length and area*.

- Effective length. As the signal propagates along the link, its power decreases because of fiber attenuation. Thus, most of the nonlinear effects occur early in the fiber span and diminish as the signal propagates. Modeling this effect can be quite complicated, but in practice, a simple model that assumes that the power is constant over this effective length L_{eff} has proved to be quite sufficient in understanding the effect of nonlinearities. The expression for L_{eff} is:

$$L_{eff} = \frac{1 - exp(-\alpha L)}{\alpha}, \tag{2.11}$$

  where α is the well known fiber attenuation and L the actual link length.

- Effective area. The effect of a nonlinearity also grows with the intensity in the fiber. For a given power, the intensity is inversely proportional to the area of the core. Since the power is not uniformly distributed within the cross section of the fiber, it is convenient to use this effective cross-sectional area A_{eff} related to the actual area A and the cross-sectional distribution of the fundamental mode $F(r, \theta)$, as

$$A_{eff} = \frac{\left(\int_r \int_\theta |F(r,\theta)|^2 r dr d\theta\right)^2}{\int_r \int_\theta |F(r,\theta)|^4 r dr d\theta}, \tag{2.12}$$

  where r and θ denote the polar coordinates. For example, the effective area of SMF is around $85\mu m^2$.

The reason why these parameters have been explained is that they will be used on the simulations of the last chapter. At the moment, we focus on the nonlinear effects.

Stimulated Brillouin Scattering, SBS. The phonons involved in the scattering interaction are acoustic phonons, and the interaction occurs over a very narrow line width. SBS does not cause any interaction between different wavelengths, as long as the wavelength spacing is much greater than 100

MHz, which is typically the case. SBS can, however, create significant distortion within a single channel. SBS produces gain in the direction opposite to the direction of propagation of the signal. Thus it depletes the transmitted signal as well as generates a potentially strong signal back toward the transmitter. In this case, the pump wave is the signal wave, and the Stokes wave is the unwanted wave that is generated due to the scattering process. Each wave has its own power due to the SBS generated intensity.

Self-Phase Modulation, SPM. SPM arises because the refractive index of the fiber has an intensity-dependent component. This nonlinear refractive index causes an induced phase shift that is proportional to the intensity of the pulse. Thus different parts of the pulse undergo different phase shifts, which gives rise to chirping of the pulses. Pulse chirping in turn enhances the pulse-broadening effects of chromatic dispersion. This chirping effect is proportional to the transmitted signal power so that SPM effects are more pronounced in systems using high transmitted powers. The SPM-induced chirp affects the pulsebroadening effects of chromatic dispersion and thus is important to consider for high-bit-rate systems that already have significant chromatic dispersion limitations.

Four-Wave Mixing. In WDM systems using the angular frequencies ω_1,...,ω_n, the intensity dependence of the refractive index not only induces phase shifts within a channel but also gives rise to signals at new frequencies such as $2\omega_i - \omega_j$ and $\omega_i + \omega_j - \omega_k$. This is the Four-Wave mixing effect and it is independent of the bit rate but is critically dependent on the channel spacing and fiber chromatic dispersion. Decreasing the channel spacing increases the four-wave mixing effect, and so does decreasing the chromatic dispersion. Thus the effects of FWM must be considered even for moderate-bit-rate systems when the channels are closely spaced and/or dispersion-shifted fibers are used.

2.4 Nonlinear Optical effects. Stimulated Raman Scattering, SRS

In this section the main theoretical point of this project will be explained and therefore it is been considered more suitable to dedicate a different section for its explanation.

It is important to show the difference between spontaneous and stimulated Raman scattering. If in the spectral bandwidth where the Raman

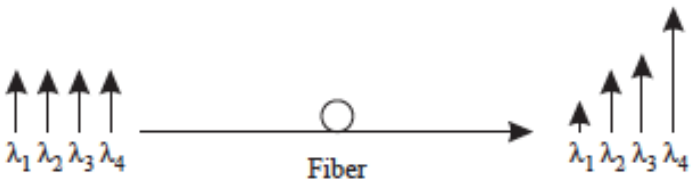

Figure 2.7: The effect of SRS. Power from lower-wavelength channels is transferred to the higher-wavelength channels.

Scattering takes place there are no propagating photons, new photons are generated, and this is the *spontaneous Raman Scattering*. But, if in the spectral bandwidth where the Raman Scattering takes place there is a flow of propagating photons (propagating optical field), energy from the pump photons is transferred to the propagating optical field and this is the *stimulated Raman scattering*.
Well, if two or more signals at different wavelengths are injected into a fiber, SRS causes power to be transferred from the lower-wavelength channels to the higher wavelength channels. Figure 2.7 shows this effect. The explanation of why are lower wavelength photon who give the power to higher wavelength photon is very simple; the energy, E, of a photon at a wavelength λ is: $E = \frac{hc}{\lambda}$ where h is Planck's constant and c is light speed in vacuum. Thus, a photon of lower wavelength has a higher energy.

As we will see, this coupling of energy from a lower wavelength signal to a higher-wavelength signal is a fundamental effect that is also the basis of optical amplification and lasers. In special for us, Raman amplifiers.

Unlike SBS, SRS is a broadband effect. Figure 2.8 shows its gain coefficient as a function of wavelength spacing. The peak gain coefficient g_R is approximately 6 x 10^{-14} m/W at 1550 nm, which is much smaller than the gain coefficient for SBS (4 x 10^{-11} m/W, independent of the wavelength).

So, channels up to 150 THz (125 nm) apart are coupled due to SRS, with the peak coupling occurring at a separation of about 13 THz. Coupling occurs for both copropagating and counterpropagating waves and also, it occurs between two channels only if power is present in both channels. Thus the SRS penalty is reduced when chromatic dispersion is present because the signals in the different channels travel at different velocities, reducing the probability of overlap between pulses at different wavelengths at any point in the fiber. Typically, chromatic dispersion reduces the SRS effect by a factor of 2.

Physically speaking, the beating of the pump with the scattered light in

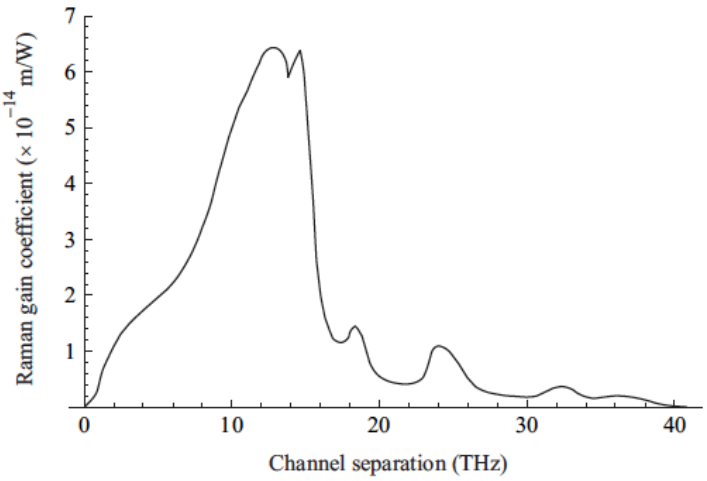

Figure 2.8: SRS gain coefficient as a function of the difference between the pump and the signal frequency for pure silica fibers.

these two directions creates a frequency component at the beat frequency $\omega_p - \omega_s$ (referring to the signal wave as the pump wave and to the unwanted wave generated by the scattering process as Stokes wave), which acts as a source that derives molecular oscillations. Since the amplitude of the scattered wave increases in response to these oscillations, a positive feedback loop sets in. It can be proved that for forward SRS, the feedback process is governed by:

$$\frac{dI_p}{dz} = -g_R I_p I_s - \alpha_p I_p, \tag{2.13}$$

$$\frac{dI_s}{dz} = g_R I_p I_s - \alpha_s I_s, \tag{2.14}$$

In the case of backward SRS, a minus sign is added in front of the derivative in equation 2.14. The threshold power P_{th} is defined as the incident power at which half of the pump power is transferred to the Stokes field at the output end of a fiber of length L. It can be aproximated as:

$$P_{th} \approx \frac{16\alpha A_{eff}}{g_R}. \tag{2.15}$$

Finally, we will introduce the variable named *capture factor*, R. This variable measures the number of photon that are back-scattered. Figure 2.9 shows a very simple representation of the effect.

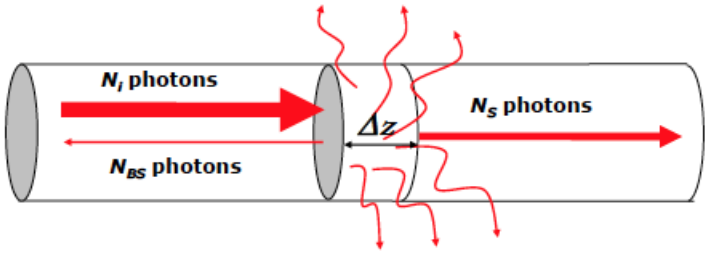

Figure 2.9: Stimulated Raman Scattering effect of rcapture factor explanation.

Considering the following equations:

$$dN_S = \alpha_R dN_i, \tag{2.16}$$

$$dN_{BS} = RdN_S = -R\alpha_R dN_i, \tag{2.17}$$

the capture factor, R, can be easily understood as the portion of input photons (N_i) that are back-scattered (N_{BS}). Usually it is specified in units of dB considering a typycal value: -30dB.

Chapter 3

Optical Amplifiers

The main function of an optical amplifier is to amplify the optical signal directly without requiring its conversion to the electric domain. They are one of the main components in optical communications becuse in an optical communication system, the optical signals from the transmitter are attenuated by the optical fiber as they propagate through it. Other optical components, such as multiplexers and couplers, also add loss. After some distance, the cumulative loss of signal strength causes the signal to become too weak to be detected. Before this happens, the signal strength has to be restored. However, amplifiers introduce additional noise, and this noise acumulates as the signal goes on until the end of the system.

3.1 Basic concepts

In this work we will study three kinds of amplification, the first one caused by EDFA's, another one caused by Raman and the last one due to HFA's amplifiers (focusing on the last one as main amplification in our system scenario).
First of all we will explain the main characteristics of optical amplification as they are explained in [10]. Once we define each kind of amplifier we will focus on its own characteristic.

Most optical amplifiers amplify incident light through stimulated emission. Its main characteristic is the optical gain realized when the amplifier is pumped (optically or electrically) to achieve population inversion (this concept should be keep in mind until it is explained). The optical gain, in general, depends not only on the frequency (or wavelength) of the incident signal, but also on the local beam intensity at any point inside the amplifier. To illustrate the main characteristics we consider the case in which the gain

medium is modeled as a homogeneously broadened two-level system. The gain coefficient of such a medium can be described as:

$$g(\omega) = \frac{g_0}{1 + (\omega - \omega_0)^2 T_2^2 + P/P_s}, \tag{3.1}$$

where g_0 is the peak value of the gain,ω is the optical frequency of the incident signal, ω_0 is the atomic transition frequency, and P is the optical power of the signal being amplified. The saturation power P_s depends on gain-medium parameters such as the fluorescence time T1 and the transition cross section. The parameter T2, known as the dipole relaxation time, is typically quite small (<1 ps). The fluorescence time T1, also called the population relaxation time, varies in the range 100 ps - 10 ms, depending on the gain medium.

3.1.1 Amplifier Gain

We define the amplification factor as:

$$G = \frac{P_{out}}{P_{in}} \tag{3.2}$$

where P_{in} and P_{out} are the input and output powers of the signal being amplified. We can also deduct the optical power at a distance z from the input end:

$$P(z) = P_{in} exp(gz). \tag{3.3}$$

By noting that $P(L) = P_{out}$ and using the amplification factor of equation 3.2, the amplification factor for an amplifier of length L is given by

$$G(\omega) = exp[g(\omega)L]. \tag{3.4}$$

3.1.2 Amplifier Noise

All amplifiers degrade the signal-to-noise ratio (SNR) of the amplified signal because of spontaneous emission that adds noise to the signal during its amplification. The SNR degradation is quantified through a parameter F_n, called the amplifier noise figure.

$$F_n = \frac{(SNR)_{in}}{(SNR)_{out}}, \tag{3.5}$$

where SNR refers to the electric power generated when the optical signal is converted into an electric current.

3.2 Erbium-doped fiber amplifier, EDFA

The Erbium-doped fiber amplifier, EDFA, is one of the well-known doped fiber amplifiers (DFA's). These amplifiers use a doped optical fiber as a gain medium to amplify an optical signal (in the case of the EDF it is a fiber doped with Er^{3+}). Erbium-doped fiber amplifiers have attracted the most attention because they operate in the wavelength region near 1550 nm. Their deployment in WDM systems revolutionized the field of fiber-optic communications and led to lightwave systems with capacities exceeding 1 Tb/s.

The structure of the EDFA can be seen on the next figure:

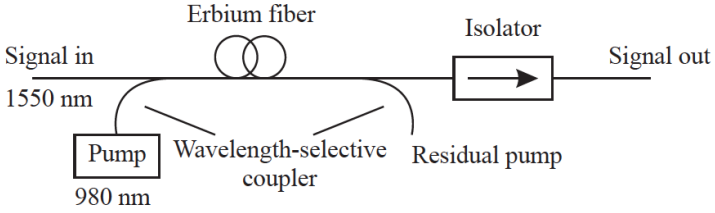

Figure 3.1: An example of erbium-doped fiber amplifier with pump at 980 nm.

The signal to be amplified and a pump laser are multiplexed into the doped fiber, and the signal is amplified through interaction with the doping ions. In order to combine the output of the pump laser with the input signal, the doped fiber is preceded by a wavelength-selective coupler. At the output, another wavelength-selective coupler may be used if needed to separate the amplified signal from any remaining pump signal power. Usually, an isolator is used at the input and/or output of any amplifier to prevent reflections into the amplifier.

3.2.1 Stimulated Emission

The EDFA is based on the physical phenomenon called stimulated emission of radiation by atoms in the presence of an electromagnetic field (in our case this field will be an optical signal). Any physical system (for example, an atom) is found in one of a discrete number of energy levels. Accordingly, consider an atom and two of its energy levels, E_1 and E_2, with $E_2 > E_1$. An electromagnetic field whose frequency f_c satisfies $hf_c = E_2 - E_1$ induces

transitions of atoms between the energy levels E_1 and E_2 (where h is Planck's constant). We describe this process on the next figure:

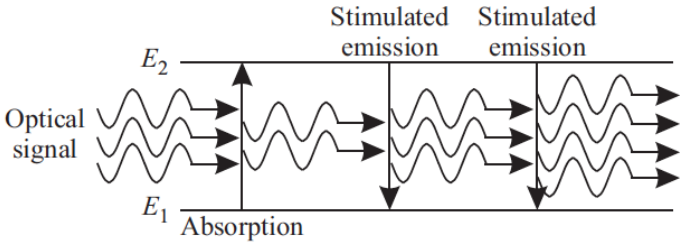

Figure 3.2: Stimulated emission and absorption in an atomic system with two energy levels.

$E_1 \rightarrow E_2$ transitions are accompanied by absorption of photons from the incident electromagnetic field. $E_2 \rightarrow E_1$ are accompanied by the emission of photons of energy hf_c, the same energy as that of the incident photons. This emission is called stimulated emission. Then the effect we are looking for, amplification, happens when stimulated emission were to dominate over absorption (because we would have a net increase in the number of photons of energy hf_c and the amplification of the signal). It follows from the theory of quantum mechanics that the rate of the $E_1 \rightarrow E_2$ transitions per atom equals the rate of the $E_2 \rightarrow E_1$ transitions per atom. If the populations (number of atoms) in the energy levels E_1 and E_2 are N_1 and N_2, respectively, we have a net increase in power (energy per unit time) of $(N_2 - N_1)rhf_c$. Where r denotes the rate of transmissions per atom. Clearly, for amplification to occur, $N_2 > N_1$. This condition is known as **population inversion**. The reason for this term is that, at thermal equilibrium, lower energy levels are more highly populated, that is, $N_2 < N_1$. Therefore, at thermal equilibrium, we have only absorption of the input signal. In order for amplification to occur, we must invert the relationship between the populations of levels E_1 and E_2 that prevails under thermal equilibrium. Population inversion can be achieved by supplying additional energy in a suitable form to pump the electrons to the higher energy level. This additional energy can be in optical or electrical form. In the case of the EDFA, the supply is carried out by the laser pump.

Focusing on the EDFA population inversion, we must say that the energy from the laser pump makes the ionized erbium ions to change to a higher energy level. After that, when a photon from the main signal arrives to the EDFA, causes that the previous excited ion to fall down to a lower energy

level, making a photon free.

On the example of the figure 3.3 we could deduce that all frequencies that correspond to the energy difference between some energy at the E_2 band and some energy at the E_1 band can be amplified. In the case of erbium ions in silica glass, the set of frequencies that can be amplified correspond to the wavelength range 1525-1570 nm. This corresponds to one of the low-attenuation windows of standard optical communications.

3.2.2 ASE Noise

Before explaining the title of this subsection we have to explain another physical process. It is named *spontaneous emission* and it is directly related to the *stimulated emission*. Consider our previous example in figure 3.3 with two energy levels. Independent of any external radiation that may be present, atoms in energy level E_2 transit to the lower energy level E_1, emitting a photon of energy hf_c. The spontaneous emission rate per atom from level E_2 to level E_1 is a characteristic of the system, and its reciprocal, denoted by τ_{21}, is called the *spontaneous emission lifetime*. Thus, if there are N_2 atoms in level E_2, the rate of spontaneous emission is N_2/τ_{21}, and the spontaneous emission power is hf_cN_2/τ_{21}.
These photons are also amplified because the amplifier treats spontaneous emission radiation as another electromagnetic field at the frequency hf_c, and the spontaneous emission also gets amplified, in addition to the incident optical signal. This *amplified spontaneous emission* (ASE) is well known as ASE noise.

It can be demonstrated that the power of the ASE noise at the ouput of the EDFA is described as:

$$P_{ASE,EDFA} = 2n_{sp}hf_c(G-1)B, \tag{3.6}$$

where n_{sp} is a constant called the spontaneous emission factor, G is the amplifier gain, and B is the optical bandwidth. The value of n_{sp} depends on the level of population inversion within the amplifier. With complete inversion $n_{sp} = 1$, but it is typically higher, around 2 - 5 for most amplifiers.

3.2.3 EDFA Gain

Because of the population levels at the various levels within a band are different, the gain of an EDFA becomes a function of the wavelength. When an EDFA is used in a WDM system, different WDM channels get different

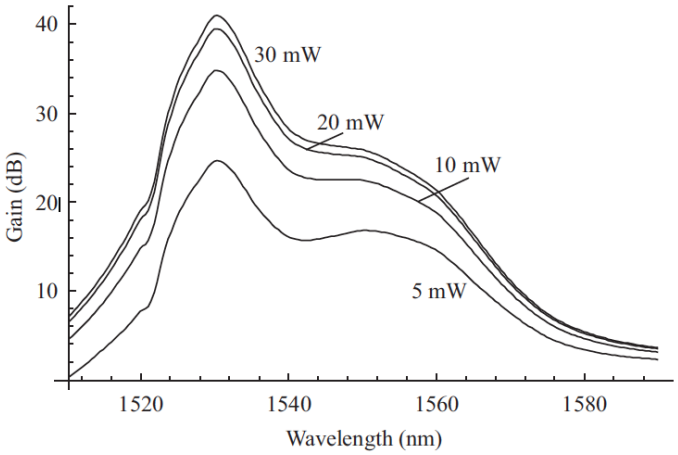

Figure 3.3: Gain of an EDFA as a function of the wavelength for four different values of the pump power.

amplification. To show this effect, an EDFA gain example for a pump at 980 nm and a fiber length of 15 m is represented on the next figure:

The gain of the EDFA is configured on the way it recovers the loss of the fiber. That is to say, if the fiber has a length L [m] and a loss coefficient α [dB/km] the gain will be:

$$G_{EDFA} = \alpha \cdot L\,[dB] \tag{3.7}$$

3.2.4 EDFA Noise Figure

The expression of the Noise Figure for an EDFA is well known as:

$$NF_{EDFA}(f) = \frac{1 + 2n_{sp,EDFA}(f)[G_{EDFA}(f) - 1]}{G_{EDFA}(f)} \tag{3.8}$$

and if $G_{EDFA}(f) >> 1$ then $NF_{EDFA}(f) \approx 2n_{sp,EDFA}$ where n_{sp} is the spontaneous emission factor that governs the spectral density os the noise at the output of the device. This density will be very usefull on the following sections and we already define it:

$$S_{ASE}^{EDFA}(f) = hfn_{sp,EDFA}(f)[G_{EDFA} - 1] \tag{3.9}$$

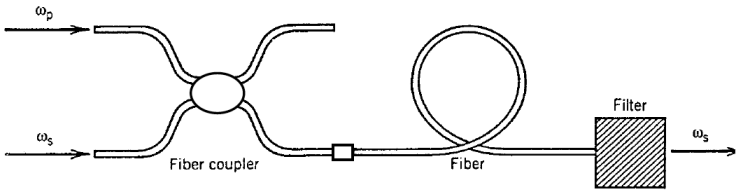

Figure 3.4: Schematic of a fiber-base Raman amplifier

3.3 Raman Amplifiers

The Raman Amplifiers are based on the non-linear effect already explained in section 2.4 called stimulated Raman scattering (SRS). This non-linearity is exploited to provide the amplification.

As it is explained in [10], whereas in the case of stimulated emission an incident photon stimulates emission of another identical photon without losing its energy, in the case of SRS the incident pump photon gives up its energy to create another photon of reduced energy at a lower frequency (inelastic scattering); the remaining energy is absorbed by the medium in the form of molecular vibrations (optical phonons). Thus, Raman amplifiers must be pumped optically to provide gain. Another difference is that we can use the Raman effect to provide gain at any wavelength (while the EDFA gain is 'centered' at 1550 nm).

On figure 3.4 we see how a Raman amplifier can be deployed with an optical fiber.

The pump and signal beams at frequencies ω_p and ω_s are injected into the fiber through a fiber coupler. The energy is transferred from the pump beam to the signal beam through SRS as the two beams copropagate inside the fiber. The pump and signal beams counterpropagate in the backward-pumping configuration.

3.3.1 Raman Gain

As it was explained in section 2.4 the Raman gain spectrum is fairly broad, and the peak of the gain is centered about 13 THz below the frequency of the pump signal used. However we recover the figure presented previously to make easier the explanation. It is the figure 3.5.

To have the maximum gain efficiency we should use a wavelength separation around 100 nm. That is to say, the raman pump frequency should be 13 THz above the main signal frequency (100 nm below). For instance, to have a RA at 1550 nm a pump at 1450 nm should be used. The pump can co-

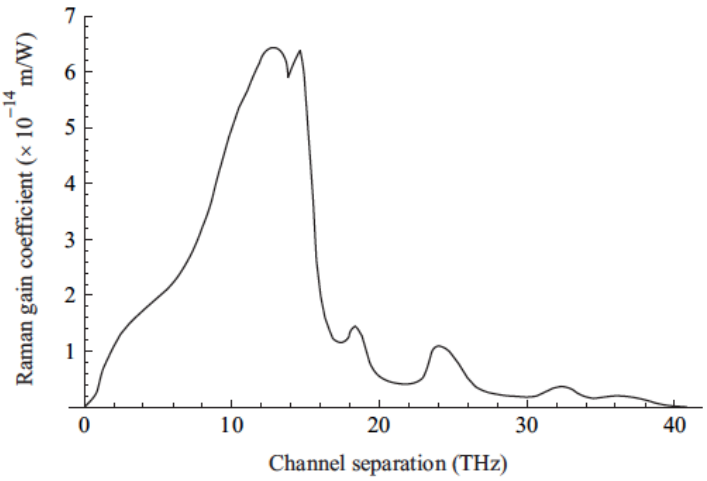

Figure 3.5: SRS gain coefficient as a function of the difference between the pump and the signal frequency for pure silica fibers.

or counter-propagate with respect to the propagation direction of the signal [12].
To describe the performance of a RA, the on-off gain is used. The on-off gain is the ratio of the power at the output to the power at the input of the fiber-span divided by the fiber loss. It is represented on the figure 3.6.

Referring to this figure, the on-off gain can be expressed as:

$$G_{on-off} = \frac{P\left(L_{span}\right)}{P(0)} \frac{1}{exp\left\{-\alpha_s L_{span}\right\}}, \tag{3.10}$$

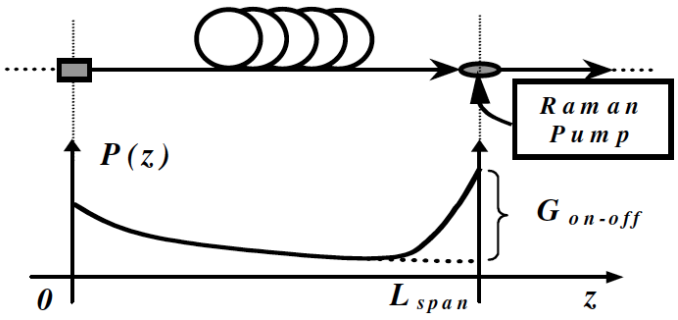

Figure 3.6: Representation of the evolution of the signal power (solid line) in a fiber-span pumped with a counter-propagating single-pump and the G_{on-off}.

and it is the gain measurable at the output of the fiber turning on and off the Raman pump.

For a single-pump configuration, and for a small-signal regime the on-off gain has the following expression:

$$G_{on-off}(f) = exp\left\{C_R(f)P_{pump}\frac{1-exp(-\alpha_p L_{span})}{\alpha_p}\right\} \tag{3.11}$$

where P_{pump} is the pump power at the beginning (counter-propagating pump) or at the end (co-propagating pump) of the fiber span, α_p is the fiber-loss coefficient at the pump frequency f_{pump} and C_R is the fiber efficiency, defined as:

$$C_R(f) = \frac{1}{k_{pol}}\frac{g_R/f_{pump} - f}{A_{eff}} \cdot \frac{f_{pump}}{f_{ref}} \tag{3.12}$$

g_R is the Raman efficiency at f_{ref} (it is different to the Raman amplifier efficieny), A_{eff} is the effective area of the fiber and f is the frequency where the gain is measured. k_{pol} is a factor that takes into account the polarization of the pump with respect to the signal polarization. If the pump is completely depolarized $k_{pol} = 2$, if the pump and the signal are aligned in terms of polarization $k_{pol} = 1$.

The noise provided by the Raman amplifier has to be also considered and the ASE noise is generated along the complete length of the fiber (because the distribution of the Raman amplifieres). The expression of the spectral density at the end of the fiber is:

$$S_{ASE}^{RA}(f) = hfC_R(f)G_{on-off}(f)exp\left\{-\alpha_s L_{span}\right\}\int_0^{L_{span}} P_{pump}(z)\cdot$$

$$exp\left\{-\int_0^z \left[C_R(f)P_{pump}(\xi) - \alpha_s\right]d\xi\right\}dz + \sum_{i=1}^{+\infty} r^i S_{ASE}^{(i)}(f) \tag{3.13}$$

where h is the Planck's constant and $r = R\alpha_s$ takes into account the Rayleigh back-scattering. R is the Capture Factor that measures the strength of the Rayleigh back-scattering. The sum of $S_{ASE}^{(i)}(f)$ takes into account of the infinite additive noise components due to the Rayleigh Back-scattering [12].

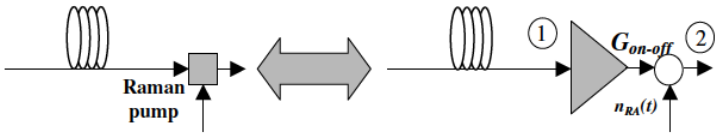

Figure 3.7: Equivalent configuration. The equivalent Noise-Figure definition is based on the ratio between the SNR's in the virtual point 1 and the one in 2.

3.3.2 Raman Noise Figure

Considering the Noise Figure definition in equation 3.5, the Noise-Figure for Raman amplifiers can be described as:

$$NF(f) = \frac{1}{exp\{-\alpha_s L\} G_{on-off}(f)} \left(1 + 2\frac{S_{ASE}(f)}{hf}\right) \tag{3.14}$$

The problem of this equation is that can not be used to compare it with the Noise Figure of the EDFA due to the different distributions of both amplifiers so as the different gain produced by them. Two possibilities might be employed to make this comparison. As it is explained in [12] one solution is to base the Noise-Figure definition on the equivalent configuration of RA which is represented on the figure 3.7

Making this configuration the NF of the Raman amplifier can be expressed:

$$NF_{RA}(f) = \frac{1 + 2n_{sp,RA}(f)\lfloor G_{on-off}(f) - 1\rfloor}{G_{on-off}(f)} \tag{3.15}$$

The other possibility to compare the EDFA and the Raman amplifier is to have in account the non-linear weight K_{NL}. This variable takes into account of the impact of the non-linearties in RA and EDFA based systems and it can be measured using the *overall non-linear phase-shift*:

$$K_{NL} = \gamma \int_0^{L_{link}} P(z)dz[rad] \tag{3.16}$$

where γ is the non-linear coefficient.

Calculating this weight for each amplifier, imposing $K_{NL}^{RA} = K_{NL}^{EDFA} = K_{NL}$ and assuming a single-span link and receiver preamplifier (RA or EDFA) that completely recovers the fiber loss, $G_{EDFA} = G_{RA} = G = exp{+}\alpha_s L_{span}$, we will obtain that:

$$SNR_{EDFA} = \frac{P_{in}^{EDFA}}{n_{sp}^{EDFA}(G-1)hfB_n} \tag{3.17}$$

$$SNR_{RA} = SNR_{EDFA}\frac{n_{sp}^{EDFA}}{n_{sp}^{RA}}\frac{L_{eff}^{EDFA}}{L_{eff}^{RA}} \tag{3.18}$$

3.3.3 Raman amplifier efficiency

Raman efficiency can be considered following the next question: How much gain does the amplifier achieve using the pump power? Expressing that question in mathematical terms:

$$\eta_{RA} = \frac{G_{on-off,dB}^{max}}{P_{pump,0}} = 18.86 \cdot \frac{C_R^{max}}{\alpha_p^{dB}} \left[\frac{dB}{W}\right], \tag{3.19}$$

where C_R has already been explained and α_p^{dB} is the attenuation that affects to the Raman pump. Usually efficiency is: 31< η_{RA} <44 dB/W.

To get to this mathematical solution, figure 3.8 shows a scheme with the formulas used [13].

$$G_{on-off,dB}(f) = 10\log_{10} e \cdot C_R(f) P_{pump,0} \frac{1-\exp[-\alpha_p L_{span}]}{\alpha_p}$$

$$G_{on-off,dB}^{max} = 10\log_{10} e \cdot C_R^{max} P_{pump,0} \frac{1-\exp[-\alpha_p L_{span}]}{\alpha_p} \leq 10\log_{10} e \cdot \frac{C_R^{max}}{\alpha_p} \cdot P_{pump,0}$$

$$\alpha_p^{dB} = 10\log_{10} e \cdot \alpha_p \qquad G_{on-off,dB}^{max} \leq (10\log_{10} e)^2 \cdot \frac{C_R^{max} P_{pump,0}}{\alpha_p^{dB}}$$

$$G_{on-off,dB}^{max} \leq 18.86 \cdot \frac{C_R^{max} P_{pump,0}}{\alpha_p^{dB}}$$

Figure 3.8: Mathematical formulas used to get to Raman Amplifier Efficiency

3.4 Hybrid Raman/Erbium-Doped Fiber Amplifiers (HFA)

Once we have seen the main characteristics of the EDFA and the Raman amplifiers and how we could compare its perfomance we focus the benefits of the 'mixed' use of the EDFA and the Raman amplifier. On this project

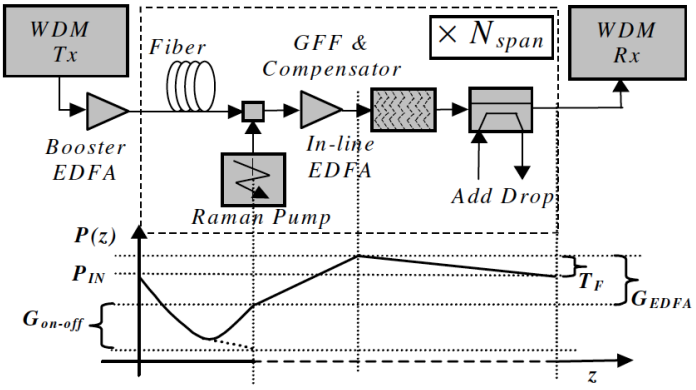

Figure 3.9: The system scenario analyzed in order to explain the HFA and its optimal configuration. The lower part of the figure shows the power-profile along each of the periods.

we will focus on the following system scenario represented in figure 3.9 and we will show this scheme and others very similar depending on what the explanation will be about.

In this case, we consider $N_{span} = 1$ and therefore the total link length will be: $L_{TOT} = L_{span}$ where this span will be backward pumped to obtain a Raman on-off gain, G_{on-off}. Each fiber is followed by an EDFA with gain G_{EDFA}, a Gain Flattening Filter (GFF), a Dispersion Compensator (DC) and an Add/Drop Multiplexer (ADM). We assume that the amplifier gains are set so as to perfectly compensate for the loss of the passive components and of the fiber in each span, yielding:

$$exp\left\{-\alpha_s L_{span}\right\} G_{on-off} T_F G_{EDFA} = 1 \tag{3.20}$$

where α_s is the fiber loss coefficient and T_F is the loss introduced by all passive components. A Raman pump with the proper power level is injected to get the required gain G_{on-off}. Under these assumptions, we found that the SNR at the output of the system has the following expression:

$$SNR = \frac{P_{IN}}{hfB_n} \cdot \frac{exp\left\{-\alpha_s \frac{L_{TOT}}{N_{span}}\right\}}{N_{span}\left(n_{eq}^{RA} + \frac{n_{eq}^{EDFA}}{G_{on-off}}\right) t} \tag{3.21}$$

where P_{IN} is the average power-per-channel at the input of each fiber span, γ is the non-linear coefficient of the fiber, h is Planck's constant, f is the optical carrier frequency, B_n is the bandwidth over which noise is

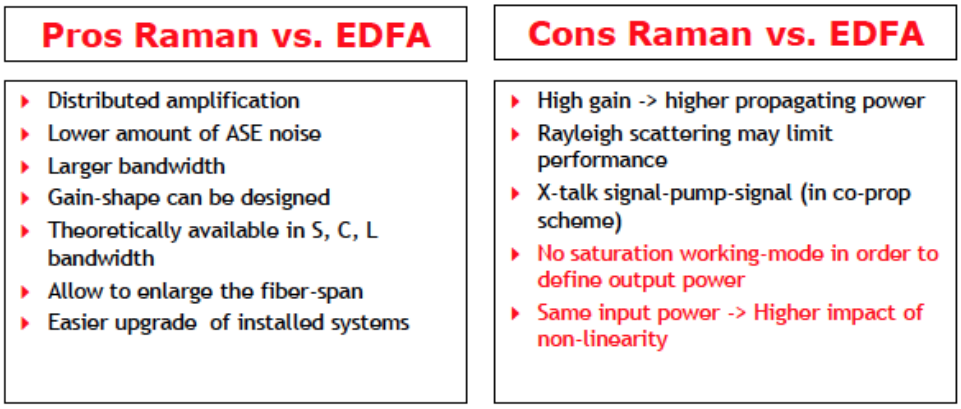

Figure 3.10: Pros and cons of Hybrid Raman Amplifiers.

integrated and n_{eq}^{RA} and $n_{eq}^{EDFA}$are the equivalent input noise factors for the in-line RA's and EDFA's. They are described as:

$$n_{eq} = n_{sp}\frac{G}{G-1} \tag{3.22}$$

Finally, it must be taken into account the physical process known as *pump depletion*. This effect, due to the SRS for high power pumps make the counter-propagating pump to deplete along the fiber.

To sum up, a table with the pros and cons of using Hybrid Raman amplifiers is showed in figure 3.10

The main objective of this project is to find the best configuration that optimizates the SNR of 3.21 (and therefore the system performance) for $N_{span} = 1$. We will find out how to make this possible in the last section but it is necessary to introduce the concept of the GN model.

Chapter 4

The GN Model

4.1 The GN Model reference formula

Nowadays, green-field installations as well as overhauling and upgrading of the existing links are being carried out through what is known as 'uncompensated' transmission (UT) technique. The UT technique is based in the avoidance of the optical dispersion compensation, or dispersion management (DM), on the fiber. This is possible because of the advent of coherent-detection systems supported by digital-signal-processing (DSP) which are able to compensate the dispersion at the receiver. It has been recognized that certain perturbative models of fiber non-linear propagation, which did not work satisfactorily with DM, can instead provide rather accurate system performance prediction with UT. In particular, recent re-consideration and extension of earlier modeling efforts has led to the formalization of the so-called Gaussian-Noise (GN) model.

We must take into account the most common modeling assumptions before explaining the GN model. These are:

1. Considering the **non-linearity relatively small** (as a perturbation compared to the useful signal). Thanks to this assumption, we could find approximate analytical solutions to the non-linear Schroedinger equation (NLSE) or the Manakov (ME) equation through the perturbation techniques.

2. "The Signal Gaussianity" assumption. It means that the **transmitted signal behaves as stationary Gaussian noise**. This assumption is not verified at the begining of the transmission but, as the signal propagates along a UT link and gets thoroughly dispersed, it tends to take on an approximately Gaussian-like distribution.

3. The signal disturbance generated by non-linearity (non-linear interference, NLI) behaves as **additive Gaussian noise** (AGN).

The GN-model reference formula (GNRF) provides the power spectral density, PSD, of NLI at the end of the link. We will call this GNLI(f). The GNRF can be written as follows [5]

$$G_{NLI} = \frac{16}{27} \int_{-\infty}^{\infty} \int_{-\infty}^{\infty} G_{WDM}(f_1) G_{WDM}(f_2) G_{WDM}(f_1 + f_2 - f)$$

$$\left| \sum_{n=1}^{N_s} \gamma_n \left[\prod_{k=1}^{n-1} exp\left(\int_0^{L_{s,k}} 3g_k(\zeta) d\zeta \right) exp\left(-3\alpha_k L_{s,k}\right) \Gamma_k^{3/2} \right] \cdot \right.$$

$$\left[\prod_{k=n}^{n-1} exp\left(\int_0^{L_{s,k}} g_k(\zeta) d\zeta \right) exp\left(-\alpha_k L_{s,k}\right) \Gamma_k^{1/2} \cdot \right]$$

$$exp\left(j4\pi^2 \left(f_1 - f\right)\left(f_2 - f\right) \cdot \sum_{k=1}^{n-1} \left[\beta_{2,k} L_{s,k} + \pi \left(f_1 + f_2\right) \beta_{3,k} L_{s,k} + \beta_{DCU,k}\right] \right) \cdot$$

$$\int_0^{L_{s,n}} \left[exp\left(\int_0^z 2g_n\left(\zeta\right) d\zeta - 2\alpha_n z \right) \right.$$

$$exp\left(j4\pi^2 \left(f_1 - f\right)\left(f_2 - f\right) \cdot \right.$$

$$\left. \left. \left[\beta_{2,n} + \pi\beta_{3,n}\left(f_1 + f_2\right)\right] z \right) \right] dz \Big|^2 df_1 f_2, \tag{4.1}$$

The symbols most frequently used in the following are listed here for convenience:
1) z: the longitudinal spatial coordinate, along the link [km]
2) α: fiber field loss coefficient $[km^{-1}]$, such that the signal power is attenuated as $exp(-2\alpha z)$
3)g(z): fiber field gain coefficient $[km^{-1}]$, possibly z-dependent, such that the signal power is amplified over a stretch of z km as $\int_0^z exp\left(2g\left(z'\right)\right) dz'$
4) Γ: lumped power gain, such as due to an EDFA
5) β_2: dispersion coefficient in $[ps^2 \cdot km^{-1}]$
6) β_3: dispersion slope in $[ps^3 \cdot km^{-1}]$
7) β_{DCU}: lumped accumulated dispersion in $[ps^2]$
8) γ: fiber non-linearity coefficient $[W^{-1} \cdot km^{-1}]$

9) L_s: span length [km]
10) L_{eff}: span effective length [km]
11) N_s : total number of spans in a link
12) $G_{WDM}(f)$: PSD of the overall WDM transmitted signal

It is important to clarify that all PSDs are assumed to be unilateral. This equation of the GNRF suppose that:
1) the transmitted signals are dual-polarization
2) a 'span' consists of a single fiber type.

Once we focus on our system scenario we will be able to reduce this equation.

4.2 The IGN Model

There exists another model, known as the 'incoherent GN model', IGN, where the coherent interference among NLI generated in different spans can be completely neglected. The expression of this model is:

$$G_{NLI}^{inc}(f) = \sum_{n=1}^{N_s} G_{NLI}^{n}(f) \tag{4.2}$$

As we can see it can be considered as an accumulative model. The question is, may the IGN model be used expecting good results?
Without going into mathematical details we can say that yes, we can. It is shown at [5] that the difference between the IGN-model, which predicts purely linear NLI accumulation versus Ns , and the GN-model , which predicts slightly super-linear NLI accumulation versus Ns, is quite small.
In essence, the IGN-model can be expected to practically coincide with the GN-model for systems with a large number of channels, that make use of a substantial part of the C-band. In these scenarios, the IGN-model becomes very attractive because its simpler analytical form makes it much easier to handle and exploit than the GN-model. For single-channel systems, the IGN model may be rather inaccurate and should not be used.

4.3 GN model in our system scenario

The next question that concerns us is: How do we use this in a real system model? Well, as we know, the performance of optical coherent systems in linearity is estimated by means of the optical signal-to-noise ratio (OSNR), defined as:

$$OSNR = \frac{P_{ch}}{P_{ASE}} \tag{4.3}$$

where P_{ch} is the average power per channel and P_{ASE} is the power of ASE noise which falls within a conventional optical noise bandwidth B_N . To find the BER, the OSNR is inserted into a suitable formula, which depends on the transmission format, the symbol rate R_s and on the chosen value for B_N. If we make the next suppositions: 1) The $H_{Rx}(f)$ baseband transfer function at the receiver is well fixed.
2) There is not inter-symbol interference (ISI).
3) $B_N = R_s$ (This produce that all OSNR versus BER laws become invariant versus the symbol rate, R_s). 4) ASE and NLI are uncorrelated. As we first explained, NLI noise is assumed to be approximately Gaussian and additive, similar to ASE.

Then, under the three first conditions the OSNR corresponds exactly to the signal-to-noise ratio, SNR, at the electrical receiver. Finally, under all the conditions, the powers of the ASE and NLI noise can be directly added at the denominator of the SNR, rising to a non-lineaity-inclusive SNR:

$$SNR_{NL} = \frac{P_{ch}}{P_{ASE} + P_{NLI}} \tag{4.4}$$

Where P_{NLI} is the power of the NLI noise.

We focus on our system scenario. As it was explained in the introduction of this work, we will work on uncompensated links and, in order to further increase spectral efficiency with respect to standard wavelength division mutiplexing (WDM), we will use the Nyquist-WDM (NyWDM) technique. NyWDM is a wavelength multiplexing technique with channel spacing approaching the symbol-rate and channel spectra shaped in order to minimize cross-talk.
The general layout of the analyzed optical links is described in the figure 4.1. It is a uncompensated multi-span link made up of N_s identical spans. Each span is composed of the transmission fiber with loss coefficient α_{dB} [dB/km], dispersion parameter D [ps/nm/km] and nonlinear coefficient γ[1/W/km]. The length of each span is L_s [km].

The fiber is possibly Raman pumped, with power P_{pump} enabling a net distributed Raman gain G_{RA} [dB] (the so-called on-off gain, equal to zero in case of no pumping), followed by an EDFA with gain G_{EDFA} [dB], recovering the residual loss. We assume *transparent* spans, i.e., $G_{RA} + G_{EDFA} = A_{s,dB}$, where $A_{s,dB}$ [dB] is the span loss, including possible insertion of passive components.
In the previous section we saw that in transmission of multilevel modulation formats over uncompensated links, nonlinearity generates a nonlinear inter-

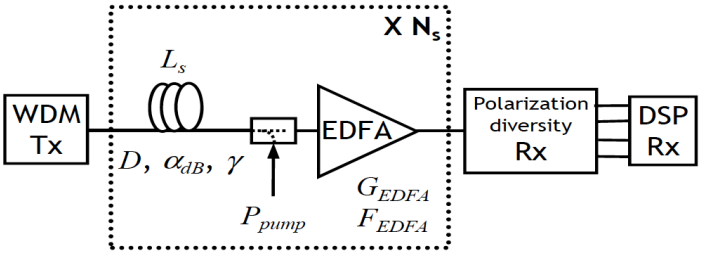

Figure 4.1: Layout of the reference optical link used for the definition of the GN-Model for NLI

ference (NLI). In equation 4.1 it was calculated the PSD of the NLI versus frequency *f*.
We have to say that equation 4.1 is quite general and therefore, we may adapt it to our system scenario. Making the mentioned assumptions:
1) the link is made up of identical spans (the homogeneous link assumption)
2) the loss of each span, including the last one, is exactly compensated for by optical amplification (the transparent link assumption).
The GNRF can be written as:

$$G_{NLI} = \frac{16}{27}\gamma^2 L_{eff}^2 \cdot \int_{-\infty}^{\infty}\int_{-\infty}^{\infty} G_{WDM}(f_1)G_{WDM}(f_2)G_{WDM}(f_1+f_2-f)\cdot$$

$$\rho\left(f_1, f_2, f\right)\cdot\chi\left(f_1, f_2, f\right)df_2df_1. \tag{4.5}$$

The physical interpretation is that the NLI PSD generated at a frequency *f*, that is $G_{NLI}(f)$, is the integrated result of all the 'infinitesimal' non-degenerate 'four wave mixing', FWM, products occurring among any three spectral components at f_1, f_2 and $f_3 = (f_1 + f_2 - f)$.
L_{eff} [km] is the generalized effective length of the fiber spans:

$$L_{eff} = \int_0^{L_s} p_{ch}(z)dz, \tag{4.6}$$

The ρ factor can be considered as the non-degenerate FWM efficiency of the beating (it is normalized so its maximum is 1).

$$\rho(f) = \frac{1}{L_{eff}^2}\left|\int_0^{L_s} p_{ch}(z)exp\{j4\pi^2\beta^2 f^2 z\}dz\right|^2, \tag{4.7}$$

We can see in both equations $p_{ch}(z)$ that is the normalized power evolution with the propagation distance z [km] defined as:

$$p_{ch}(z) = exp\left\{-2\left[\int_0^z \alpha + g(\zeta)d\zeta\right]\right\}, \tag{4.8}$$

The last factor, χ considers the NLI accumulation along the fiber. It has the folloing form:

$$\chi(f_1, f_2, f_3) = \frac{\sin^2\left[2N_s\pi^2(f_1 - f)(f_2 - f)\beta_2 L_s\right]}{\sin^2\left[2\pi^2(f_1 - f)(f_2 - f)\beta_2 L_s\right]}, \tag{4.9}$$

Applying that $R_s = \Delta f$ (due to the channel spacing of the NyWDM transmission) we can make a change of variables based on hyperbolic coordinates, i.e., $\nu^2 = f_1 \cdot f_2$, to equation 4.5. Remembering that the NLI disturbance can be considered as a white random process (because of $G_{NLI}(f)$ variation with f on the center channel is negligible), the aproximation for the NLI power spectral density at the receiver is:

$$G_{NLI} \cong \frac{256}{27}\frac{\gamma^2 L_{eff}^2 P_{ch}^3}{R_s^3}\int_0^{\frac{B_{opt}}{2}} \rho(\nu)\nu\frac{\sin^2\left[2N_s\pi^2\nu^2\beta_2 L_s\right]}{\sin^2\left[2\pi^2\nu^2\beta_2 L_s\right]}\log\left(\frac{B_{opt}}{2\nu}\right)d\nu, \tag{4.10}$$

where $P_{ch}[W]$ is the transmitted power per channel, N_s is the number of spans, R_s [sym/s] is the symbol rate and $B_{opt} = N_{ch} \cdot Rs$ [Hz] is the overall bandwidth occupied by the channel comb.
If the fiber is composed of just one span, then $\chi = 1$.

In our case, the pump produced by the Raman amplifier will be mainly counter-propagating to the main signal. We have to distinguish between depleted and undepleted pump. The last one is well verified when using HFA's, whereby the Raman on-off gain is substantially less than span loss. If this happens, the distributed amplification can be analytically described by the following formula:

$$g(z) = \frac{1}{2}C_R P_{pump} e^{-2\alpha_p(L_s - z)} \tag{4.11}$$

$C_R[1/W/km]$ is the fiber efficiency described as: $\frac{g_R}{A_eff}$ with $g_R = 0.33e-13m/W$, $P_pump[W]$ is the launched un-polarized pump power and α_p [1/km] is the fiber loss at the pump wavelength. We recall from Raman amplifiers section the Raman gain as on-off gain:

$$G_{RA} = 10log_{10}\left\{exp\left[2\int_0^{L_s} g(\zeta)d\zeta\right]\right\} = 10log_{10}(e)C_R Ppump\frac{1-e^{-2\alpha_p L_s}}{2\alpha_p}[dB]. \tag{4.12}$$

Chapter 5

Simulation Results

In this chapter the results of the simulation are presented. These simulations have been carried out using the multi-paradigm numerical computing environment MATLAB® and OptSim™. First a short explanation of the code performance will be done. After that, the theory of the simulations is showed, explaining what are we looking for on this project and why it is been carried out on this way (making some considerations). Finally, the different simulation results are exposed

5.1 Code Performance

To obtain the results, the main part of the simulation has been developed using MATLAB®. In MATLAB® code, four parts can be differentiated:

- **Variable declaration**. In this part, the different variables such as the input power signal are declared. Also, the kind of fiber is defined.
- **Call to OptSim subroutine**. Once the variables are declared, Matlab calls a C function defined on a different file. This function contains the call to the Raman Amplifier subroutine included in OptSim™ program. So, instead of running OptSim to obtain the Raman pump evolution along the fiber, the losses of the pump and the G_{on-off}, this part of the Matlab code gives us the results.
- **Mathematical model**. Using the Raman pump evolution of the previous subroutine, we calculate the input signal evolution along the fiber as:

$$G(z) = exp\left\{-2\alpha z + g(z)\right\}, \tag{5.1}$$

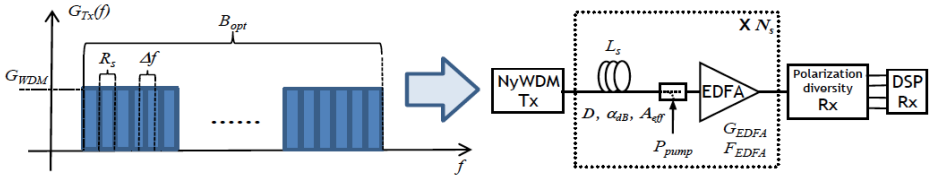

Figure 5.1: Representation of the basic link used on this work.

where g(z) is the distributed Raman amplification. Then, we are able to calculate the NLI efficiency, η [5]. To calculate this parameter different approximations are carried out, obtaining results with an accuracy of 10^{-6}.

- **Obtaining OSNR and saving the results**. Once we obtain the results, the OSNR and other parameters (they will be exposed soon) are calculated. Finally all of them are saved in different files depending on the configuration of the fiber to be showed on different comparisons.

5.2 Analyzed scenario

We focus on the system described in figure 5.1, i.e., transmission over the entire C-band in uniform, uncompensated amplified links. Amplification is hybrid Raman/EDFA (HFA) and recovers completely for the span loss As (G_{HFA}=A_s). We assume the transmitter DSP being able to shape a perfectly squared spectrum for each transmitted channel, so the channel spacing Δf is equal to the symbol rate R_s. Hence, the spectrum of the optical field sent into the link is a flat power spectral density (PSD) G_{WDM} on the entire optical bandwidth B_{opt}=$N_{ch}R_s$, where N_{ch} is the number of channels. Then, the power per channel is P_{ch}=G_{WDM}·R_s.

Recovering the results of the SNR_{NL} from the GN-Model chapter, we can obtain the $OSNR_{NL}$ in R_s including both the ASE noise and the NLI disturbance.

$$OSNR_{NL} = \frac{P_{ch}}{N_s\left(P_{ASE} + \eta P_{ch}^3\right)} = \frac{G_{WDM}}{N_s E_{ph}\left(F_{eq}A_s + E_{ph}^2 \eta R_s^2 \frac{G_{WDM}^3}{E_0^3}\right)} = \frac{N_{ph}}{N_s\left(F_{eq}A_s + \Gamma_{NLI} N_{ph}^3\right)} \tag{5.2}$$

where η is the NLI efficiency [5, 6], N_s is the number of spans, F_{eq} is the HFA noise figure and N_{ph} is the PSD expressed as average number of photons. E_{ph}=hf_0, h is the Plank's constant, f_0 is the center frequency.

Γ_{NLI} is the normalized NLI efficiency. We saw its expression in equation 4.10, but in this case we assume N_s=1 and therefore it assumes the following expression:

$$\Gamma_{NLI} = \frac{256}{27} E_0^2 \gamma^2 \int_0^{\frac{B_{opt}}{2}} \left| \int_0^{L_s} G(z) exp\left\{ j4\pi^2 \beta_2 f^2 z \right\} dz \right|^2 flog\left(\frac{B_{opt}}{2f} \right) df \tag{5.3}$$

where G(z) is described in equation 5.1.

If we want to maximize the reach, the link can be desgined to give a target OSNR depending on the modulation format and Tx/Rx characterization. Therefore, the maximum reach vs. the PSD expressed as average number of photons has the following expression:

$$N_s = \frac{N_{ph}}{OSNR_T(F_{eq}A_s + \Gamma_{NLI} N_{ph}^3}. \tag{5.4}$$

If we compare equations 5.2 and 5.4, they have the same dependence on system parameters, so both the maximum reach $N_{s,max}$ and the maximum $ONSR_{NL}$=$OSNR_{max}$ are given by the same optimal $N_{ph,opt}$, i.e., the value of N_{ph} corresponding to:

$$\frac{\delta N_s}{\delta N_{ph}} = \frac{\delta(OSNR_{NL})}{\delta N_{ph}} = 0. \tag{5.5}$$

In general, due to the Raman pump depletion, both F_{eq} and Γ_{NLI} depend on Nph and therefore the optimization of hybrid amplification needs an accurate characterization of F_{eq} and Γ_{NLI} vs. (P_{pump},N_{ph}) before deriving the optimal working point solving the equation 5.5.

If we consider the system scenario based on HFA amplification, we can suppose the moderate pumping regime roughly corresponding to $P_{pump} \leq$500 mW. In such a scenario pump depletion can be neglected as well as multi-path interference (MPI) and so both F_{eq} and Γ_{NLI} can be assumed constant, yielding:

$$N_{ph,opt} = \frac{1}{\Gamma_{NLI}^{1/3}} \left(\frac{A_s F_{eq}}{2} \right)^{1/3}, \tag{5.6}$$

$$N_{s,max} = \frac{1}{OSNR_T} \frac{1}{\Gamma_{NLI}^{1/3}} \frac{1}{(4A_s F_{eq})^{2/3}}, \tag{5.7}$$

$$OSNR_{max} = \frac{1}{N_s} \frac{1}{\Gamma_{NLI}^{1/3}} \frac{1}{(4A_s F_{eq})^{2/3}}. \tag{5.8}$$

Now we are able to define a merit parameter for Raman amplification:

$$\Delta_{RA} = 10log_{10}\left(\frac{N_{s,max,HFA}}{N_{s,max,EDFA}}\right) = 10log_{10}\left(\frac{OSNR_{max,HFA}}{OSNR_{max,EDFA}}\right) = \frac{1}{3}\left(2\Delta F_{eq} - \Delta\Gamma_{NLI}\right), \tag{5.9}$$

where

$$\Delta F_{eq} = F_{eq,EDFA,dB} - F_{eq,HFA,dB} \tag{5.10}$$

always positive, is the noise reduction and

$$\Delta\Gamma_{NLI} = 10log_{10}\left(\frac{\Gamma_{NLI,HFA}}{\Gamma_{NLI,EDFA}}\right) \tag{5.11}$$

always positive as well, is the NLI enhancement due to the power re-growth at the fiber end.

The result of these equations give us the reason of this project. Knowing how Δ_{RA} is, we can decide whether the use of the HFA or not, and what is the input power value and Raman pump that give us the target OSNR.

5.2.1 Simulation considerations

Before showing the results, some consideratios must be explained:

Fiber types. To run the simulations different kind of fibers have been used each characterized by different parameters already explained.

- NZDSF
  - α_{dB}=0.222 dB/km
  - D=3.8 ps/nm/km
  - A_{eff}=70 μm^2
- SMF
  - α_{dB}=0.2 dB/km
  - D=16.7 ps/nm/km
  - A_{eff}=80 μm^2
- PSCF
  - α_{dB}=0.166 dB/km
  - D=21 ps/nm/km
  - A_{eff}=135 μm^2

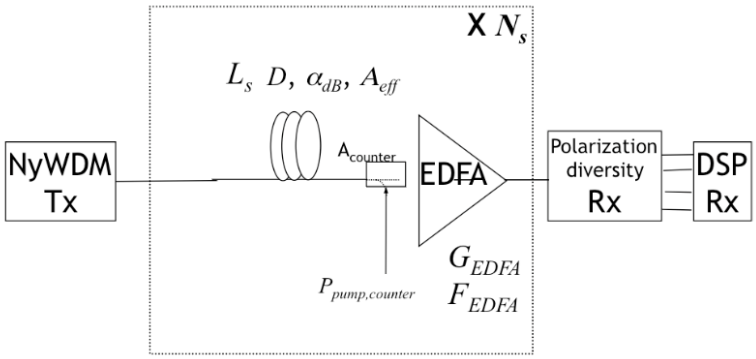

Figure 5.2: Layout of the first simulated scenario.

General hypotheses.

- As Raman efficiency for depolarized pumps it is considered the approximation C_R=g_{R0}/A_{eff} constant with respect to the frequency.
- g_{R0}=0.33e-13 m/W for all fibers.
- Raman pump(s) supposed to be depolarized.
- No relative intensity noise, RIN, transfer from pump(s) to signals.
- Loss coefficient for pump exceeding by 0.05 dB the C-band loss.
- Rayleigh backscattering: ideal (R=-∞) or R=-27 dB. Where R is the capture factor.
- Full C-band (4 THz) transmission.
- The F_{eq} (Noise Figure) for the EDFA is 4.5 dB.

5.3 First Scenario. Counter propagating Pump, No extra losses when RA is on

The first simulated scenario is showed in figure 5.2.

The simulation consists on a single span (N_s=1) composed of a NyWDM transmitter, a fiber characterized by the parameters of the previous section and L_s=A_s/α_{dB} (where A_s varies according to: A_s=16, 18, 20, 22, 24 dB but only the simulations results for 16, 20 and 24 dB will be shown), a coupler for the Raman pump (so, extra losses due to pump insertion can be

considered through the $A_{counter}$ parameter) and a EDFA (characterized by its gain, G_{EDFA} and its noise figure, F_{EDFA}).

In this scenario no extra losses due to pump insertion are considered ($A_{counter}$=0 dB) and the pump power values goes from 0 mW to $P_{pump,full-RA}$, that is to say:

$$P_{pump,full-RA} = \frac{\alpha_{dB} L_s + A_{counter}}{10 log_{10}(e) \frac{g_{r0}}{A_{eff}} L_{eff,p}}, \tag{5.12}$$

where $L_{eff,p}$ is the effective length considering the pump attenuation coefficient, α_p.

The figures showing the results have different curves depending on:

- If the results come from **closed-form expressions for undepleted pump**. These results are represented under the **UP$_{theor}$** curve.
- If the results come from **numerical integrals** (that is to say, Matlab theoretical simulation) for **undepleted pump**. These results are represented under the **UP** curve.
- If the results **don't include Rayleigh scattering** but consider **pump depletion** (they come from the OptSim simulation). These results are represented under the **DP** curve.
- If the results consider the **MPI from Rayleigh scattering** and the **pump depletion**. These results are represented under the **DP RS-ON** curve.

The following sections show the results for each fiber and a comparison between the three different fibers. On the figures of: Γ_{NLI},F_{eq} and $OSNR_{NL}$ for each fiber results ten lines are represented for each kind of curve. Each line represents a Raman pump power value (from 0 to $P_{pump,full-RA}$).

5.3.1 NZDSF results

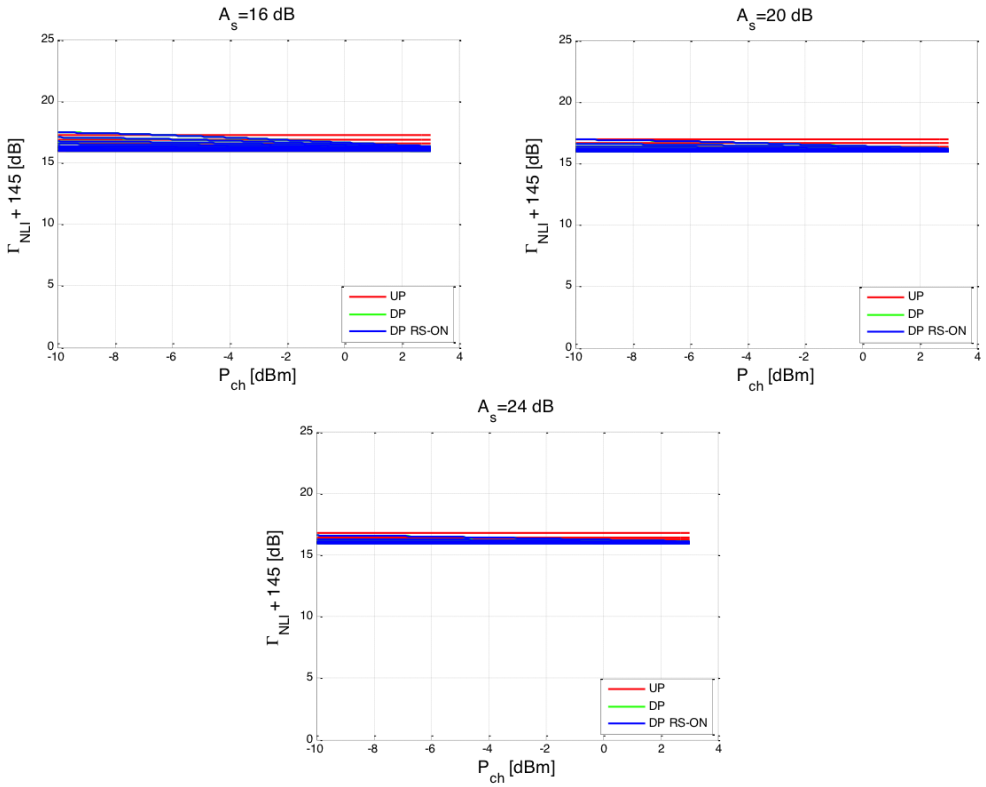

Figure 5.3: Γ_{NLI} [dB] for A_s=16, 20 and 22 [dB] vs. the channel input power, P_{ch} [dBm].

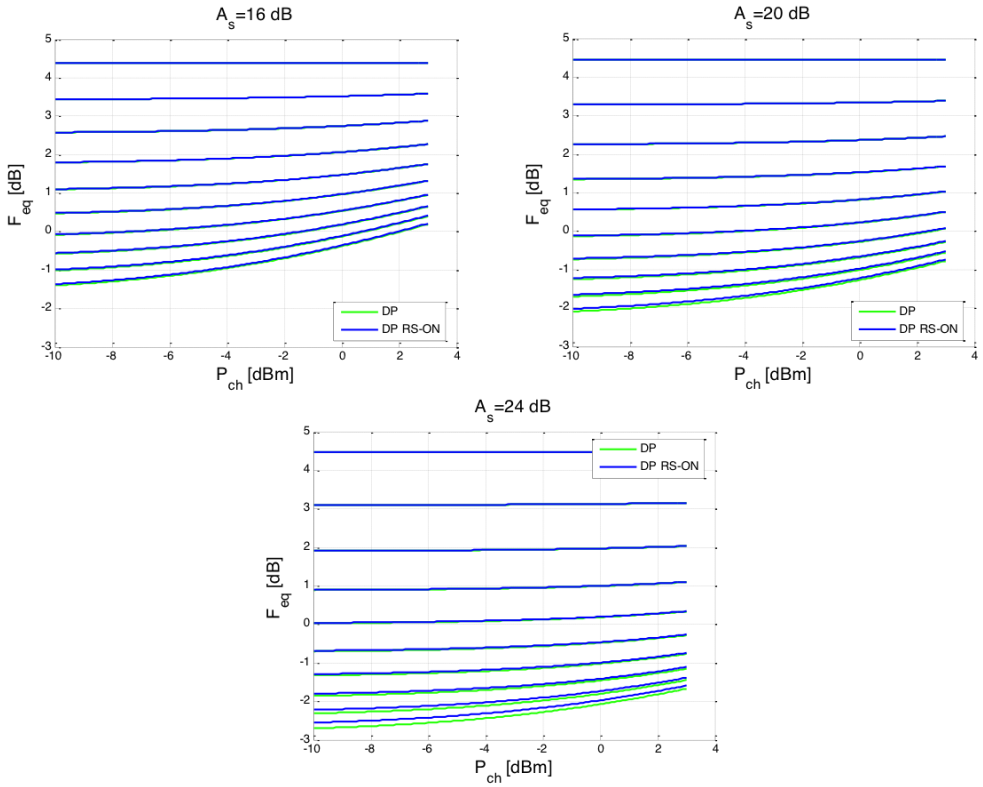

Figure 5.4: F_{eq} [dB] for A_s=16, 20 and 22 [dB] vs. the channel input power, P_{ch} [dBm].

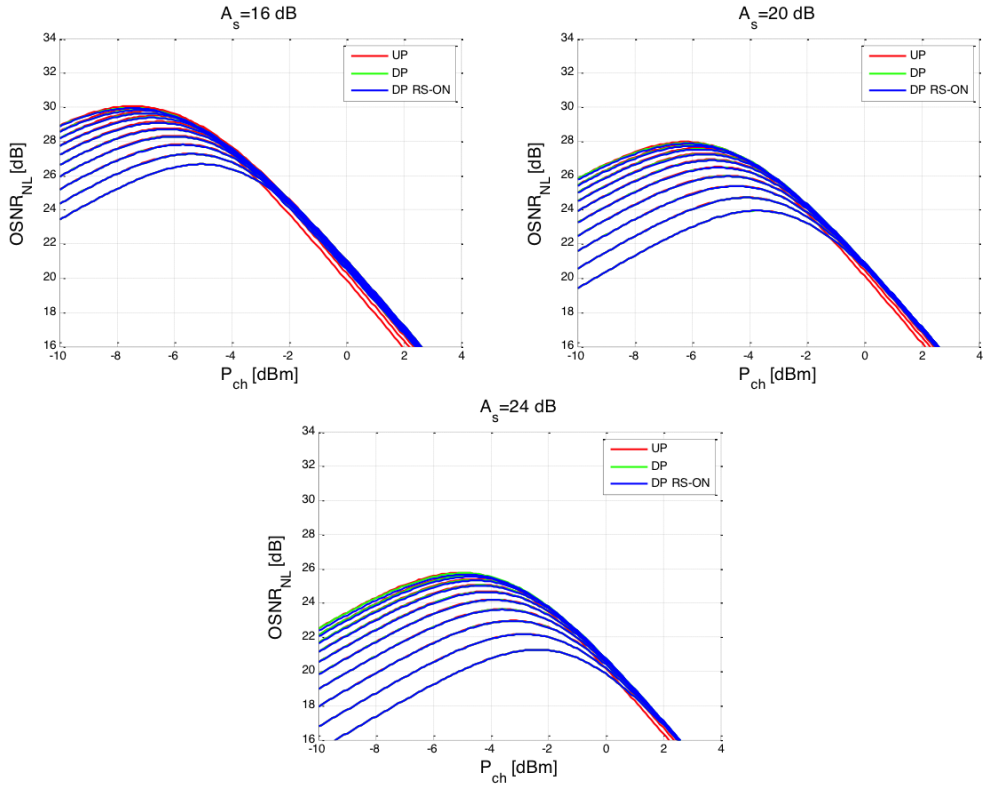

Figure 5.5: $OSNR_{NL}$ [dB] for A_s=16, 20 and 22 [dB] vs. the channel input power, P_{ch} [dBm].

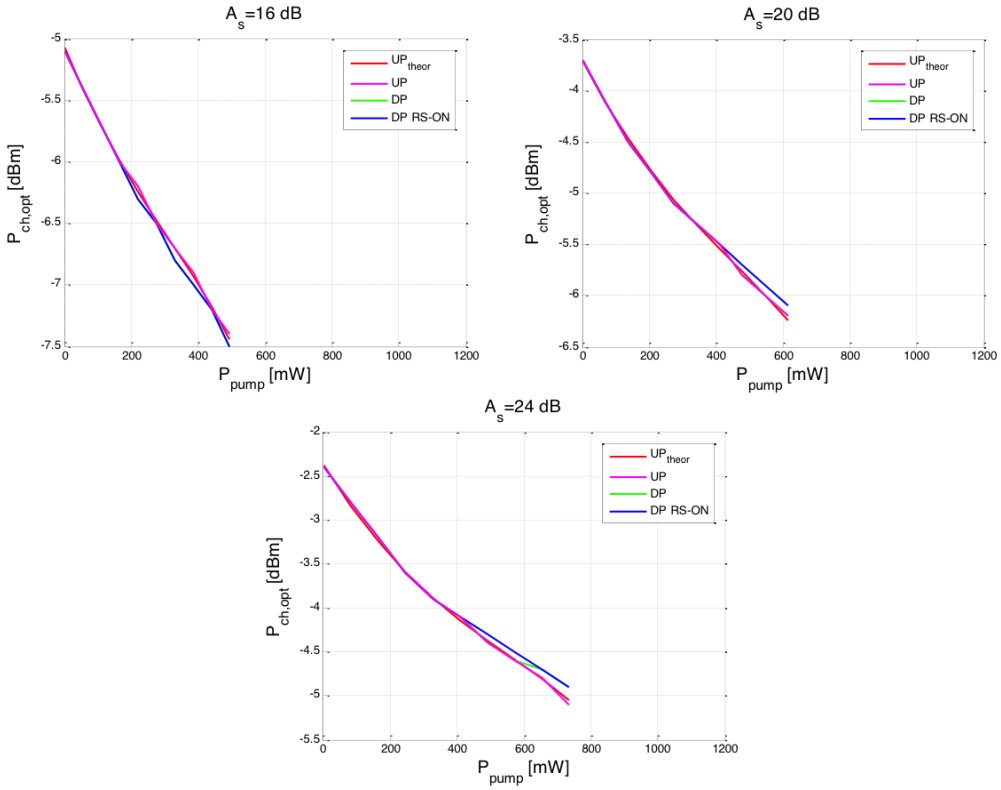

Figure 5.6: $P_{ch,opt}$ [dBm] for A_s=16, 20 and 22 [dB] vs. the Raman pump power, P_{pump} [mW].

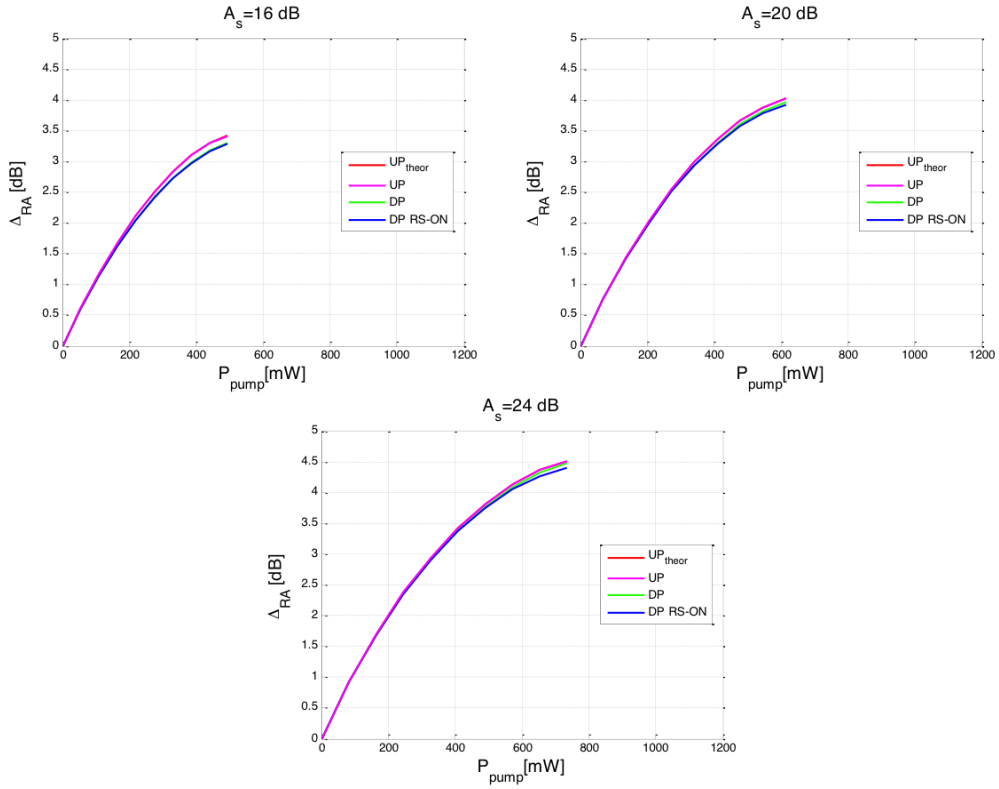

Figure 5.7: Δ_{RA} [dB] for A_s=16, 20 and 22 [dB] vs. the Raman pump power, P_{pump} [mW].

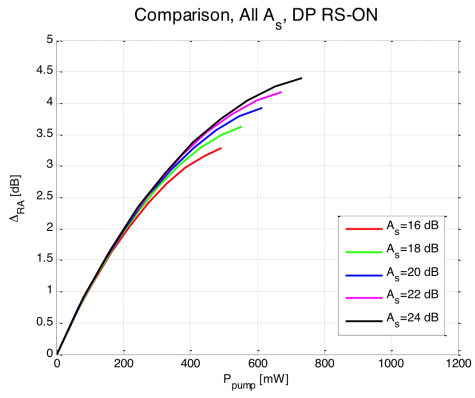

Figure 5.8: Δ_{RA} [dB] for A_s=16, 18, 20, 22 and 24 [dB] vs. the Raman pump power, P_{pump} [mW].

5.3.2 SMF results

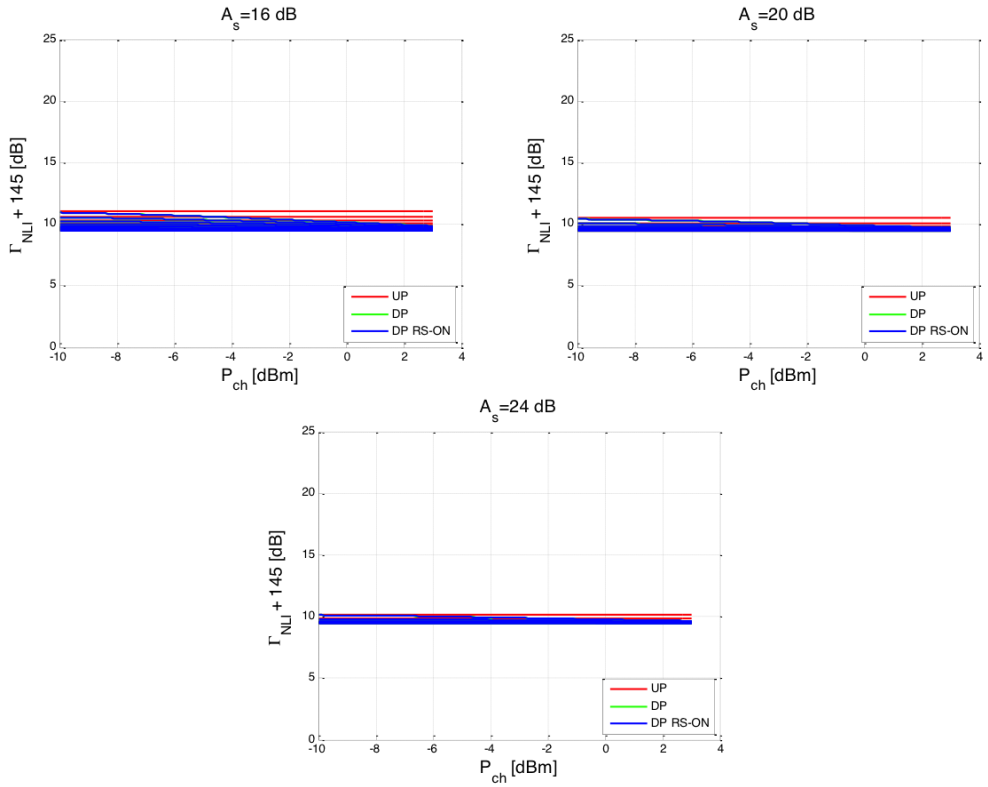

Figure 5.9: Γ_{NLI} [dB] for A_s=16, 20 and 22 [dB] vs. the channel input power, P_{ch} [dBm].

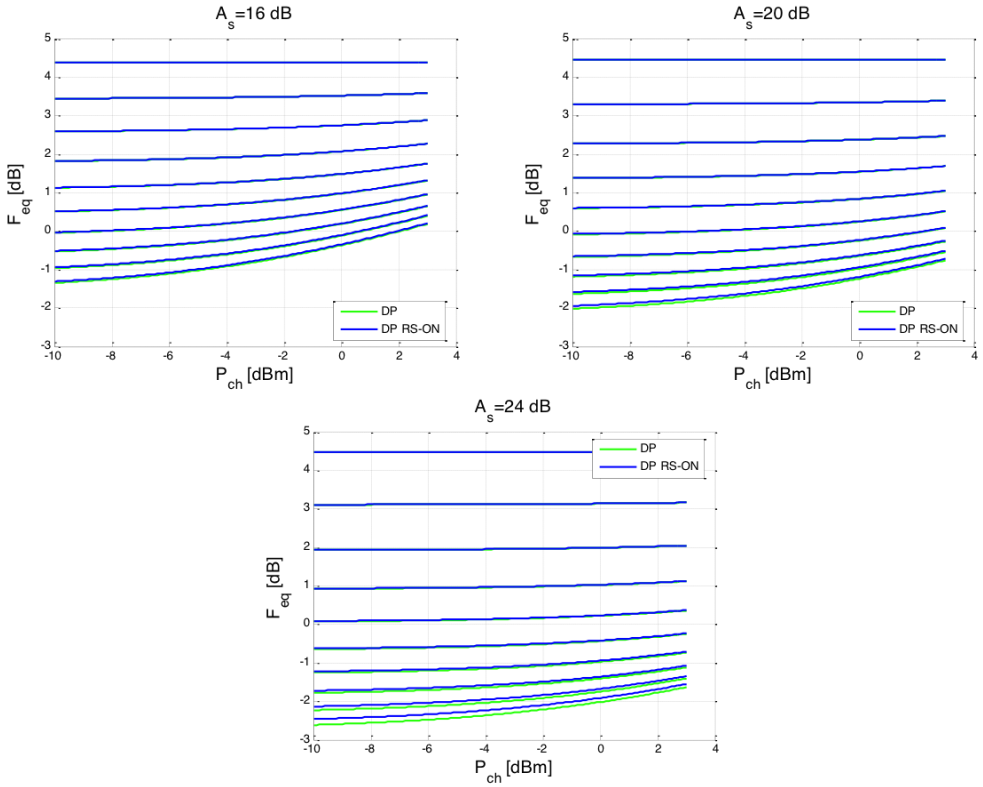

Figure 5.10: F_{eq} [dB] for A_s=16, 20 and 22 [dB] vs. the channel input power, P_{ch} [dBm].

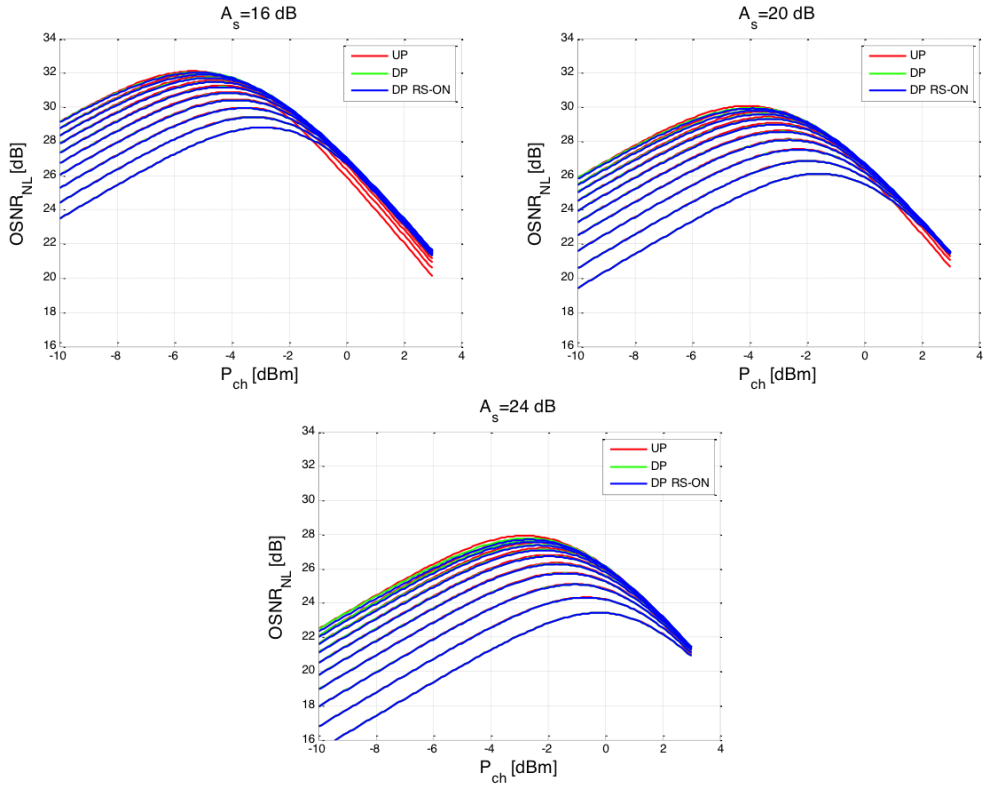

Figure 5.11: $OSNR_{NL}$ [dB] for A_s=16, 20 and 22 [dB] vs. the channel input power, P_{ch} [dBm].

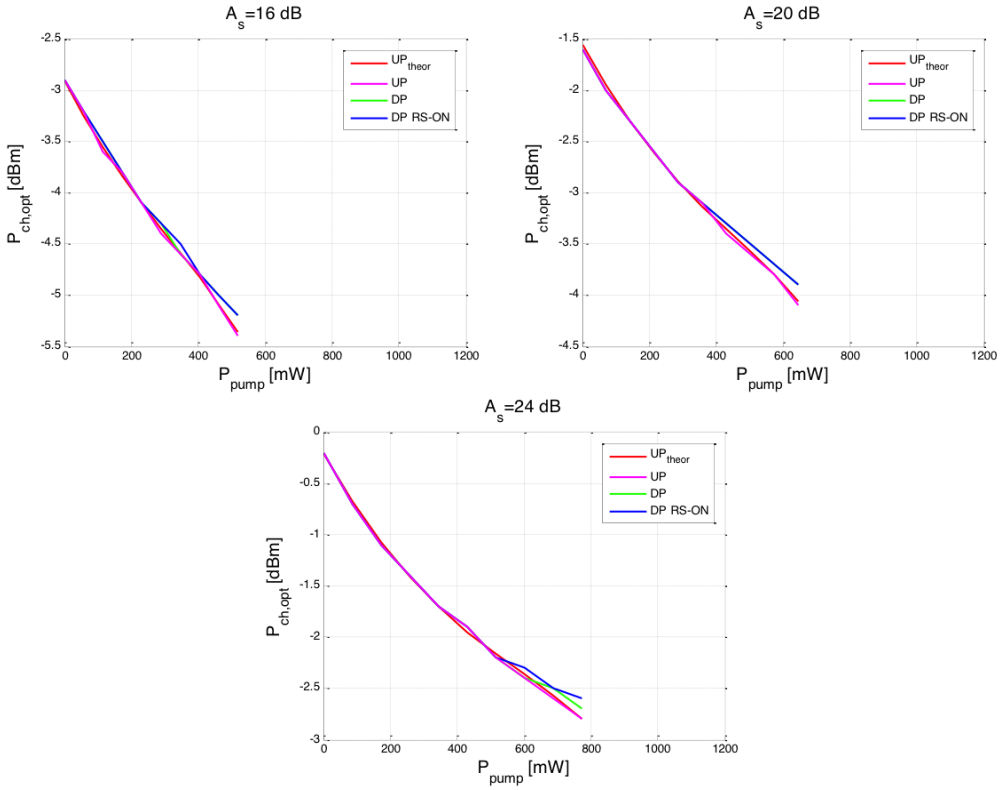

Figure 5.12: $P_{ch,opt}$ [dBm] for A_s=16, 20 and 22 [dB] vs. the Raman pump power, P_{pump} [mW].

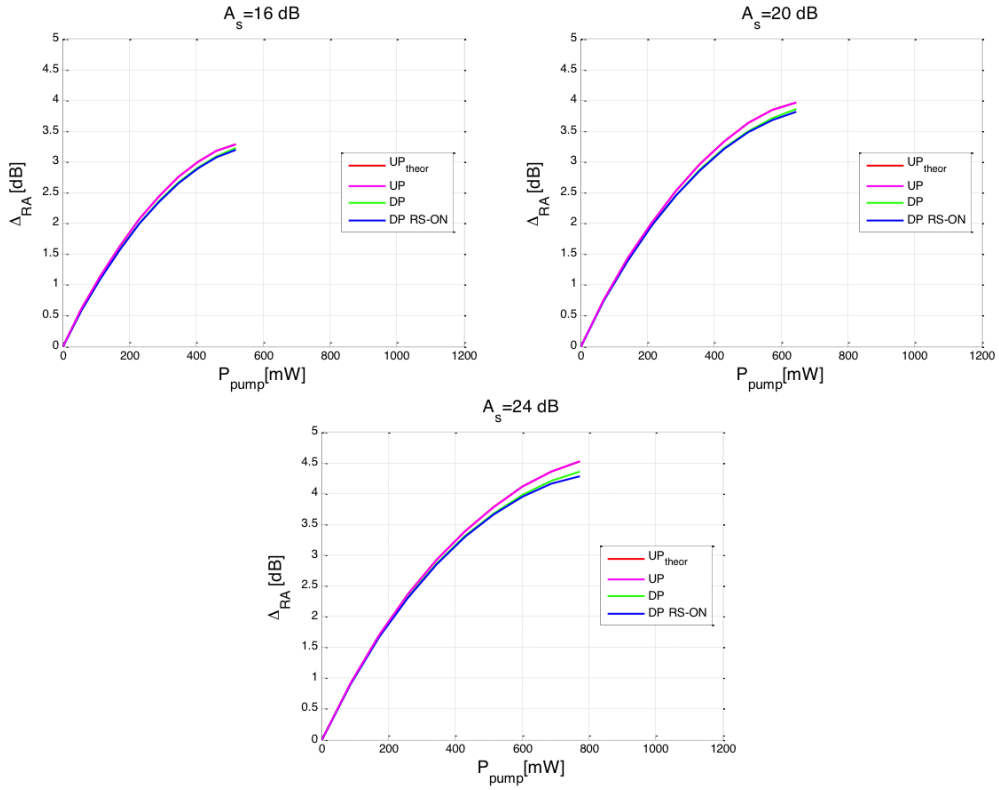

Figure 5.13: Δ_{RA} [dB] for A_s=16, 20 and 22 [dB] vs. the Raman pump power, P_{pump} [mW].

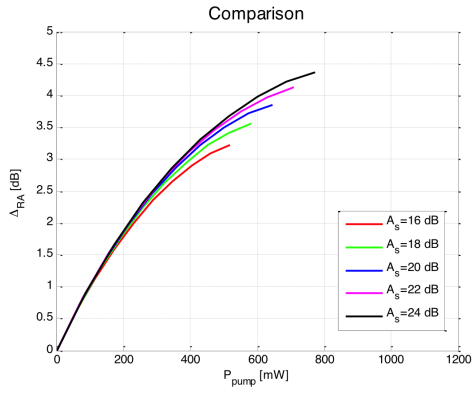

Figure 5.14: Δ_{RA} [dB] for A_s=16, 18, 20, 22 and 24 [dB] vs. the Raman pump power, P_{pump} [mW].

5.3.3 PSCF results

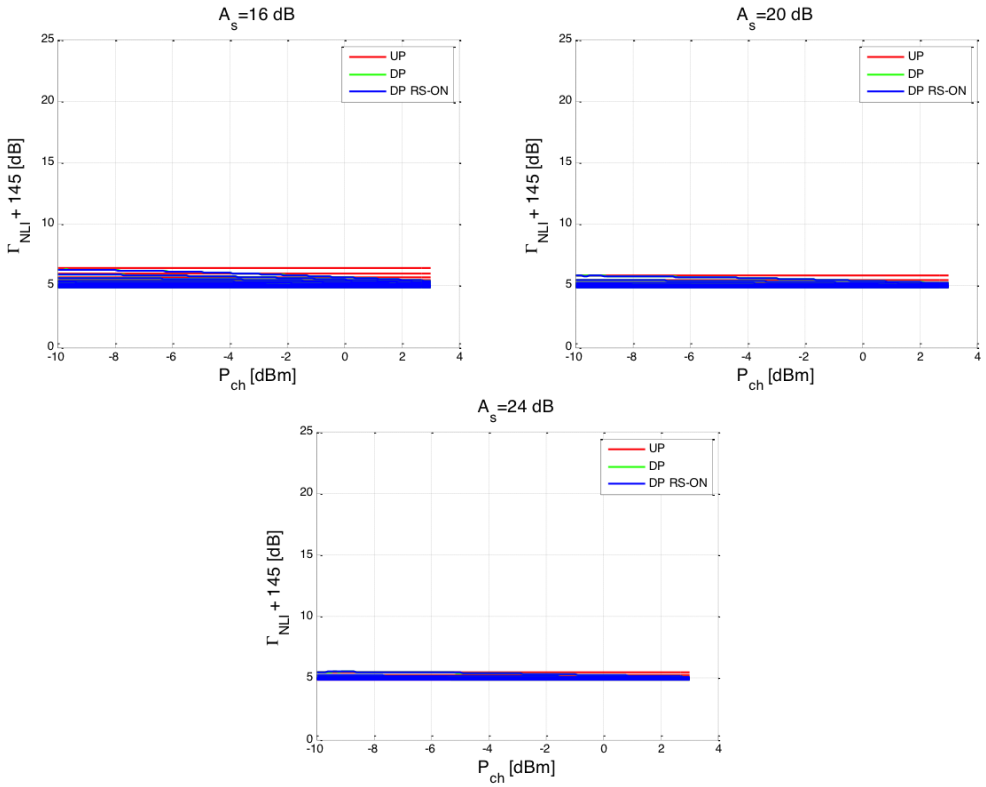

Figure 5.15: Γ_{NLI} [dB] for A_s=16, 20 and 22 [dB] vs. the channel input power, P_{ch} [dBm].

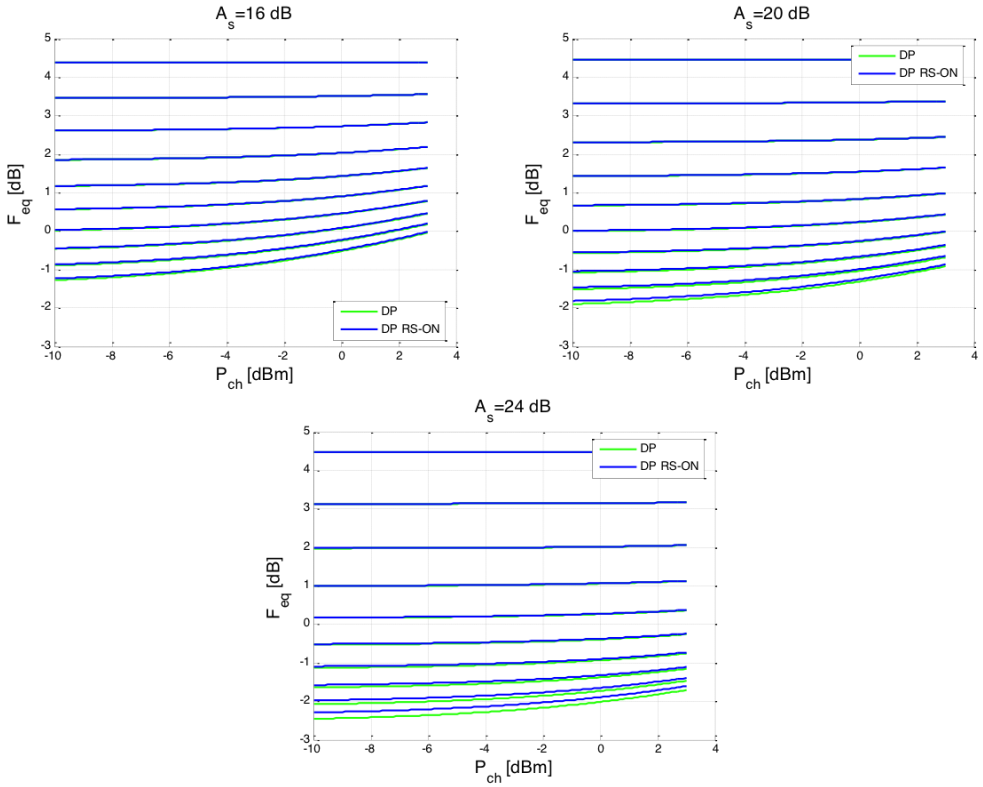

Figure 5.16: F_{eq} [dB] for A_s=16, 20 and 22 [dB] vs. the channel input power, P_{ch} [dBm].

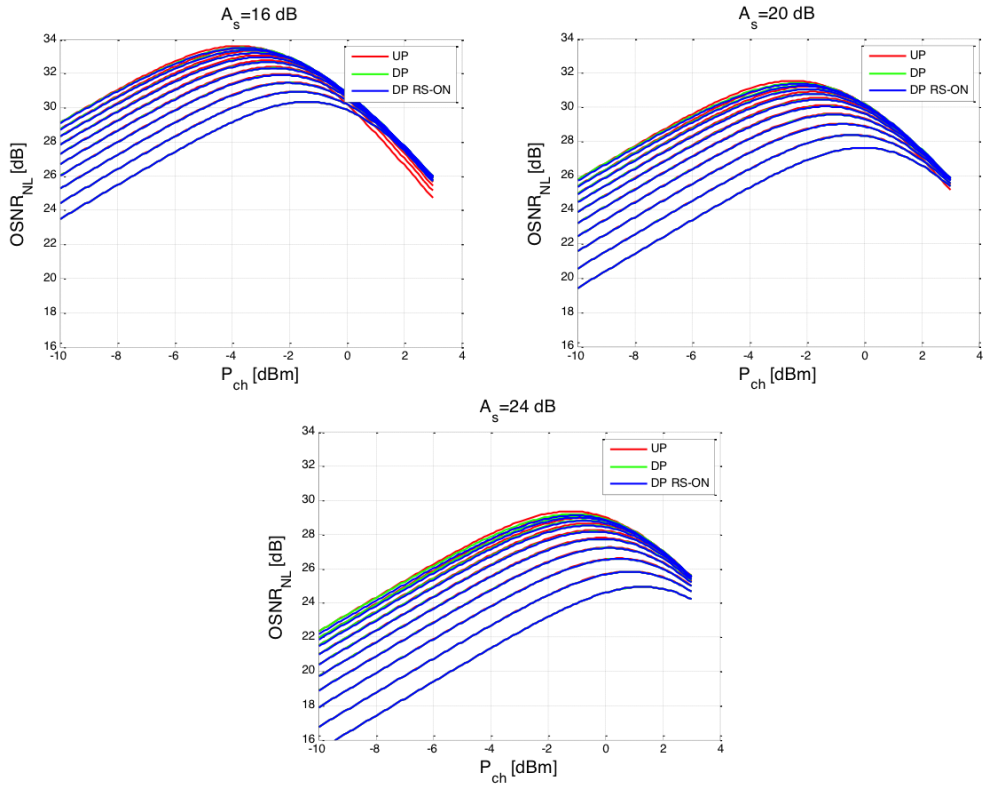

Figure 5.17: $OSNR_{NL}$ [dB] for A_s=16, 20 and 22 [dB] vs. the channel input power, P_{ch} [dBm].

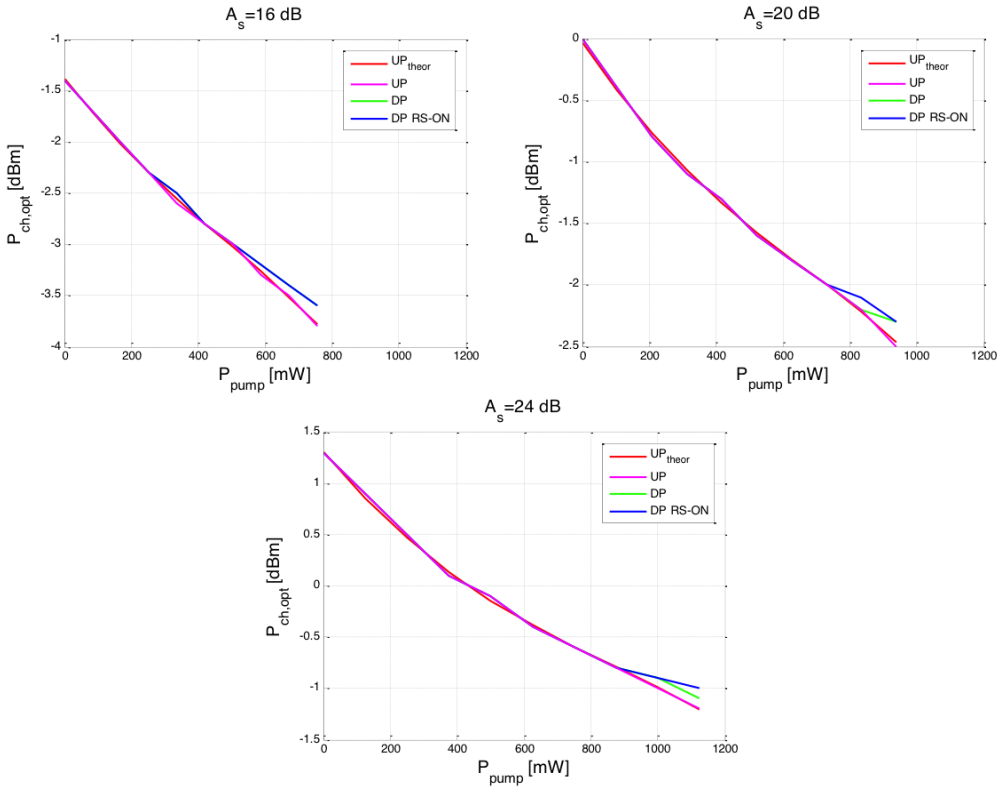

Figure 5.18: $P_{ch,opt}$ [dBm] for A_s=16, 20 and 22 [dB] vs. the Raman pump power, P_{pump} [mW].

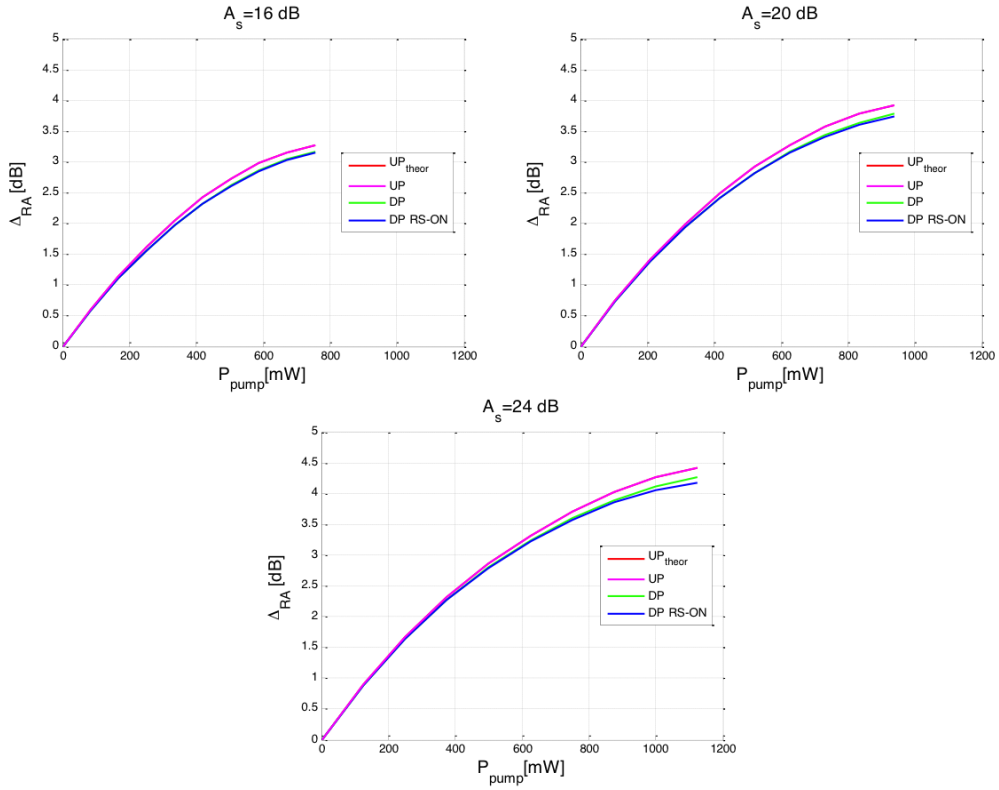

Figure 5.19: Δ_{RA} [dB] for A_s=16, 20 and 22 [dB] vs. the Raman pump power, P_{pump} [mW].

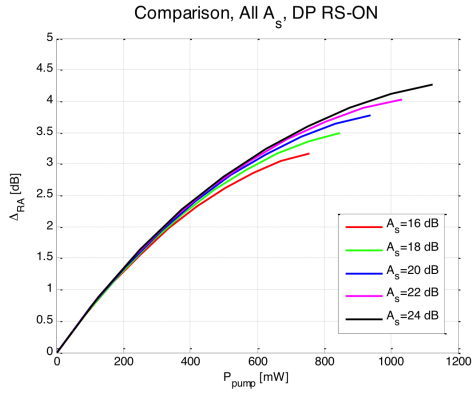

Figure 5.20: Δ_{RA} [dB] for A_s=16, 18, 20, 22 and 24 [dB] vs. the Raman pump power, P_{pump} [mW].

5.3.4 Comparison between fibers

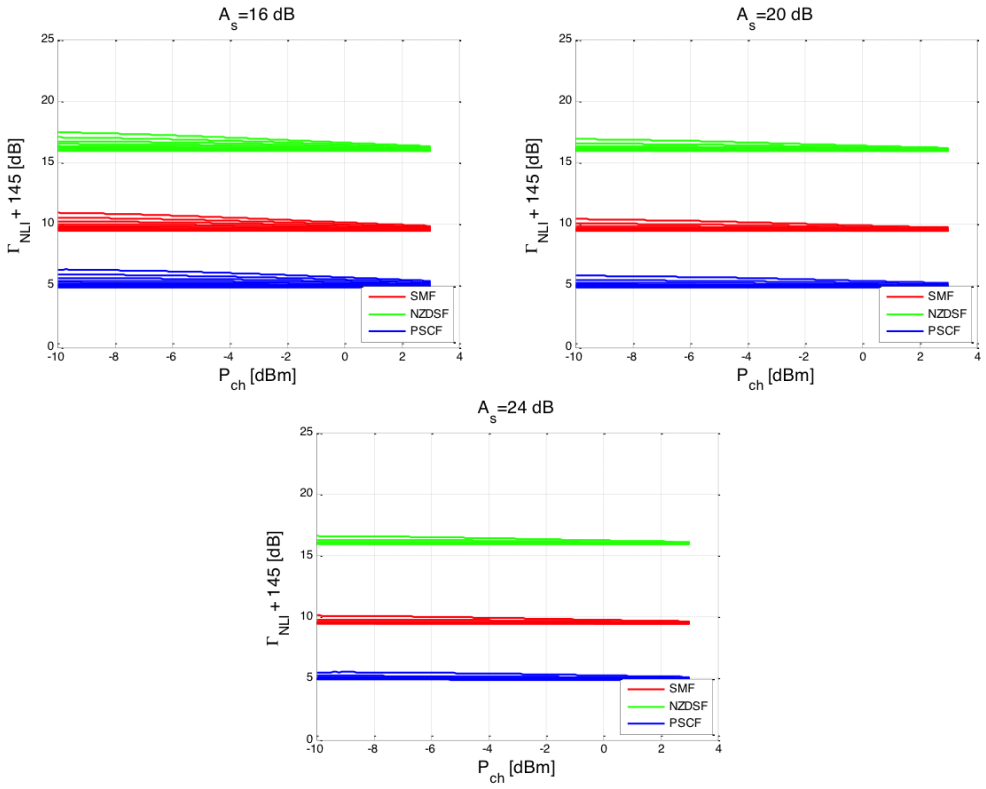

Figure 5.21: Γ_{NLI} [dB] for the different fibers vs. the channel input power, P_{ch} [dBm].

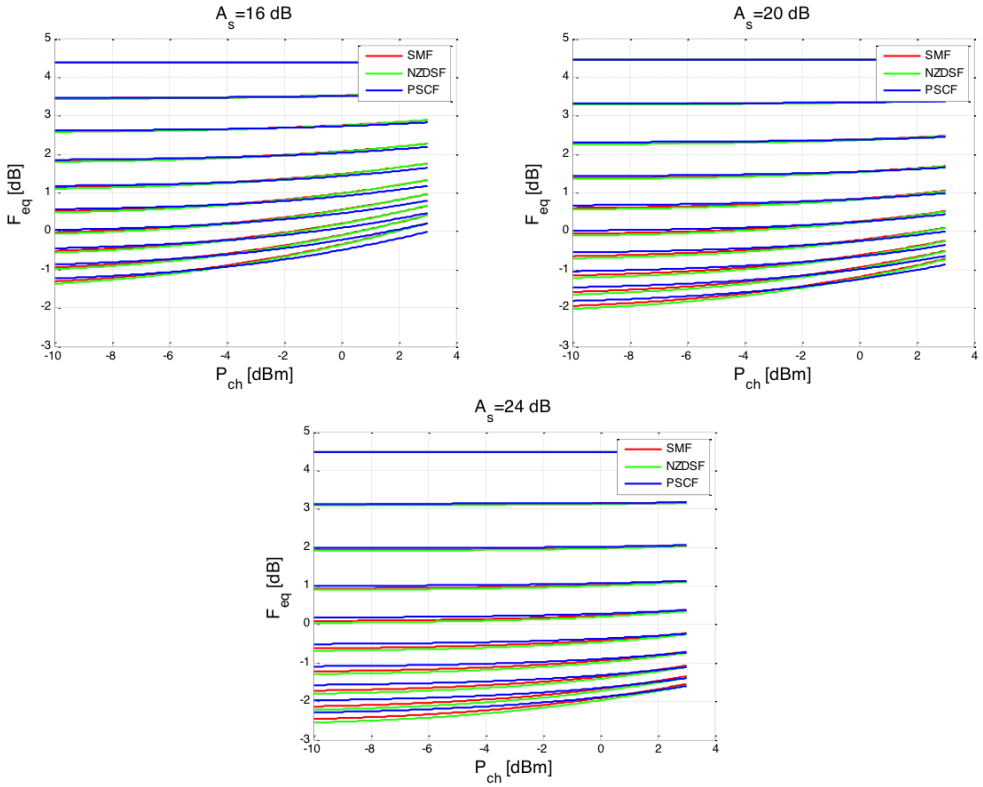

Figure 5.22: F_{eq} [dB] for the different fibers vs. the channel input power, P_{ch} [dBm].

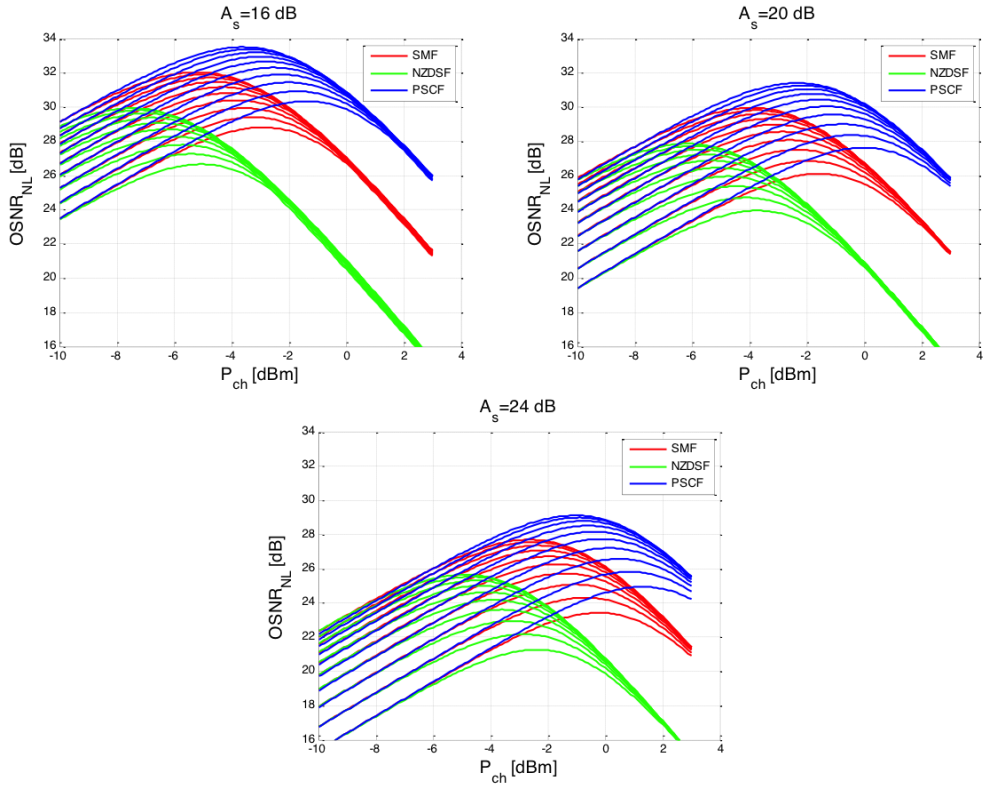

Figure 5.23: OSNR_{NL} [dB] for the different fibers vs. the channel input power, P_{ch} [dBm].

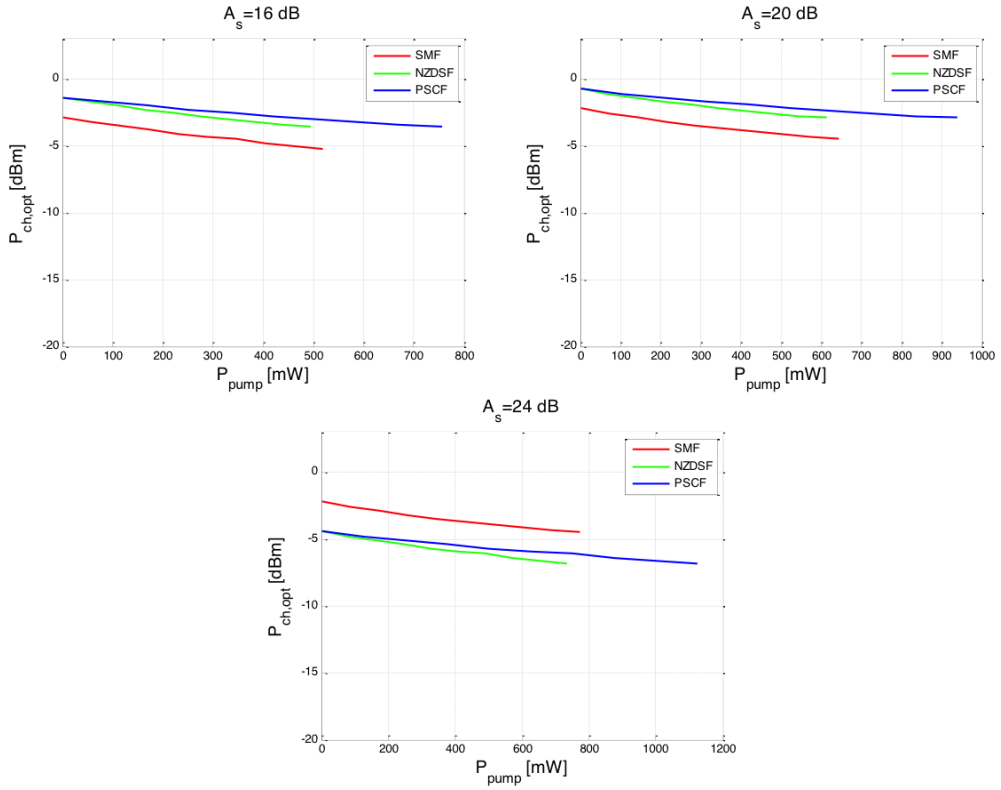

Figure 5.24: $P_{ch,opt}$ [dB] for the different fibers vs. Raman pump power, P_{pump} [mW].

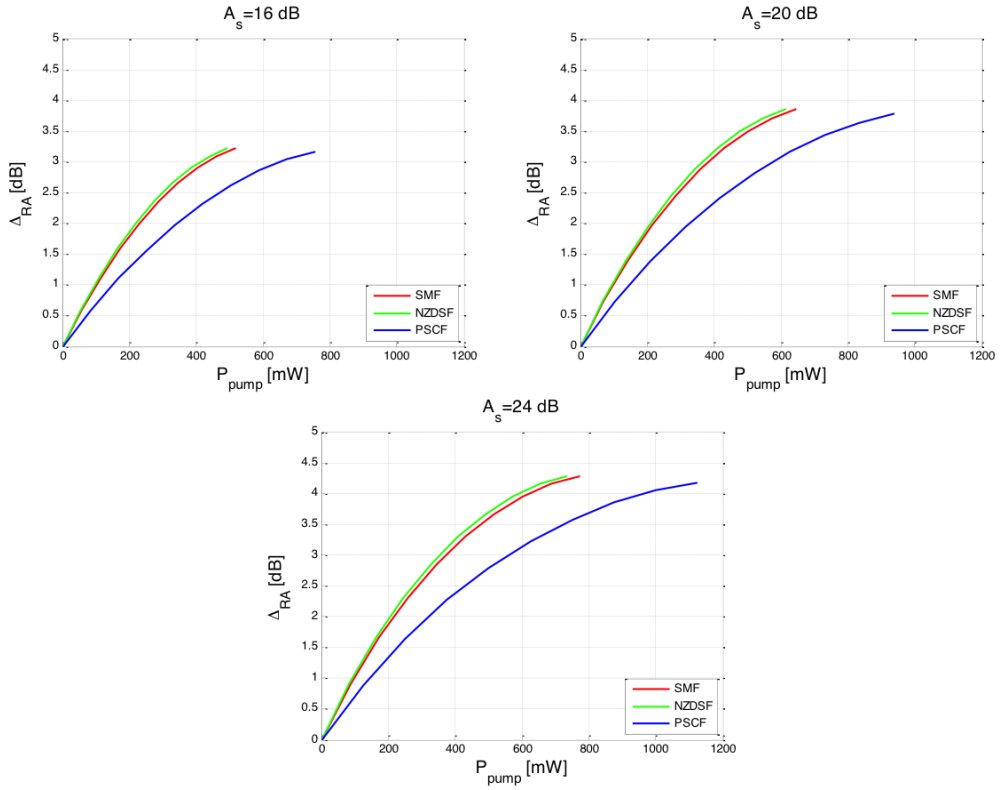

Figure 5.25: Δ_{RA} [dB] for the different fibers vs. Raman pump power, P_{pump} [mW].

5.4 Second Scenario. Co and Counter propagating Pump, No extra losses with RA on

The second simulated scenario is showed in figure 5.26. The simulation is very similar to that carried out on the first scenario with the differences of the co-propagating coupler for Raman pump and the fixed value A_s=20 dB for every simulation. As in the previous scenario, we will not take into account the coupler losses, and therefore A_{co}=$A_{counter}$=0 dB.

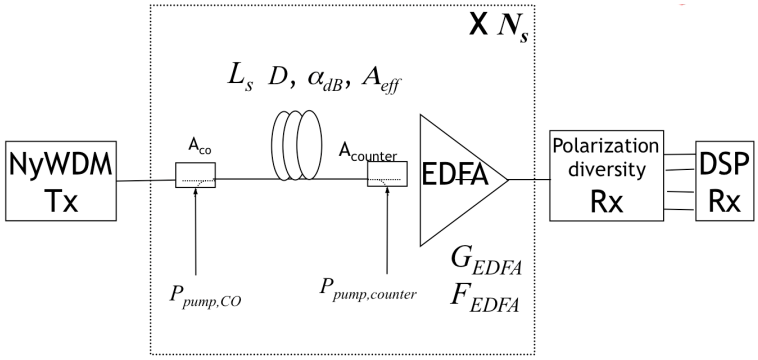

Figure 5.26: Layout of the second simulated scenario.

In this case the maximum value of the Raman pump power will be:

$$P_{pump,full-RA} = \frac{\alpha_{dB} L_s + A_{counter} + A_{co}}{10 log_{10}(e) \frac{g_{r0}}{A_{eff}} L_{eff,p}}, \tag{5.13}$$

and the pump power will be the contribution of both propagating directions power:

$$P_{pump} = P_{pump,co} + P_{pump,counter} \tag{5.14}$$

where:

$$P_{pump,co} = P_{pump} \frac{perc_{co}}{100} \quad and \quad P_{pump,counter} = P_{pump} \left(1 - \frac{perc_{co}}{100}\right). \tag{5.15}$$

For each pump level (we define 10 values from full-EDFA, P_{pump}=0 mW, to full-RA, $P_{pump,full-RA}$) $perc_{co}$ = 0% (full counter), 25%, 50%, 75%, 100% (full co).

5.4.1 NZDSF results

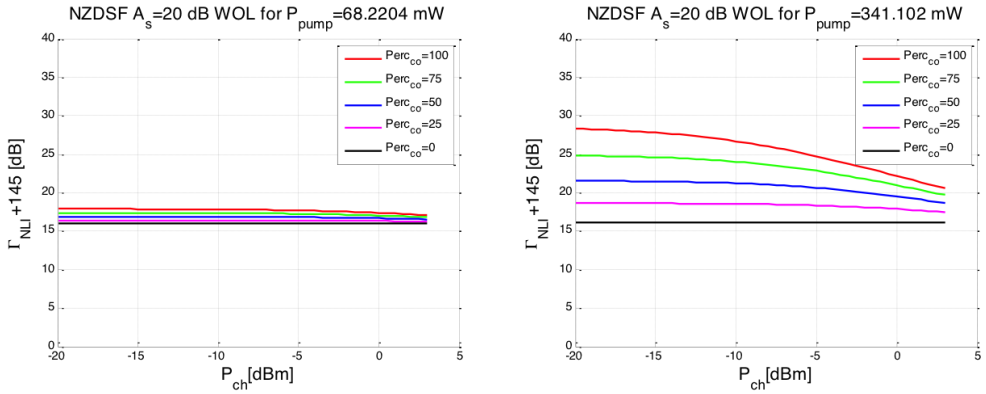

(a) P_{pump} = 68.2204 mW (b) P_{pump} = 341.102 mW

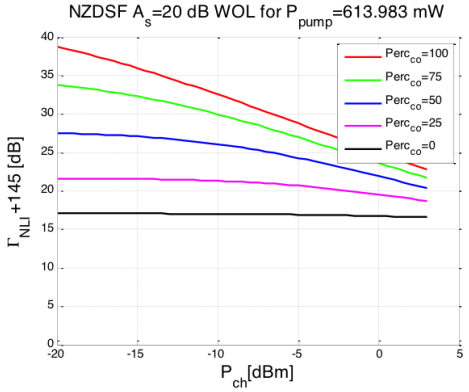

(c) P_{pump} = 613.983 mW

Figure 5.27: Γ_{NLI} [dB] vs. channel input power, P_{ch} [dBm].

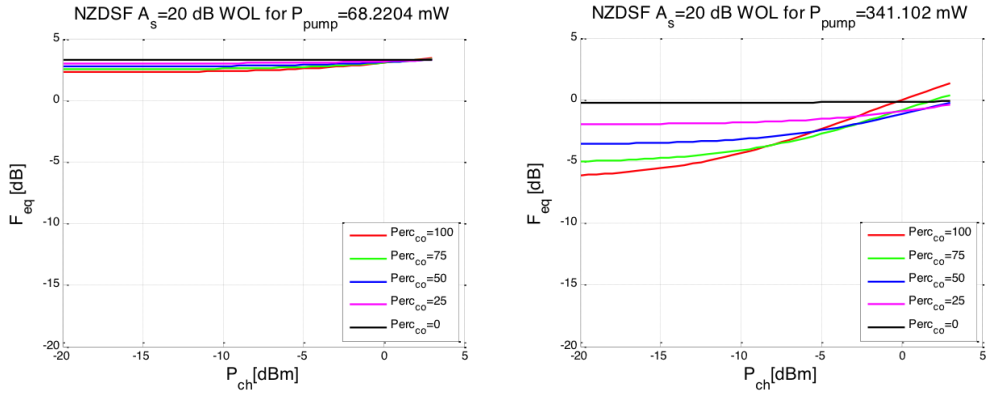

(a) P_{pump} = 68.2204 mW (b) P_{pump} = 341.102 mW

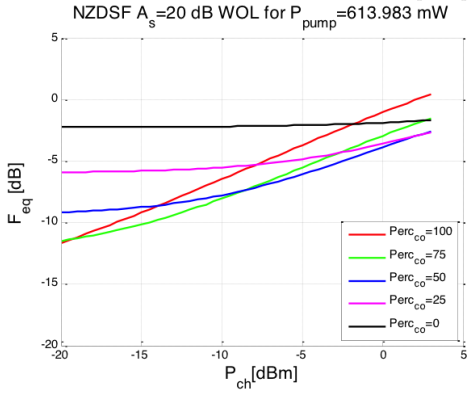

(c) P_{pump} = 613.983 mW

Figure 5.28: F_{eq} [dB] vs. channel input power, P_{ch} [dBm].

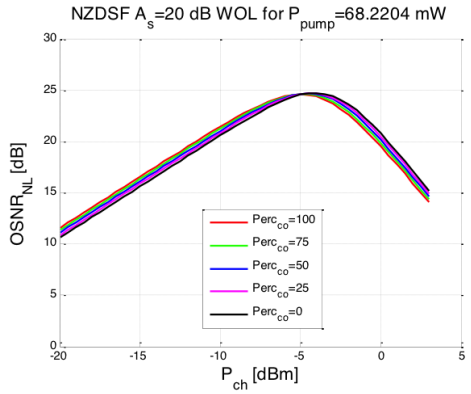

(a) P_{pump} = 68.2204 mW

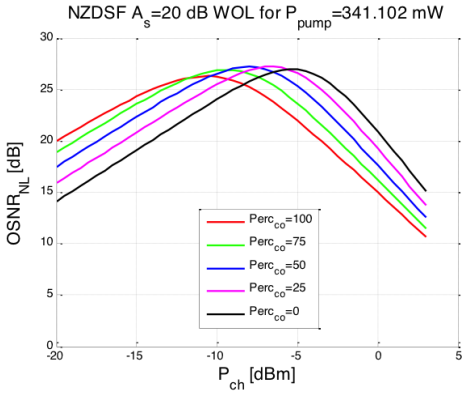

(b) P_{pump} = 341.102 mW

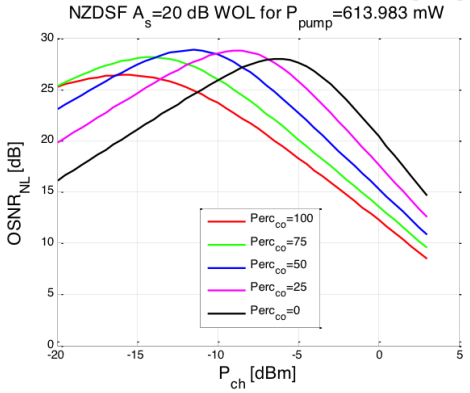

(c) P_{pump} = 613.983 mW

Figure 5.29: $OSNR_{NL}$ [dB] vs. channel input power, P_{ch} [dBm].

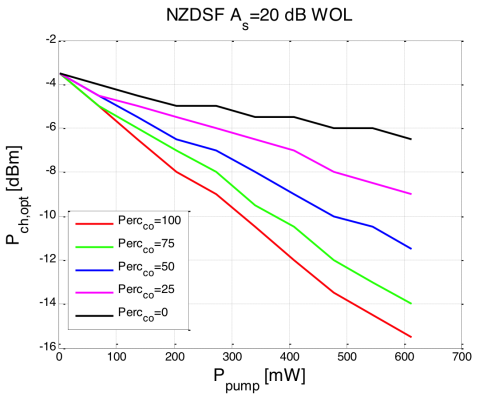

(a) $P_{ch,opt}$ [dBm] vs. P_{pump} [mW]

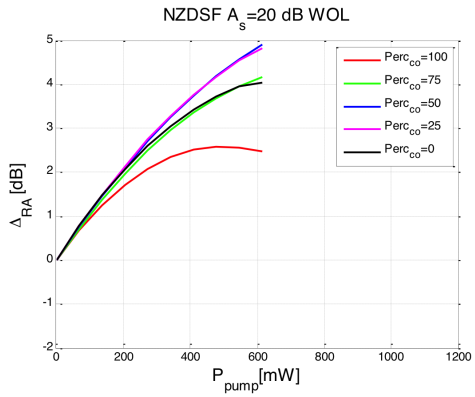

(b) Δ_{RA} [dB] vs. P_{pump} [mW]

5.4.2 SMF results

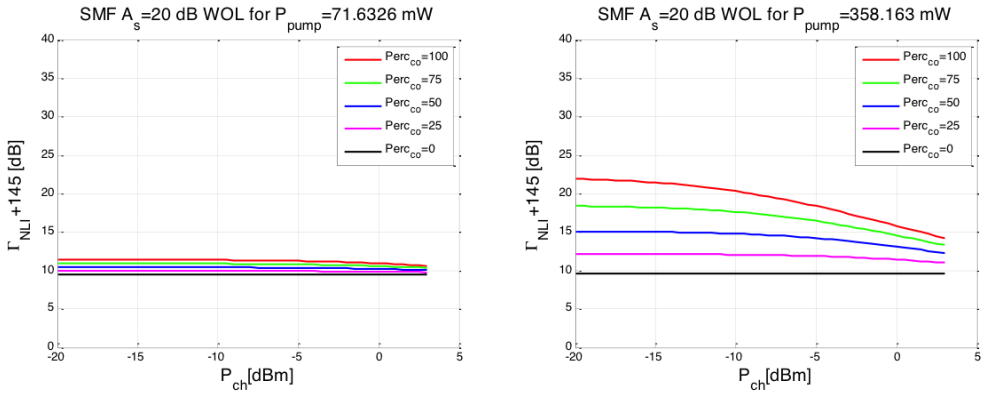

(a) P_{pump} = 68.2204 mW (b) P_{pump} = 341.102 mW

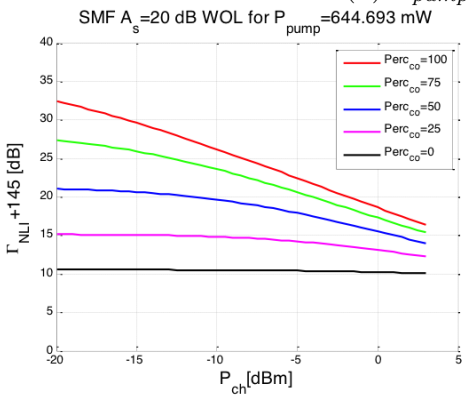

(c) P_{pump} = 613.983 mW

Figure 5.31: Γ_{NLI} [dB] vs. channel input power, P_{ch} [dBm].

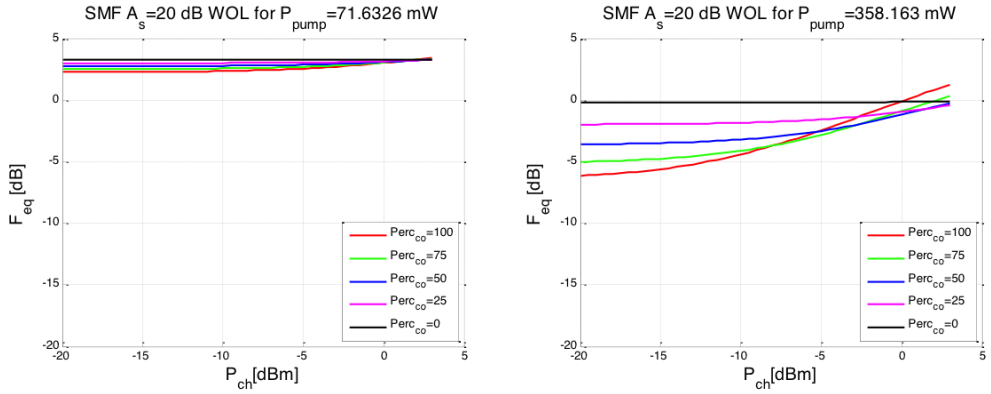

(a) P_{pump} = 68.2204 mW (b) P_{pump} = 341.102 mW

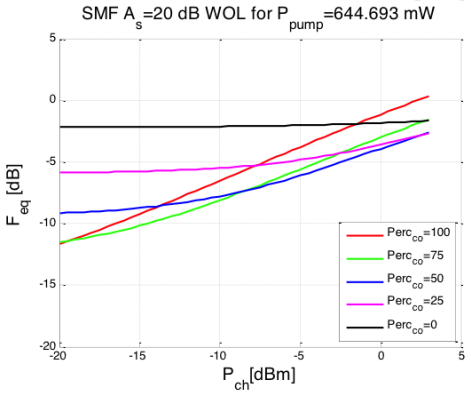

(c) P_{pump} = 613.983 mW

Figure 5.32: F_{eq} [dB] vs. channel input power, P_{ch} [dBm].

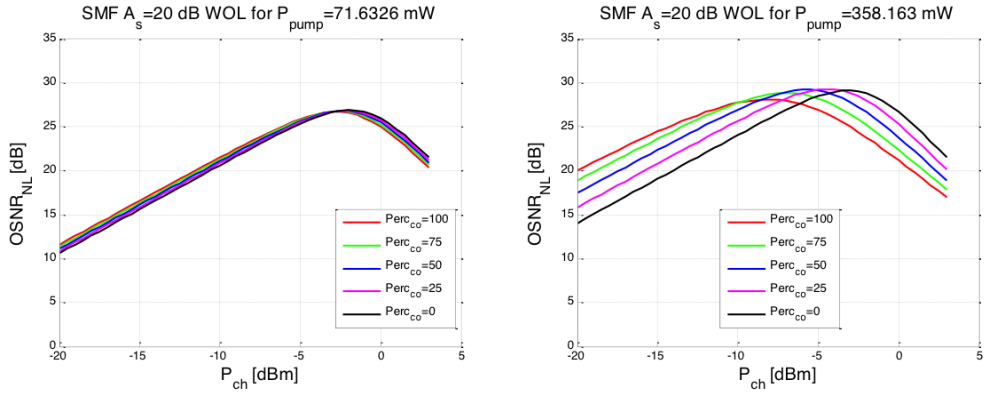

(a) P_{pump} = 68.2204 mW (b) P_{pump} = 341.102 mW

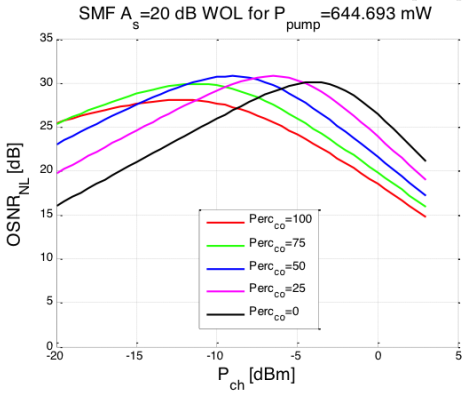

(c) P_{pump} = 613.983 mW

Figure 5.33: $OSNR_{NL}$ [dB] vs. channel input power, P_{ch} [dBm].

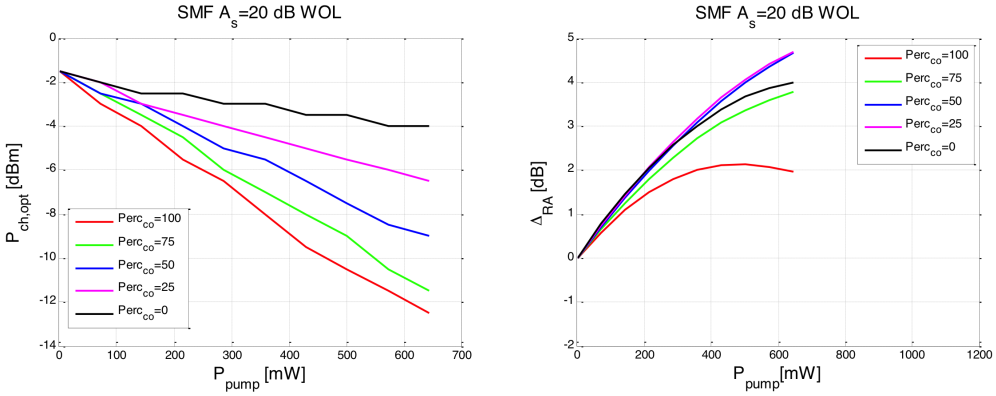

(a) $P_{ch,opt}$ [dBm] vs. P_{pump} [mW] (b) Δ_{RA} [dB] vs. P_{pump} [mW]

5.4.3 PSCF results

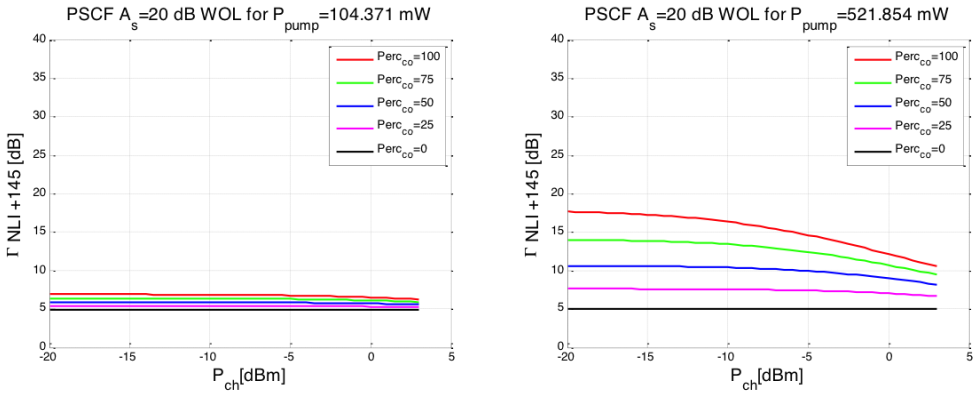

(a) P_{pump} = 68.2204 mW (b) P_{pump} = 341.102 mW

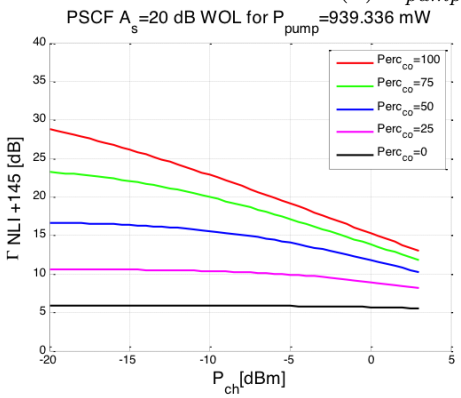

(c) P_{pump} = 613.983 mW

Figure 5.35: Γ_{NLI} [dB] vs. channel input power, P_{ch} [dBm].

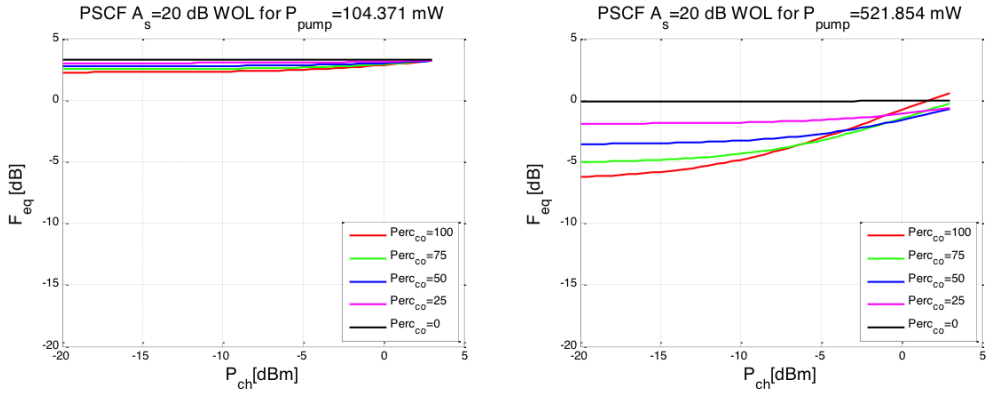

(a) P_{pump} = 68.2204 mW (b) P_{pump} = 341.102 mW

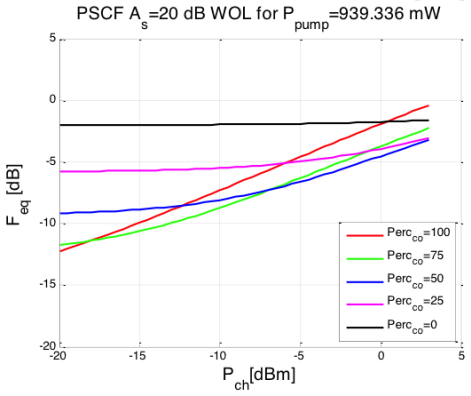

(c) P_{pump} = 613.983 mW

Figure 5.36: F_{eq} [dB] vs. channel input power, P_{ch} [dBm].

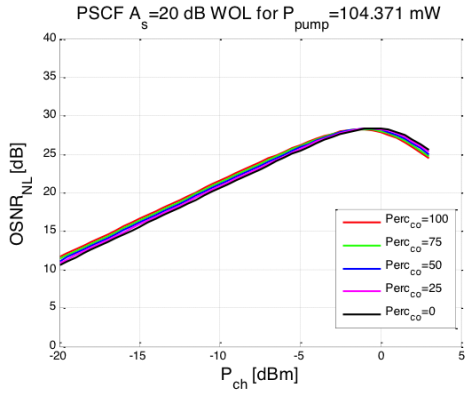

(a) P_{pump} = 68.2204 mW

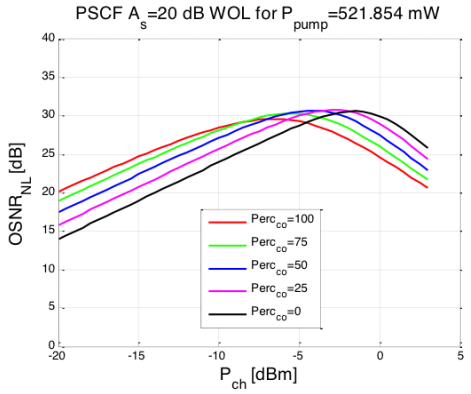

(b) P_{pump} = 341.102 mW

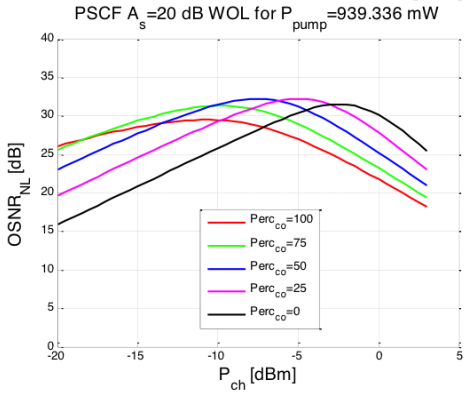

(c) P_{pump} = 613.983 mW

Figure 5.37: $OSNR_{NL}$ [dB] vs. channel input power, P_{ch} [dBm].

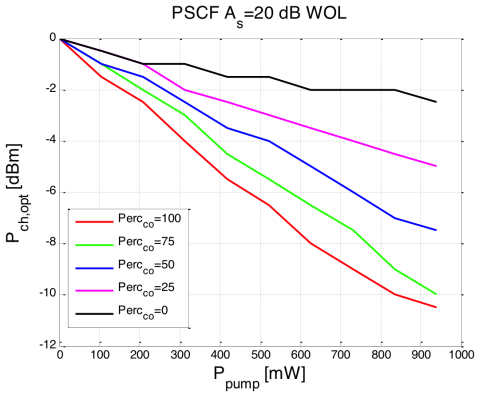

(a) $P_{ch,opt}$ [dBm] vs. P_{pump} [mW]

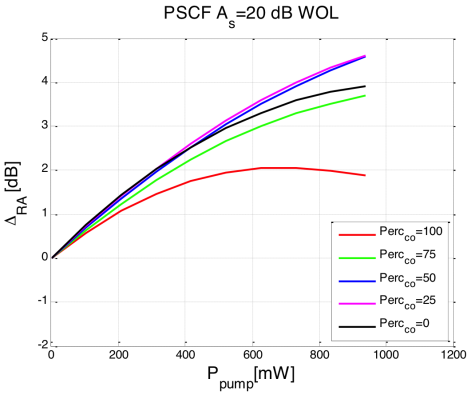

(b) Δ_{RA} [dB] vs. P_{pump} [mW]

5.4.4 Comparison between fibers

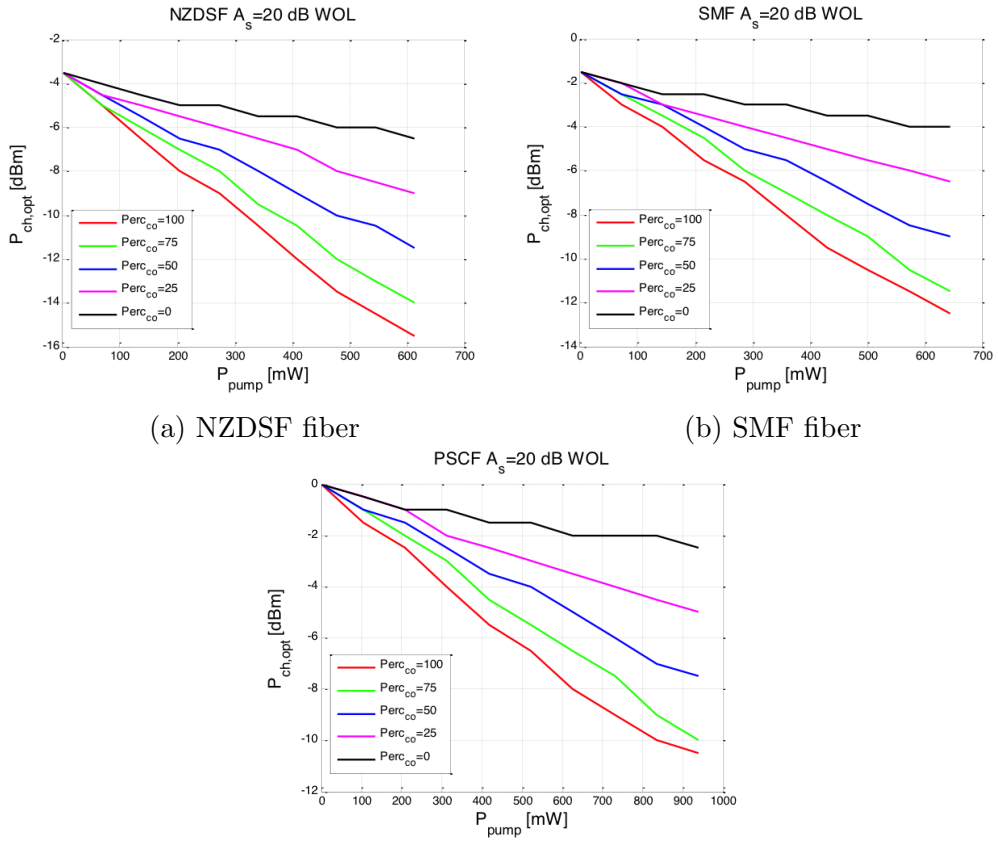

(a) NZDSF fiber

(b) SMF fiber

(c) PSCF fiber

Figure 5.39: $P_{ch,opt}$ [dBm] vs. P_{pump} [mW] for each fiber.

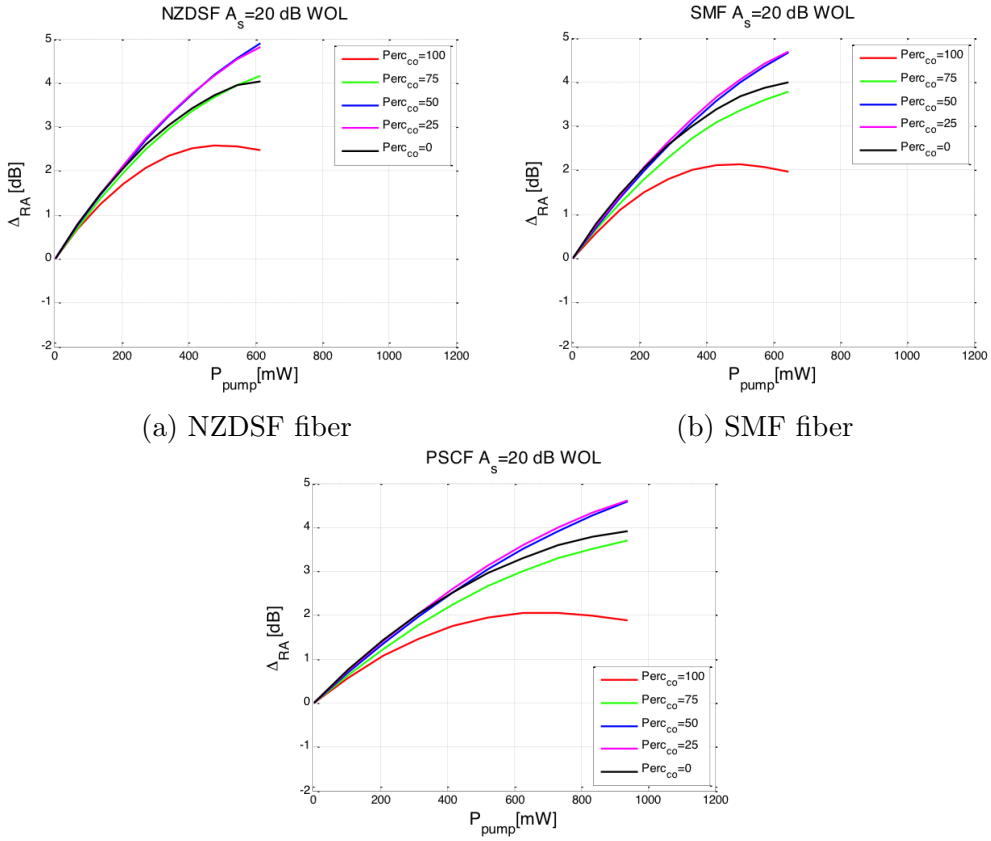

(a) NZDSF fiber

(b) SMF fiber

(c) PSCF fiber

Figure 5.40: F_{eq} [dB] vs. P_{pump} [mW] for each fiber.

5.5 Third Scenario. Co and Counter propagating Pump, Extra losses with RA on

This simulated scenario is identical to the second scenario, in exception of the inclusion of both co and counter coupler losses. The losses are defined as:

$$A_{xx} = \begin{cases} 0 & dB \quad if \quad P_{pump,xx} = 0 \quad mW \\ 1 & dB \quad if \quad P_{pump,xx} > 0 \quad mW \end{cases} \tag{5.16}$$

where A_{xx} might be A_{co} or $A_{counter}$. Due to the extra losses, A_s=20 dB + pump insertion loss(es) (if the pump is greater than zero).

5.5.1 NZDSF results

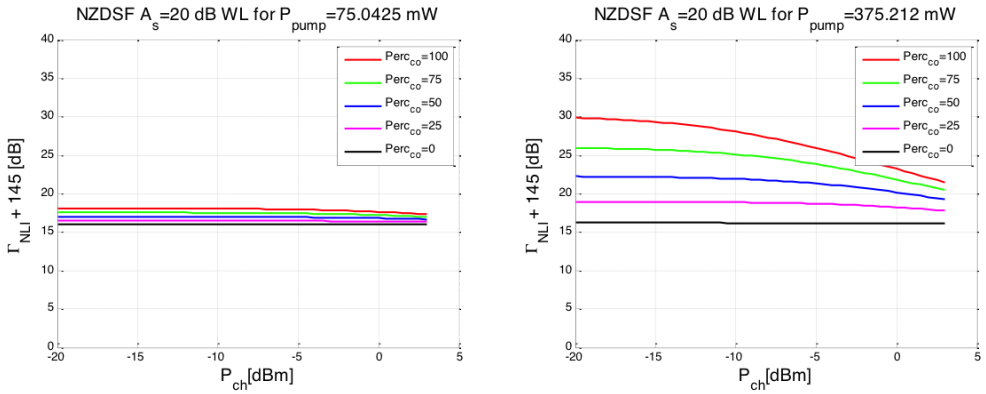

(a) P_{pump} = 75.0425 mW (b) P_{pump} = 375.212 mW

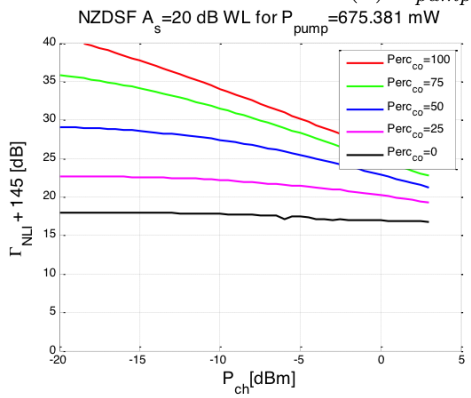

(c) P_{pump} = 675.381 mW

Figure 5.41: Γ_{NLI} [dB] vs. channel input power, P_{ch} [dBm].

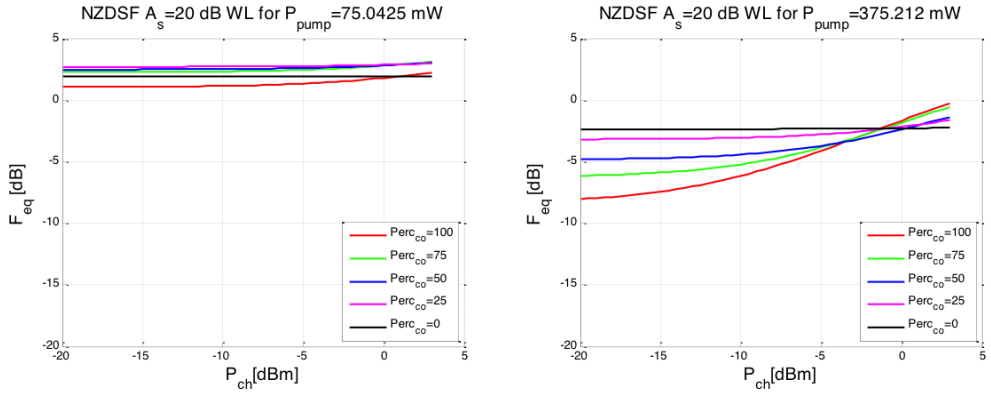

(a) P_{pump} = 75.0425 mW (b) P_{pump} = 375.212 mW

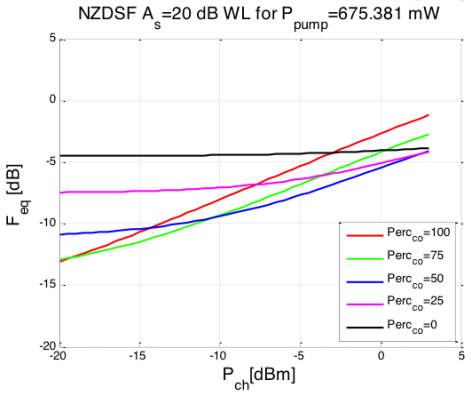

(c) P_{pump} = 675.381 mW

Figure 5.42: F_{eq} [dB] vs. channel input power, P_{ch} [dBm].

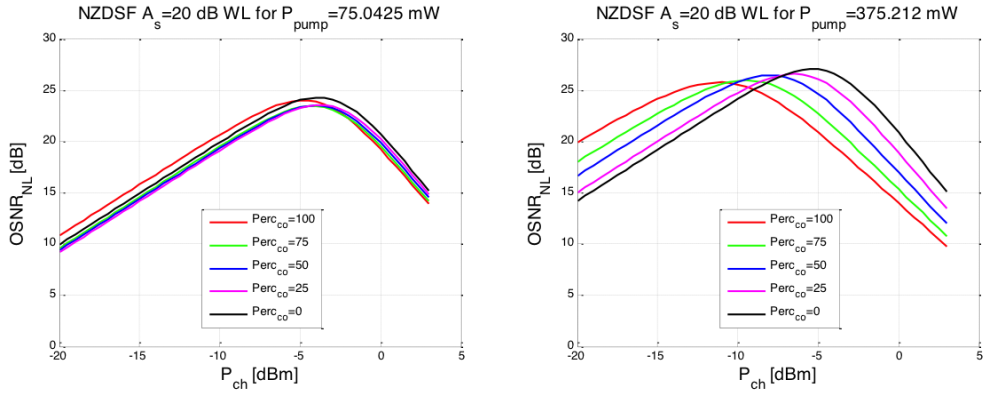

(a) P_{pump} = 75.0425 mW (b) P_{pump} = 375.212 mW

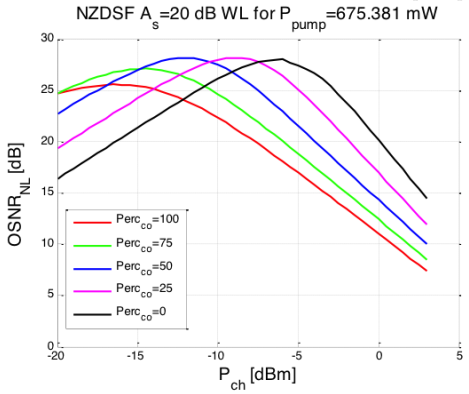

(c) P_{pump} = 675.381 mW

Figure 5.43: $OSNR_{NL}$ [dB] vs. channel input power, P_{ch} [dBm].

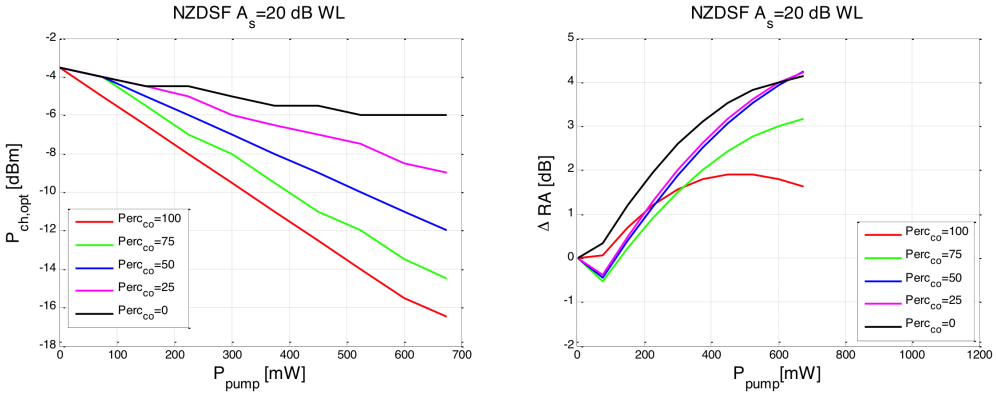

(a) $P_{ch,opt}$ [dBm] vs. P_{pump} [mW] (b) Δ_{RA} [dB] vs. P_{pump} [mW]

5.5.2 SMF results

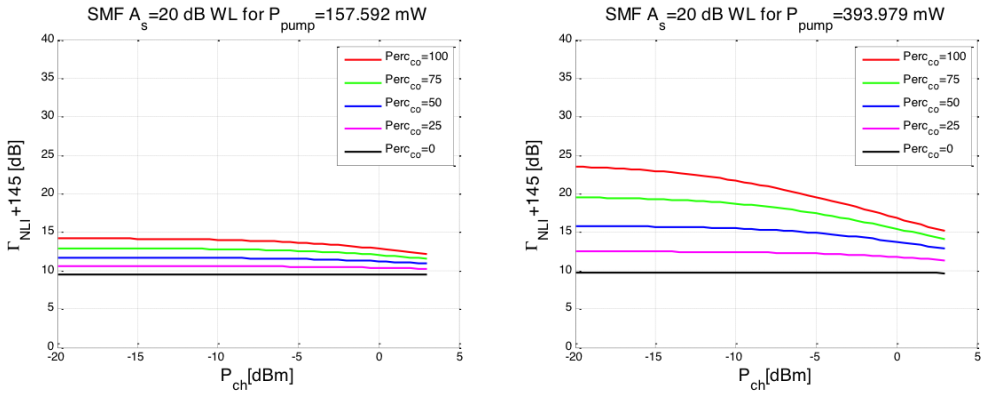

(a) P_{pump} = 75.0425 mW (b) P_{pump} = 375.212 mW

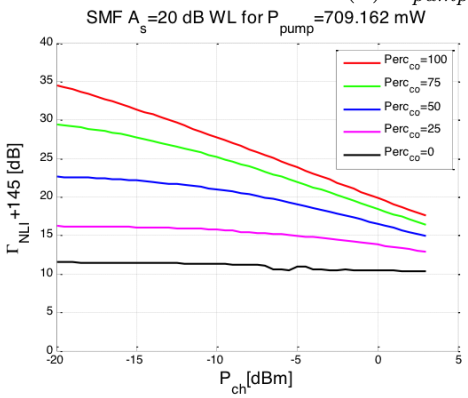

(c) P_{pump} = 675.381 mW

Figure 5.45: Γ_{NLI} [dB] vs. channel input power, P_{ch} [dBm].

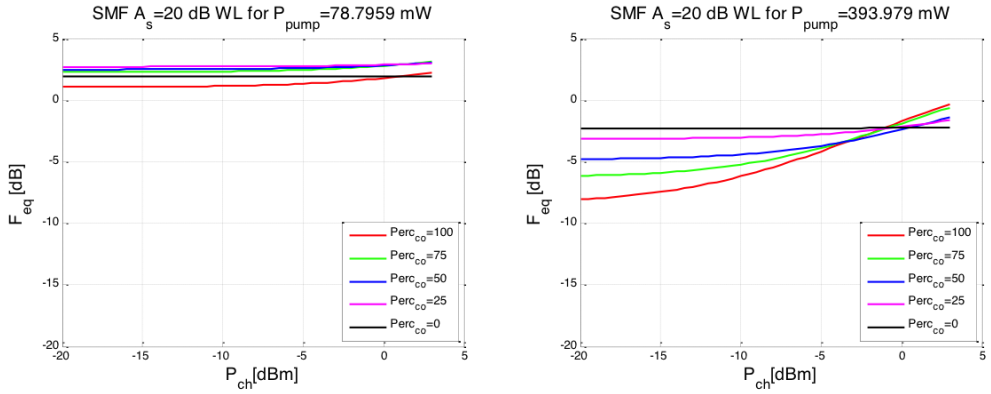

(a) P_{pump} = 75.0425 mW (b) P_{pump} = 375.212 mW

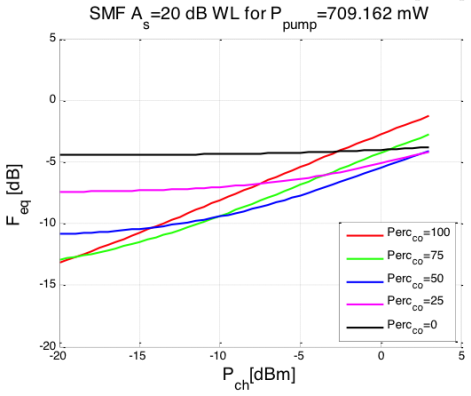

(c) P_{pump} = 675.381 mW

Figure 5.46: F_{eq} [dB] vs. channel input power, P_{ch} [dBm].

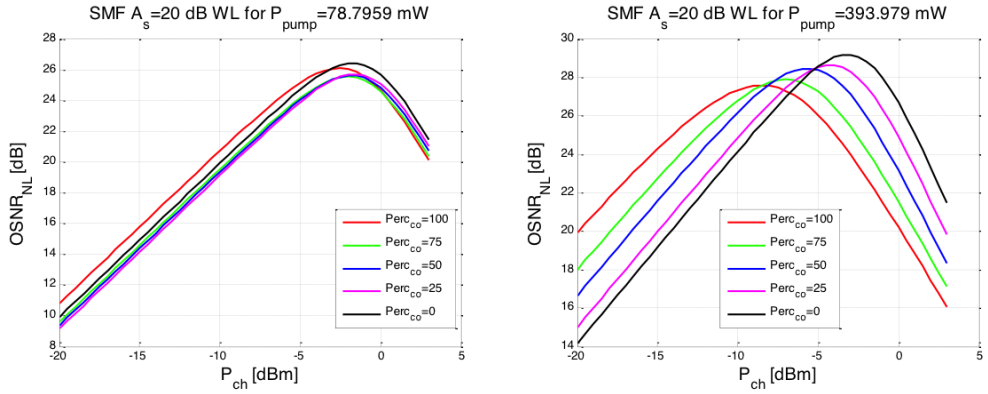

(a) P_{pump} = 75.0425 mW

(b) P_{pump} = 375.212 mW

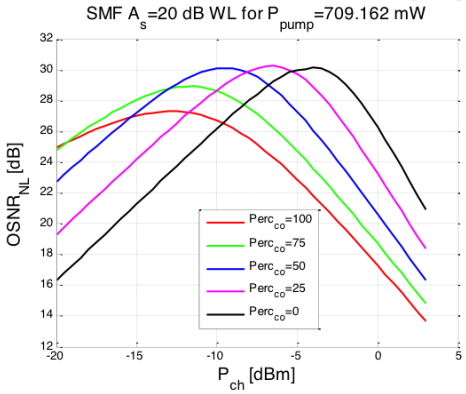

(c) P_{pump} = 675.381 mW

Figure 5.47: $OSNR_{NL}$ [dB] vs. channel input power, P_{ch} [dBm].

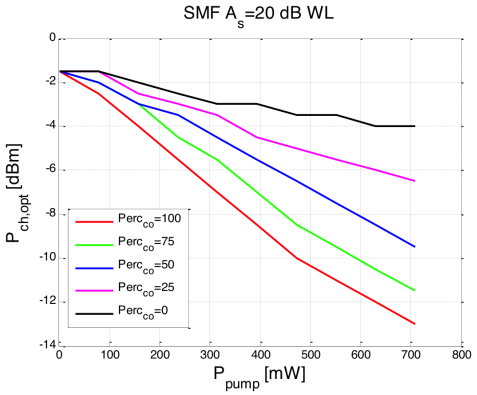

(a) $P_{ch,opt}$ [dBm] vs. P_{pump} [mW]

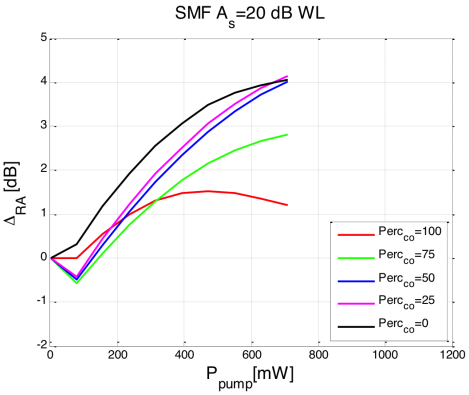

(b) Δ_{RA} [dB] vs. P_{pump} [mW]

5.5.3 PSCF results

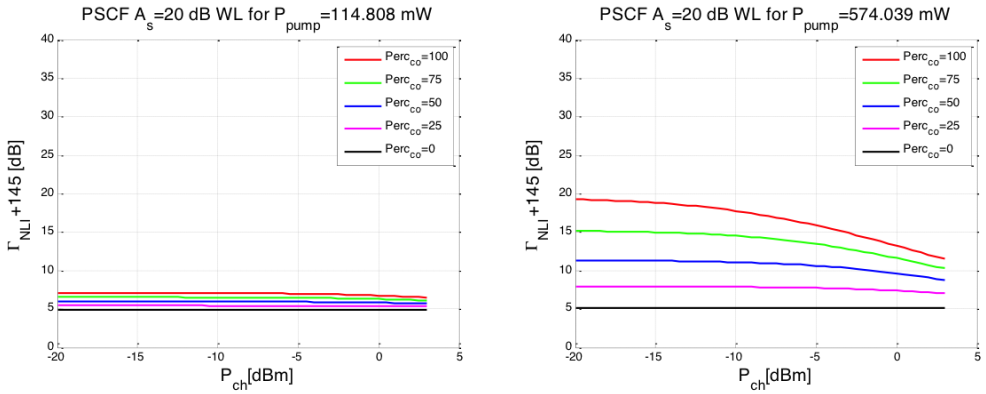

(a) P_{pump} = 75.0425 mW (b) P_{pump} = 375.212 mW

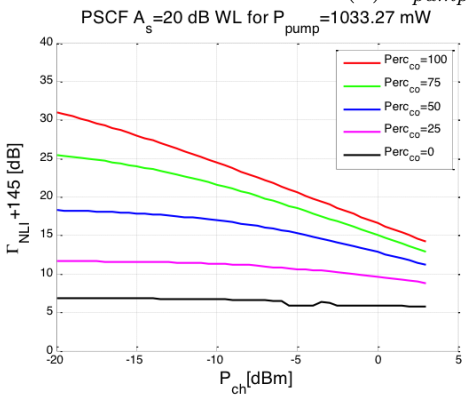

(c) P_{pump} = 675.381 mW

Figure 5.49: Γ_{NLI} [dB] vs. channel input power, P_{ch} [dBm].

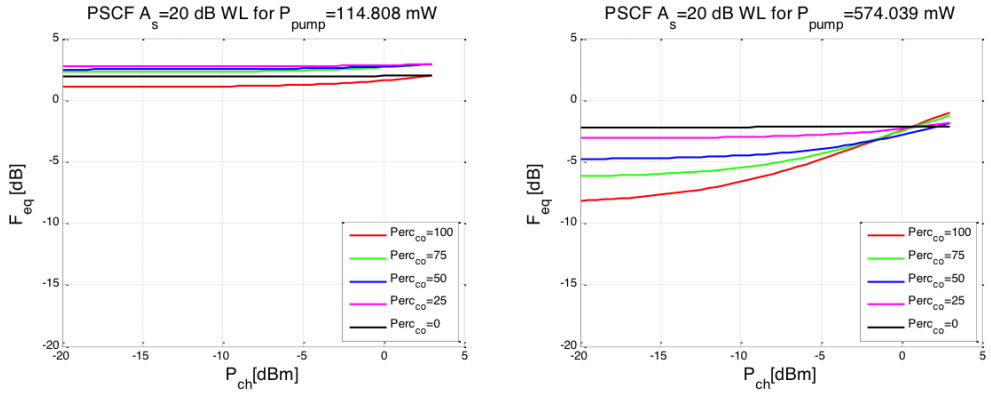

(a) P_{pump} = 75.0425 mW (b) P_{pump} = 375.212 mW

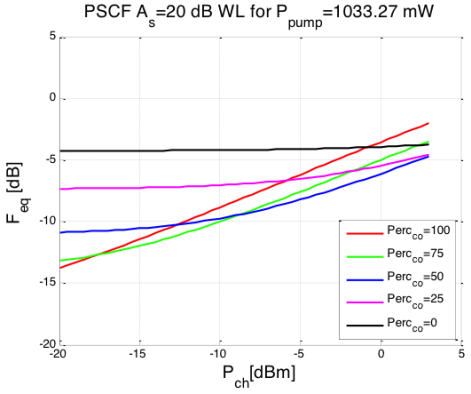

(c) P_{pump} = 675.381 mW

Figure 5.50: F_{eq} [dB] vs. channel input power, P_{ch} [dBm].

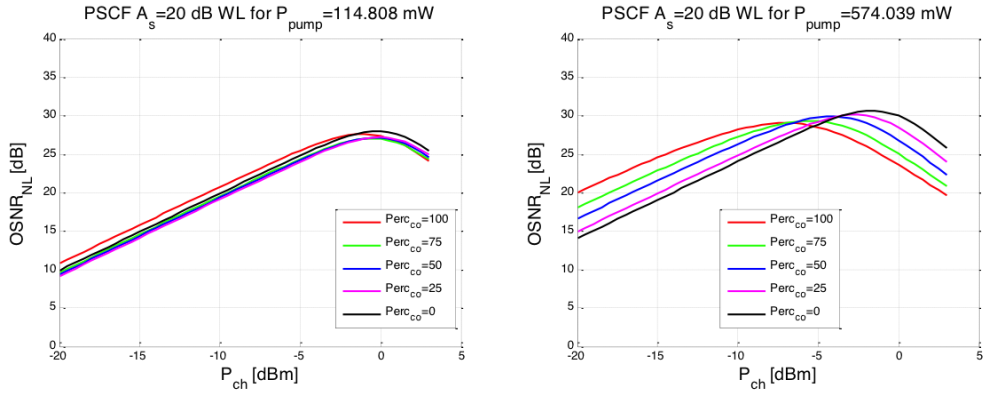

(a) P_{pump} = 75.0425 mW (b) P_{pump} = 375.212 mW

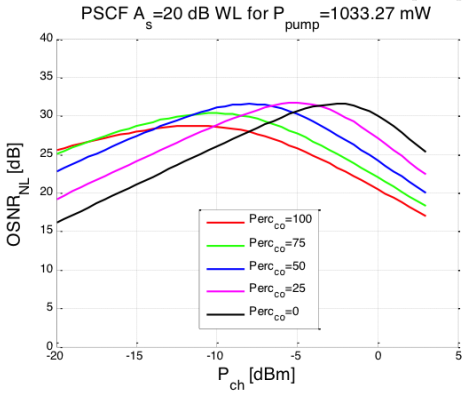

(c) P_{pump} = 675.381 mW

Figure 5.51: $OSNR_{NL}$ [dB] vs. channel input power, P_{ch} [dBm].

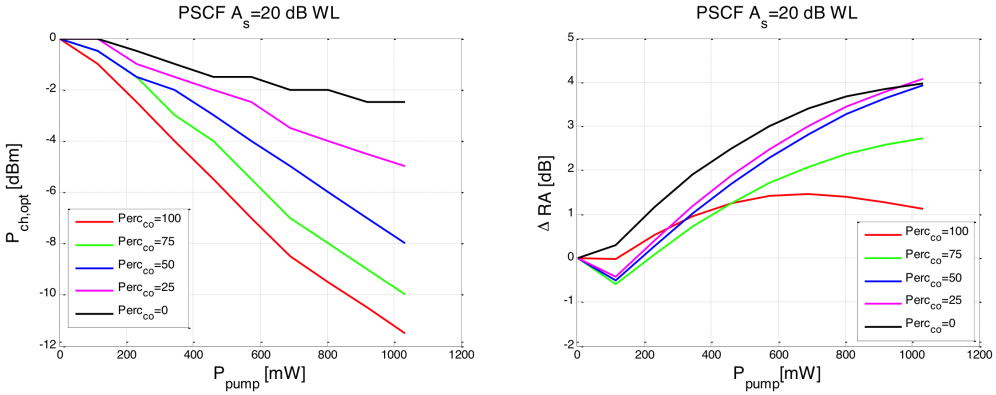

(a) $P_{ch,opt}$ [dBm] vs. P_{pump} [mW] (b) Δ_{RA} [dB] vs. P_{pump} [mW]

5.5.4 Comparison between fibers

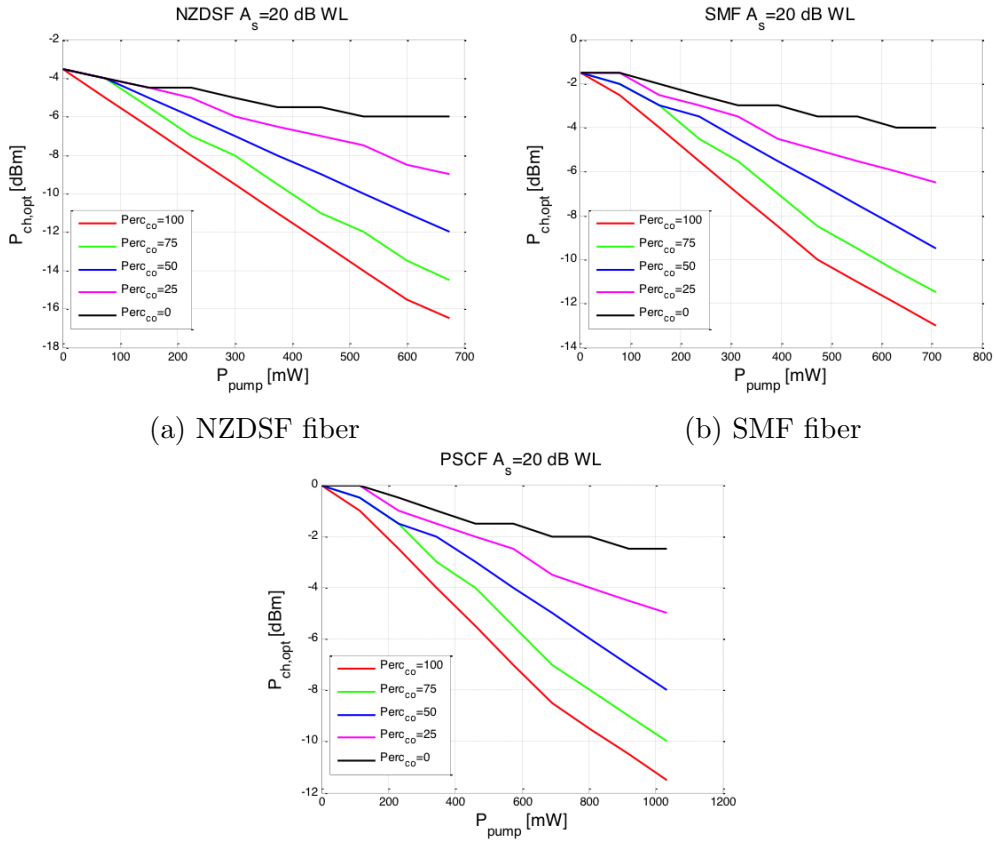

(a) NZDSF fiber

(b) SMF fiber

(c) PSCF fiber

Figure 5.53: $P_{ch,opt}$ [dBm] vs. P_{pump} [mW] for each fiber.

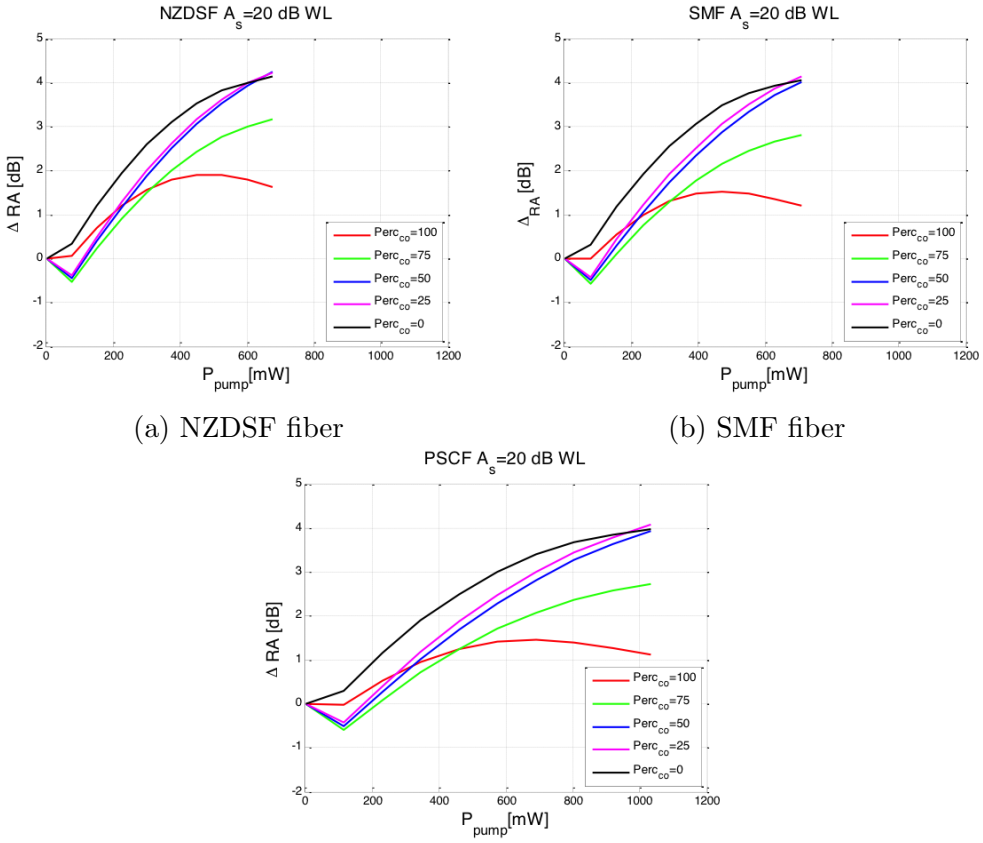

(a) NZDSF fiber

(b) SMF fiber

(c) PSCF fiber

Figure 5.54: F_{eq} [dB] vs. P_{pump} [mW] for each fiber.

5.6 Comparison between Second Scenario and Third Scenario

In order to see the differences whether the consideration of the coupler loss or not, we will show the results for $P_{ch,opt}$ and Δ_{RA} for each fiber.

5.6.1 NZDSF comparison

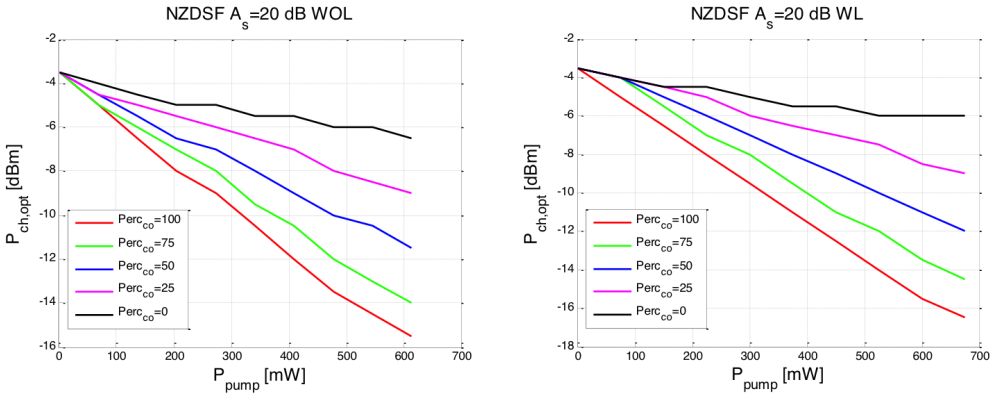

(a) Without considering coupler losses (b) Considering coupler losses

Figure 5.55: $P_{ch,opt}$ [dBm] vs. P_{pump} [mW] for NZDSF fiber.

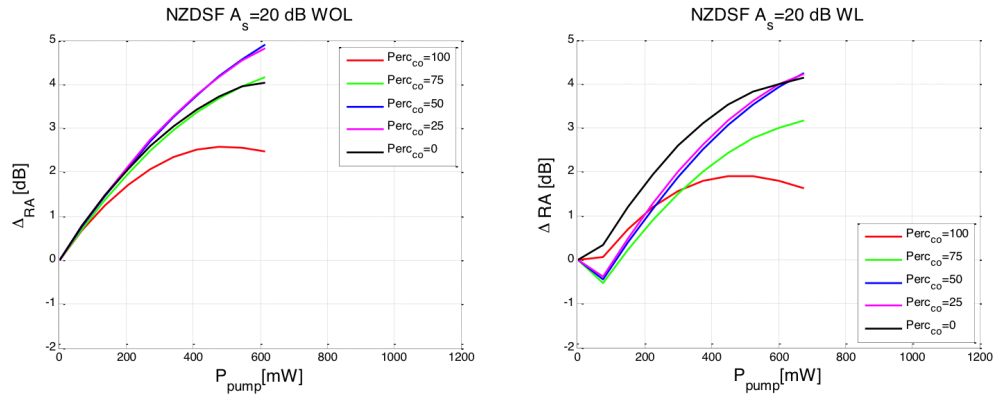

(a) Without considering coupler losses (b) Considering coupler losses

Figure 5.56: Δ_{RA} [dB] vs. P_{pump} [mW] for NZDSF fiber.

5.6.2 SMF comparison

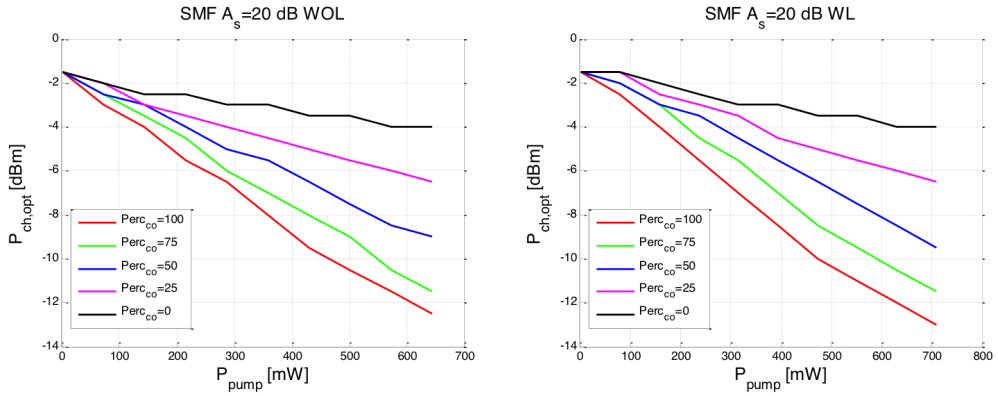

(a) Without considering coupler losses (b) Considering coupler losses

Figure 5.57: $P_{ch,opt}$ [dBm] vs. P_{pump} [mW] for SMF fiber.

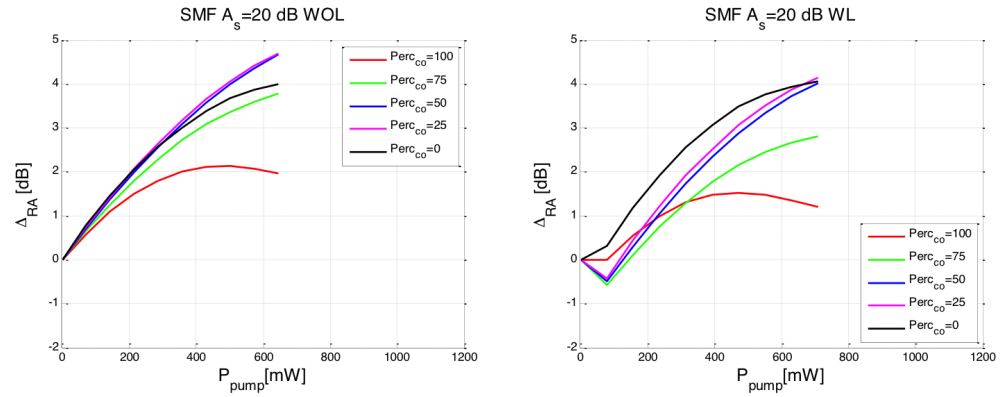

(a) Without considering coupler losses (b) Considering coupler losses

Figure 5.58: Δ_{RA} [dB] vs. P_{pump} [mW] for SMF fiber.

5.6.3 PSCF comparison

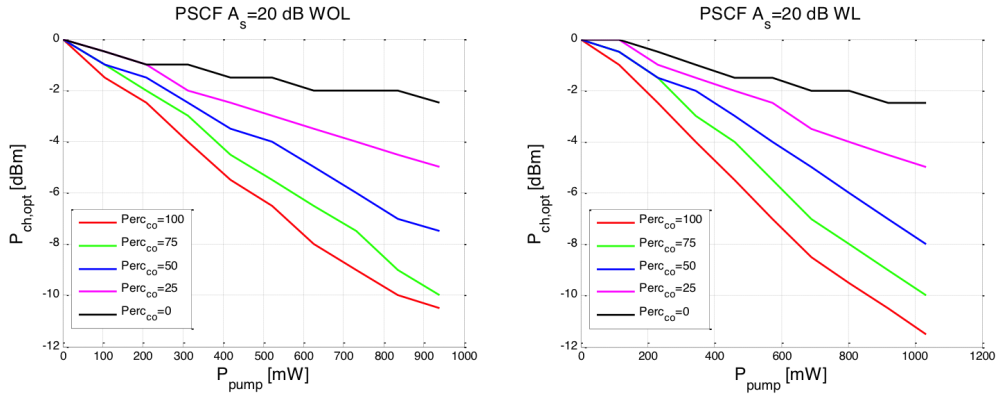

(a) Without considering coupler losses (b) Considering coupler losses

Figure 5.59: $P_{ch,opt}$ [dBm] vs. P_{pump} [mW] for PSCF fiber.

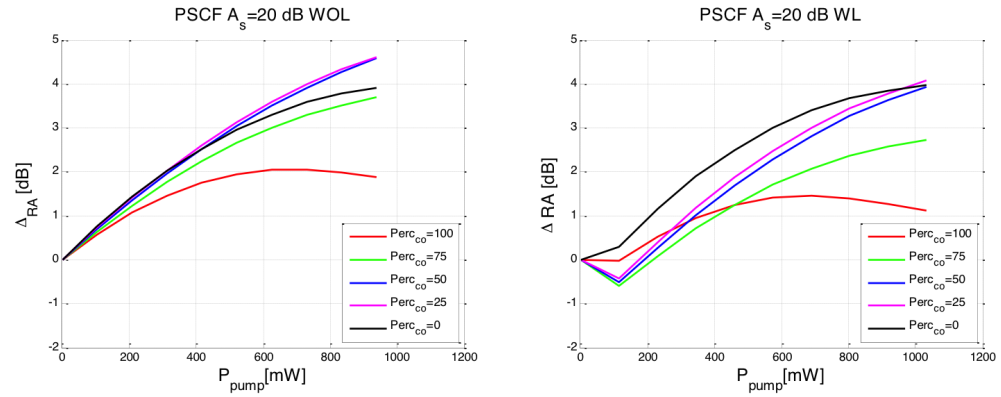

(a) Without considering coupler losses (b) Considering coupler losses

Figure 5.60: Δ_{RA} [dB] vs. P_{pump} [mW] for PSCF fiber.

Chapter 6

Conclusions

The very first conclusion that we see is that in therms of Γ_{NLI} we have to take into account its low value in dB, being the F_{eq} the parameter that really determines the Δ_{RA} of each fiber.

We may say that the first scenario is focused to prove the correct performance of the simulations comparing the theoretical and the practical results (under the undepleted or depleted pump assumptions). The behaviour of the different parameters is very similar in different fibers (the curve shapes are similar). Depending on what we are looking for, we might choose between different solutions; for example, PSCF fiber seems to have the best $OSNR_{NL}$ but we will need more Raman pump power to reach a close value in therms of Δ_{RA} comparing with SMF and NZDSF.
The second scenario includes the co-propagating pump. The main difference whether not using co-propagating pump or using it, is the dependence of the Γ_{NLI} and F_{eq} with the input power. In therms of $OSNR_{NL}$, the results are very similar in exception where there is not counter propagating pump. Δ_{RA} reachs its maximum value when $perc_{co} = 50$ or 25 instead of $perc_{co} = 0$ as it was expected. Finally, it must be said that an use of just a co propagating pump instead of both pumps, is not adviced due to the bad performance in therms of both $OSNR_{NL}$ and Δ_{RA}.
Including the coupler losses changes all the results of the $OSNR_{NL}$ and Δ_{RA} parameters. This what is shown on the third scenario. Here, the $OSNR_{NL}$ is similar when $perc_{co} > 50$ and Δ_{RA} shows a very similar behaviour when $perc_{co} = 25$, 50 or 100.

To sum up, in this project we propose optimization rules for HFA aimed at maximizing the reach or the OSNR at the receiver in NyWDM transmission over uniform and uncompensated links. We show that in general the optimization needs a careful HFA characterization in terms of pump depletion and DRB-induced MPI. For scenarios where coupler losses are not included

and the Raman pump power does not reach the full-RA power, undepleted results can be taken into account instead of depleted results, that is to say, pump depletion and MPI can be neglected and a unique merit parameter can be defined for each fiber type. We present results for three typical fiber types showing that Raman-induced noise reduction is always dominant on NLI enhancement.

Acknowledgements Thanks to Prof Curri and Prof Carena (Politecnico di Torino).

Bibliography

[1] Cisco Visual Networking Index:, Forecast and Methodology, 2013-2018

[2] G. Wellbrock, "How Will Optical Transport Deal With Future Network Traffic Growth?", ECOC 2014, Th.1.2.1 (2014)

[3] Jin-Xing Cai, *et al*, "54 Tb/s Transmission over 9,150 km with optimized Hybrid Raman-EDFA amplification...", ECOC 2014, PD3.3 (2014)

[4] G. Charlet, *et al*, "Ultra High Capacity Transmission over Transoceanic Distances", ECOC 2014, Tu.1.5.1 (2014)

[5] P. Poggiolini, *et al*, "The GN-Model of Fiber Non-Linear Propagation and its Applications", JLT, 32, 694-721 (2014)

[6] V. Curri, *et al*, "Extension and validation of the GN model..." OpExp, 21, 3308-3317 (2013)

[7] P. B. Hansen, *et al*, "Rayleigh Scattering Limitations in Distributed Raman Pre-Amplifiers," PTL, 10, 159-161 (1998)

[8] E. Pincemin, *et al*, "Raman gain efficiencies of modern ...," Nonlinear Guided Waves and Their Applications 2002, Paper NLTuC2 (2002)

[9] A. Carena, *et al*, "On the optimization of hybrid Raman/erbium-doped fiber amplifiers", PTL, 13, 1170-1172 (2001)

[10] Govind P. Agrawal, *Fiber-Optic Communications Systems*, John Wiley & Sons, Inc., third Edition, 2002

[11] R. Ramaswami, K. N. Sivarajan and G. H. Sasaki, *Optical Networks: A Practical Perspective*, Morgan Kaufmann Publishers, third edition, 2010

[12] V. Curri, "System advantages of Raman amplifiers"

[13] V. Curri, "Raman amplification", Master in Optical Communications and Photonic Technologies, Politecnico di Torino